

# Investigation of mixing time and relative concentration effects in adhesive mixtures for drug inhalation

**Simon Åslund**

---

Master Thesis in Engineering Nanoscience

Ergonomics and Aerosol Technology  
Department of Design Sciences  
Faculty of Engineering, LTH  
Lund University

EAT 2015



## Abstract

A common approach to treat respiratory diseases is with adhesive powder mixtures. These are dispersed into an aerosol upon inhalation. It has been found that the performance of such mixtures can be improved by adding fine particle lactose, but exactly why is yet to be established. Several theories have been proposed by previous studies, but the fundamental mechanism is still unknown.

This study was done in order to examine the impact of lactose fines (LF) in adhesive mixtures. This was approached by manufacturing different formulations using a high shear mixer. The concentration of added fines was kept at a constant 8% for all batches, whereas the relative concentration between the active pharmaceutical ingredient (API) Beclomethasone Dipropionate (BDP) and LF was varied systematically. Two sets of formulations were made, one containing a force control additive (1% Magnesium Stearate), referred to as coated formulations, whereas the other contained no such additive, referred to standard formulations. Several samples were extracted at different time points during the mixing stage in order to get a better understanding on how the mixing process influences the dispersion properties.

The aerodynamic particle size distributions of the API and LF were assessed using a Next Generation Impactor (NGI), which is a widely practiced technique within pharmaceutical development work. Quantification of BDP component was done using a well-developed method consisting of an ultra-performance liquid chromatography -system and an internal standard solution. However, this technique is not suitable to quantify the LF component. Overall, the analysis of lactose intended for inhalation is poorly described in literature. Therefore, one objective of this thesis was to find and evaluate such method. Two techniques were tried out; the first one being LC-PAD system based on electrochemical analysis. This was however disregarded due to instrumental errors and instead, a high pressure liquid chromatography system coupled with a mass spectrometer was used. However, this technique needs more tuning to be as good as the one used for BDP, as the assessed results did sometime display unreasonably high values and it is still unclear how much impact the carriers have on the analysis.

Regarding the performance of the manufactured batches, it was observed that the Fine Particle Fraction (FPF) for the coated formulations were consistently higher than for the standard formulations, as was expected. The coated formulations did also show a dependency on the mixing process as regards the FPF values. No such effect could be seen for the standard formulations. It was also found that the FPF of LF were consistently higher than the FPF of BDP. The FPF of BDP was consistently higher for formulations with a higher amount of LF. It was proposed that the LF and BDP form co-agglomerates during mixing, which lies in agreement with one of the existing theories that explains the behavior of LF.

The NGI is, despite yielding high quality results, a rather time consuming method which bottlenecks the pharmaceutical development process. A faster method to assess the PSD of an adhesive mixture is by the usage of Laser Diffraction (LD). This technique is however chemically non-specific, which render analysis of adhesive mixtures including both LF and API a bit troublesome. It would be favorable for future work if there was a way of correcting for LF when analyzing using LD, and a second part of this thesis was thus to evaluate how well data assessed from the NGI correlated with data assessed with LD setups.

It was found that it is possible to screen a formulation using LD if an appropriate dispersion method is used. However, in order to correct for LF in LD measurements, more research is needed as the LF seems to disperse differently in different formulations. Formulations with only LF as added fines correlated well with data assessed by the NGI.

## **Acknowledgements**

This diploma work was done at AstraZeneca R&D Mölndal. I would like to thank my supervisors Kyrre Thalberg and Patrik Andersson for all their invaluable support, guidance and admirable commitment throughout this work. Their knowledge and experience in the field have really been a great help and asset for me when conducting this thesis.

Likewise, I would also like to express my deepest gratitude to my examiner at LTH, Anders Gudmundsson, for taking part in this thesis and making it possible.

Furthermore, special thanks go to Marcus Skogevall for all his patience and helpful assistance throughout the analysis work. Other persons I would like to thank are Magnus Olsson and Lars Dalmin for helping me out in the lab. I would also like to acknowledge Johan Arnehed for assisting me with SEM images.

Simon Åslund, April 2015

## List of abbreviations

<b>API</b>	Active Pharmaceutical Ingredient
<b>BDP</b>	Beclomethasone Dipropionate
<b>COPD</b>	Chronic obstructive pulmonary disease
<b>DPI</b>	Dry Powder Inhaler
<b>F<sub>5</sub></b>	Cumulative volume fraction <5 μm
<b>FCA</b>	Force Control Additive
<b>FPF</b>	Fine Particle Fraction
<b>FPmode</b>	Fine particle mode
<b>HPLC</b>	High pressure liquid chromatography
<b>LC</b>	Liquid chromatography
<b>LD</b>	Laser diffraction
<b>LF</b>	Lactose Fines
<b>MgSt</b>	Magnesium Stearate
<b>MMD</b>	Mass Median Diameter
<b>MMAD</b>	Mass Median Aerodynamic Diameter
<b>MS</b>	Mass spectrometry
<b>NGI</b>	Next Generation Impactor
<b>PSD</b>	Particle size distribution
<b>RSD</b>	Relative Standard Deviation
<b>TOF-SIMS</b>	Time Of Flight – Secondary Ion Mass Spectroscopy
<b>UPLC</b>	Ultra performance liquid chromatography

## Table of Contents

Abstract.....	2
Acknowledgements.....	4
List of abbreviations .....	5
1. Introduction.....	7
1.1 Theory.....	7
1.2 Measuring adhesive mixtures .....	11
1.3 Aim of the study.....	14
2. Materials and manufacturing .....	15
2.1. Materials .....	15
2.2. Manufacturing of adhesive mixtures .....	16
3. Analytical methods .....	18
3.1 Next Generation Impactor.....	18
3.2. Liquid Chromotography.....	19
3.3 Laser diffraction measurements .....	22
3.3.1 Sympatec RODOS.....	22
3.3.2 Sympatec Inhaler .....	22
4. Results.....	24
4.1 NGI .....	24
4.1.1. Formulations with MgSt.....	24
4.1.2 Standard formulations .....	31
4.2 Laser diffraction.....	35
4.2.1. Sympatec RODOS.....	35
4.2.2. Sympatec Inhaler.....	39
4.3 Relaxation effect of formulations. ....	44
4.4 Effect of intrinsic fines.....	45
4.5 Images from scanning electron microscopy .....	46
5. Discussion.....	49
5.1 Behavior of the adhesive mixtures.....	49
5.1.1 Effect of coating agent.....	49
5.1.2 Influence of different mixing times .....	50
5.1.2.1 Mathematical modeling of FPF of BDP.....	54
5.1.3. Effect of different concentrations between BDP and LF .....	56
5.1.4 Formation of agglomerates.....	57
5.2. Comparison between NGI and Laser Diffraction .....	58
6. Conclusions and further work.....	65
6.1 Conclusions.....	65
6.2 Further work.....	66
7. References.....	68
Appendix I – Raw data from measurements.....	70
Appendix II – Correlation plots .....	80

# 1. Introduction

This thesis has been carried out in order to obtain fundamental understanding about the dispersion properties of powder formulations intended for inhalation. The focus has been in investigating the impact of adding fine particle lactose into such powder mixtures. This chapter will provide a brief background to the field, followed by a description of what was sought for when conducting this thesis.

## 1.1 Theory

Throughout history there have been several ways of treating different diseases, ranging from trepanation to phlebotomy, some methods better than others. One way, that even the old Greeks employed, was to inhale medicinal herbs into the lungs. Today, inhalation science is a well-established field of research and there are several pharmaceutical products on the market that employs the respiratory tract as a route of delivering medication. This has several advantages over oral or intravenous treatment including direct delivery to the target as well as rapid onset of drug action. Furthermore, systematic side effects are fewer as the dose can be smaller and unlike oral administration of the drug the lungs exhibit low metabolic activity. [1]

When treating respiratory diseases, such as asthma or chronic obstructive pulmonary disease (COPD), the active pharmaceutical ingredient (API) is delivered to the lungs in the form of an aerosol cloud. An aerosol is defined as a two phase system of solid particles or liquid droplets dispersed in a gaseous phase such as air [2]. On entering the respiratory tract there are numerous ways that the inhaled particles can interact with the surrounding tissue, depending on their aerodynamic diameter. This is defined as the diameter of a unit-density sphere having the same settling velocity as the particle in question and is one of the most important properties of respirable particles [2].

In order to reach the lower respiratory tract of the lungs, a generally accepted size interval for respirable particles is approximately between 1-5  $\mu\text{m}$  (aerodynamic diameter), depending on the desired target site. Larger particles than this are likely to deposit earlier in the airway system and smaller particles are likely to be exhaled. [3]

To deliver the particles to the targeted lung-regions there are different devices on the market that can be utilized, each one of them employing different techniques to create the aerosol cloud. A commonly used type is the Dry Powder Inhaler (DPI), in which the API is stored as a dry powder formulation. The driving force to create an aerosol from a static powder bed is the actuation generated by the patient's inhalation effort, entraining the powder into the air flow. The dispersion is furthermore aided by the structure of the device. [4]

To achieve full dispersion of the powder, the formulation has to be carefully designed in order to overcome various difficulties respirable particles may experience. Particles of this size range are naturally cohesive due to their large surface area compared to mass, which leads to poor dispersion as well as poor handling properties of the powder within the DPI. [4]

To overcome these problems there are commonly two approaches employed. The first one is to form larger, loose agglomerates (defined as a system where primary particles of different sizes are held together by inter particulate contact forces) of the drug particles that are both easily broken and dispersed upon inhalation as well as more suitable to handle within the DPI. These agglomerates can also be made up by API and some inert excipient in the same size interval (typically 1-10  $\mu\text{m}$ ) to further ease de-agglomeration upon inhalation. [5] A schematic view of this can be seen in Fig.1.1.

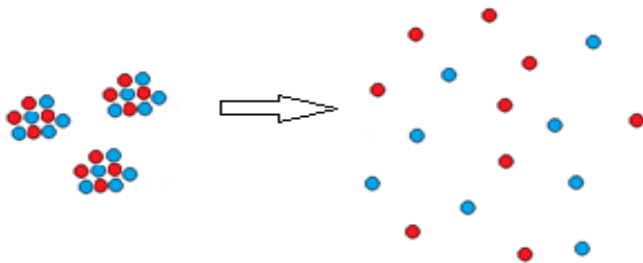


**Figure 1.1: A schematic view of agglomerates consisting of API and excipients that are dispersed upon inhalation. The arrow in the middle signifies the dispersion of the powder into an aerosol. The red spheres represent the API, where the blue spheres represent inert excipients.**

The other type of powder formulation intended for usage in a DPI is built up by a mixture of API particles along with coarser particles, referred to as carriers. These are typically 50-200  $\mu\text{m}$  in diameter and consist of an inert material, often lactose monohydrate. The principle behind these mixtures is that the API will adhere to the surface of the carrier particles and upon inhalation, the API will liberate from the carriers and continue downwards the lower airways, while the carrier particles will deposit in the earlier stages of the lungs. [5]

These kinds of mixtures, built up by coarse carriers and finer API-particles, are often referred to as adhesive or ordered mixtures. The carriers are generally less cohesive than the API and have better flow and fluidization properties, thus making these types of mixtures suitable to handle in a DPI[5]. A schematic view of the dispersion process for an adhesive mixture is shown in Fig 1.2.



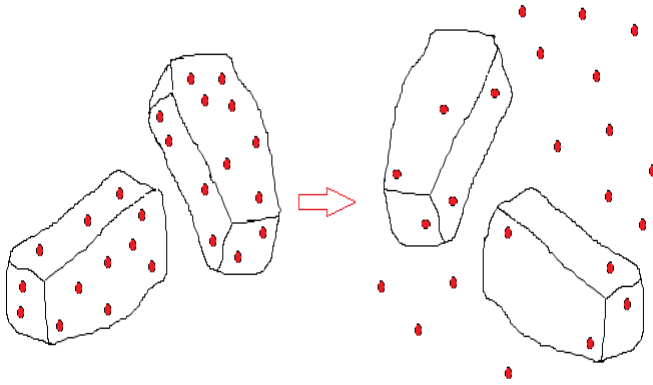


**Figure 1.2: A schematic view of API particles liberating from the surface of carriers upon inhalation. The arrow in the middle resembles the inhalation process which disperses the powder into an aerosol. The red spheres represent the API adhering to the carriers, which are shown as white blocks.**

The molecular forces responsible for the adhesion and separation between particles are mainly van der Waals forces and Columbic (electrostatic) forces, but also mechanical forces caused by surface roughness and irregularly shaped particles [6]

If the adhesive forces between the API and the carrier are stronger than the inhalation forces induced upon inhalation, the API does not liberate from the carrier surface. By introducing a force control additive (FCA), also referred to as a coating agent, into an adhesive mixture it has been found that the adhesive forces between the API and carriers are reduced. It is believed that this additive is smeared onto the carriers or API particles as a thin layer, thus allowing for easier de-aggregation upon inhalation due to reduced van der Waals attractions. [7]

To further improve the dispersion performance of an adhesive mixture it has been found that introduction of additional excipients within the same size range as the API can aid this cause. A commonly used material for this is lactose monohydrate. This excipient has been the focus of this thesis work and will hereby be referred to as lactose fines (LF). The mechanism of why the introduction of LF increases the dispersion performance of an adhesive mixture is still unknown, but different theoretical explanations have been proposed in literature. However, each of them has some drawbacks and further research is needed.

A review by Jones et al. [8] refers to two main theories to explain the effect of LF:

#### *Active sites*

The surface of the carriers inhibits so called “active sites”, which are areas that are more adhesive than others. This results in a higher chance of smaller particles to adhere there first and the idea is that the LF saturates these sites, leaving the rest of the surface for

the API. The API adhere thus to less adhesive areas and are consequently more easily liberated from the carriers upon inhalation.

#### *Formation of agglomerates*

This theory states that instead of adhering to active sites, the finer particles (API and LF) form agglomerates during mixing. These agglomerates are then evenly distributed onto the carriers. Upon inhalation, these clusters are liberated from the carriers to be shattered and a higher dispersion of the API is achieved, compared to if the fines would adhere to the carriers alone.

Furthermore, there is another, more recent theory, proposed by Shur *et al.* [9] to account for:

#### *Increased cohesion*

Formulations including fine lactose have shown to increase the cohesive strength of the bulk powder and by so, the minimum energy that is required for fluidization of the powder bed is increased and so is the energy available for dispersion.

Another theory proposed by Dickhoff *et al* [10] is also found in literature:

#### *Fines acting as buffers*

During mixing, LF coarser than the API may protect the API from compression and act as a buffer between colliding particles.

As stated previously, none of these theories are proven, but Kinnunen *et al* [11] suggests that the explanation might lie within a combination of these theories.

## 1.2 Measuring adhesive mixtures

In order to study different formulations it is important to know the particle size distribution (PSD) of the aerosol cloud. There are different ways of assessing the PSD and a widely practiced technique is to use a cascade impactor, such as the Next Generation Impactor (NGI) shown in Fig. 1.3.



Figure 1.3 : The image to the left displays an open NGI. The image to the right displays an NGI connected to a United States Pharmacopeia (USP) induction port and a pre-separator, mimicking the upper airways of the lungs. Typically a DPI is connected the inlet of the NGI, in which the powder is drawn from. In this work, a prototype device, described in chapter 3, was used. The airflow is lead from left to right, and the small cavities seen in the left figure fractionates the aerosol by impaction. [12, 13]

The NGI is based on the principle that particles following an airstream will separate depending on their size and ability to adjust for sharp turns. Particles with high inertia will continue in their original direction and can thus impact on a collector plate, while smaller particles can follow the sudden change of the air stream. By coupling several collector plates in series and by letting the airstream pass through smaller and smaller nozzles thus increasing its speed, the aerosol can be fractionated according to the particles aerodynamic diameter.

In the NGI the air flow is lead through a saw tooth pattern in a series of nozzles containing progressively reducing jet diameters. Different air flows give different cut-off diameters. There are 8 stages of collector plates in the form of a removable tray that can be changed between each measurement. The NGI typically gives a PSD interval of 0.1 – 10  $\mu\text{m}$ . [13]

The NGI has 3 distinct advantages when it comes to measuring aerosols intended for respiratory medication; firstly, it gives the aerodynamic diameter of the particles, which is relevant for the intended deposition site in the lungs. Secondly, it gives the opportunity to analyze the collected particles with regards to their chemical

composition. Thus, the distribution of the API can be assessed; giving information on how much of the API that can reach down to the final stages of the lungs. Finally, it is a method approved by governments and it is described in various Pharmacopeias. However, drawbacks with this method is the long analysis times and high labor consumption, which easily can bottleneck the pharmaceutical development process.

Another way of assessing the PSD of an aerosol is by the usage of laser diffraction (LD). The aerosol passes through a laser beam and the particles will then, depending on their size and refractive index, scatter the beam differently.

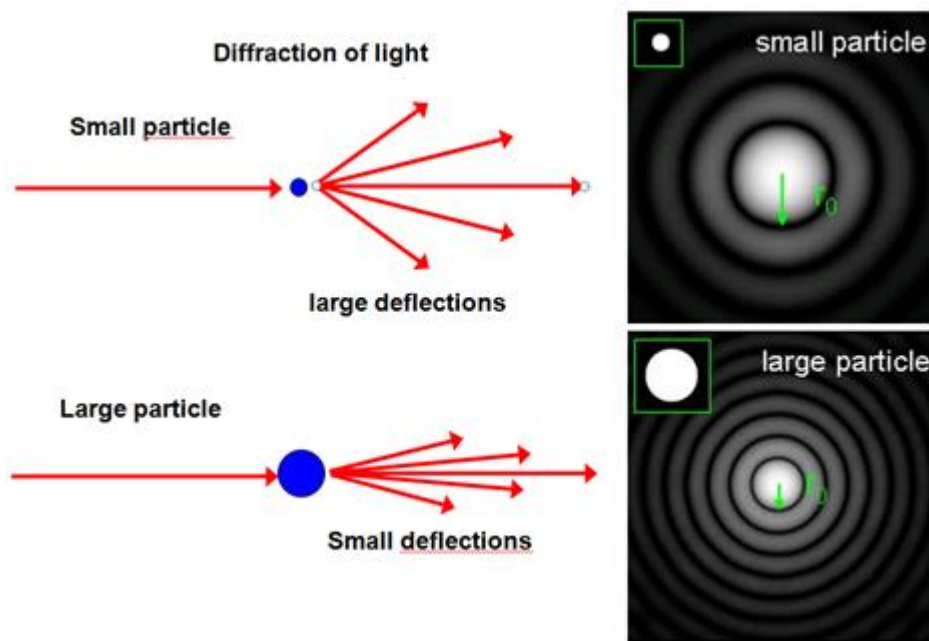


Figure 1.4: A schematic view on how the light scatters differently depending on the particle size. Displayed to the right is the diffraction pattern of smaller respectively large particles. By courtesy of Patrik Andersson [14]

A fourier lens is used to focus the scattered light onto a detector. With the help of computational power the PSD can be calculated from the acquired signal, using existing mathematical theories and assumptions (Mie and Fraunhofer) [14]. A typical PSD interval using LD is 0.5 - 200  $\mu\text{m}$  but this depends on the lens used in the measurement. [14]

The LD provides a fast and cheap screening method in comparison to the NGI, but it comes with some drawbacks. Firstly, the technique cannot differentiate between different chemical components such as the API and other excipients. Secondly, it

measures the geometrical diameter and thirdly, the mathematical calculations assume spherical particles which rarely are the case for ordered mixtures.

By knowing the PSD of a formulation, the amount of API that reaches the intended regions in the lungs can be evaluated. Using the NGI, the fine particle fraction (FPF) is commonly sought for. This is defined as the fraction of particles of the total API-dose below a set cut-off value (usually  $5\ \mu\text{m}$ ). Another important value given from the PSD is the mass median diameter (MMD) which is defined as the diameter at which 50% of the particles by mass are larger and 50% are smaller. For aerodynamic particles, which are relevant for inhalation, the mass median aerodynamic diameter (MMAD) is used. [2].

The FPF equivalent for LD is Cumulative Volume Fraction  $< 5\ \mu\text{m}$  (here denoted as  $F_5$ ). Note that this value may include both API and excipients, such as LF, since the method cannot differentiate between different compounds. In this work the LD equivalent to MMAD is referred to as Fine Particle mode (FPmode), which is the peak value of fraction of finer particles, shown in Fig. 1.5.

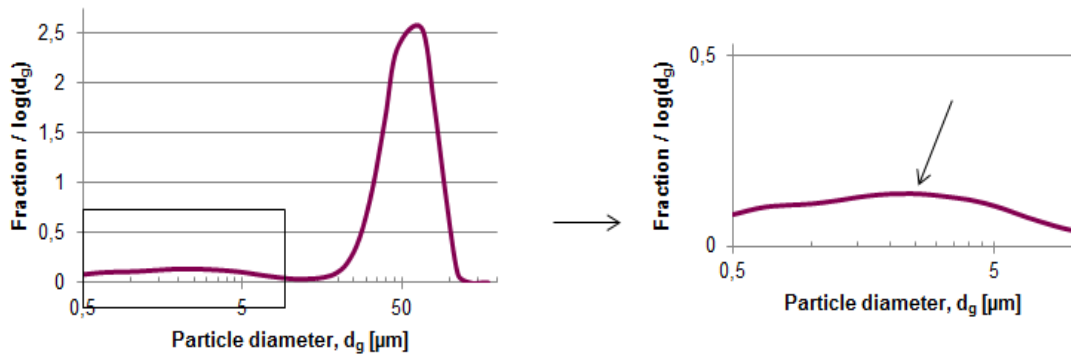


**Figure 1.5:** The left image displays a typical PSD from laser diffraction measurement and the right image resembles a zoomed in view of the particles below  $5\ \mu\text{m}$ . From this the FPmode can be assessed, shown by the arrow.

### **1.3 Aim of the study**

The aim of this thesis was to obtain further understanding of the behavior and effect of LF within an adhesive powder mixture. This was targeted by manufacturing several formulations containing different amount of LF and API. The analysis work was constructed around two main objectives, where the first involved measurements using the standard method NGI. For this part the following topics were dealt with:

- How does LF behave in different formulations and how do they affect the performance of the API?
- How are adhesive mixtures with API and LF influenced by different processing times?
- How does addition of a coating agent affect the formulations?

As LD measurements provides a faster screening of formulations compared to the NGI, it would be beneficial for future development if there is a way to correct for LF when evaluating the performance of an API. Therefore, the other main objective for this thesis was to compare results given by the NGI with results given by LD measurements with the following question in mind:

- Is there a way to correct for LF using LD method, in order to predict the FPF of the API?

## 2. Materials and manufacturing

This work included manufacturing of adhesive mixtures, divided into two sets of mixing. In the following sections the materials that were used are presented, followed by a description of the manufacturing processes.

### 2.1. Materials

The carrier in the formulations was an inhalable form of lactose, Respitose SV003, with an intrinsic amount of fines of roughly 1 %. The term intrinsic fines refer to finer particles inherent from the production process. The API was micronized Beclomethasone Dipropionate (BDP), which is a glucocorticoid steroid with anti-inflammatory properties. The LF were micronized and conditioned lactose, where conditioning refers to re-crystallization of amorphous regions formed during micronisation. For the first set of mixing Magnesium Stearate (MgSt) was added as a coating agent. For the second set no such coating additive was present. The different formulations will be referred to as coated formulations and standard formulations, respectively.

The total amount of added fine particle (API and LF) was set to 8 wt% for all formulations, as it has been observed that the concentration of total fines relates to the performance of an adhesive mixture [15], where 8% lies within the region of neither being too much nor little.

An overview on the materials used for manufacturing in this work is presented in table 2.1. and in table 2.2 the relative weight concentrations are given.

**Table 2.1.** List of raw material used in this work.

Material	Batch#	MMD ( $\mu\text{m}$ )	Supplier
Carrier Lactose, Respitose SV003	1301	60.0*	DFE Pharma
Coating agent Magnesium Stearate	30003501	5.0*	Peter Greven
API and fines Beclomethasone Dipropionate, Micr.	03220520	1.3*	Meridian Pharmaceuticals Inc.
Lactose, Micr. and cond.	309001	2.4*	AstraZeneca

\* Measured at AstraZeneca

## 2.2. Manufacturing of adhesive mixtures

Production and mixing of the formulations were done using a Diosna P1-6 high shear mixer equipped with a mixing vessel of 1.2 liter made of stainless steel, displayed in Fig. 2.1. The speed of the mixing blade was set to 800 rpm and the mixing was performed inside an isolator-box to avoid contact with the drug. The relative humidity of the isolator box was set to around 20 % and the temperature was around 22° C. Between each mixing of a batch the isolator box including the mixing vessel was dry cleaned using a vacuum hose.



Figure 2.1: An image of the high shear mixer used in this work, Diosna P1-6 [16].

8 sets of formulations were manufactured, divided into two sets of mixing, with a total mixing time of 120 minutes for each batch. The mixing was stopped 8 times at different time points for sampling and thus a total of 9 samples were extracted from each batch, including the end-point. The specific time points where the blending was stopped was 2, 5, 10, 20, 30, 45, 60, 90 and finally 120 minutes for all batches. The extracted samples were roughly 25 grams each and the total amount of material for each batch was 350 gram.

In the first set of mixing, a pre-coating step of the carrier was performed. Half of the carrier was added evenly into the mixing vessel, followed by the MgSt and then the rest of the carriers. This pre-blending step was done at 70 rpm for 2 minutes and 350 rpm for 1 minute, followed by 10 minutes of mixing at 800 rpm. This was done in order to smear out the MgSt on the carrier surface. The LF and API were then added layer-wise and mixed for 2 min at 70 rpm and 1 min at 350 rpm before the mixing at full speed of 800 rpm was started. The conditions for second set of mixing were the same as for the first mixing set, but without the coating step. The components were added layer wise, starting with half of the carrier followed by API and LF and then the rest of the carrier.



**Table 2.2.** List of the weight concentration of each component in the manufactured batches.

**Coated formulations**

Batch#	Carriers	LF	BDP	MgSt	Yield
EB14-032125	91 %	8%	0%	1%	87,4%
EB14-032126	91 %	6%	2%	1%	86,8%
EB14-032127	91 %	4%	4%	1%	87,4%
EB14-032128	91 %	2%	6%	1%	83,1%
EB14-032129	91 %	0%	8%	1%	84,7%

**Standard formulations**

EB14-023132	92 %	8%	0%	-	56,6%
EB14-023133	92 %	6%	2%	-	91,3%
EB14-023134	92 %	4%	4%	-	95,7%

The 120 min sample from the 8% LF mixture was unfortunately exposed to water when emptying the mixing bowl (due to residual water that had been left in cooling pipes of the mixing vessel after the previous cleaning) and thus damaged. Therefore, no analysis of this point could be made.

### 3. Analytical methods

A variety of different techniques and measurement instruments were employed throughout this work. In the following chapter a description of these will be given followed by the settings and conditions applied in each measurement.

#### 3.1 Next Generation Impactor

To acquire the FPF of the formulations an NGI was used. A prototype inhaler device, referred to as screenhaler and displayed in Fig 3.1, was fitted to the USP throat of the NGI.

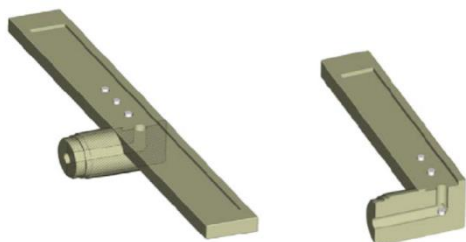


**Figure 3.1: A schematic view [15] of the device, referred to as screenhaler, used during NGI measurements. The screenhaler is a rather simple device with no inherent deaggregation mechanism, where the dispersion of the powder relies basically on the applied airflow. The device consists of L-shaped cylindrical channel with a diameter of 7 mm made of stainless steel.**

The powder was weighted into the screenhaler using a spatula. An airstream through the impactor was created by using a trig box, giving a defined air flow rate and a fixed measurement time, connected at the end of the impactor.

A pre-separator was connected between the USP throat and the impactor-body. Standard settings for measurements were applied, where the pressure drop was set to 1.5 kPa, the measurement time was set to 3.1 s and the flow rate was set to 77 lpm. Impactor plates were coated with a Brij-solution in prior to each measurement in order to reduce bounce off effects. Each measurement consisted of a total of three doses of roughly 5 mg of formulation / dose. In Fig 3.2 the cut-off sizes for the flow used in NGI measurement can be seen along with the PSD of an API within an adhesive mixture

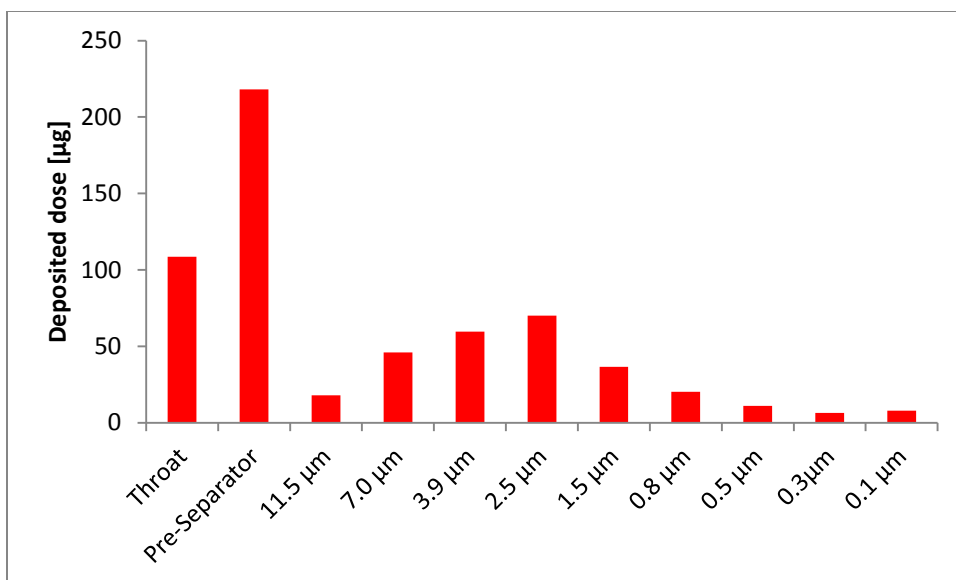


**Figure 3.2: Deposition curve within the NGI for coated formulation containing 2% BDP and 6% LF. The cut-off values for the used airflow are given on the X-axis.**

After each measurement, the NGI was disassembled. The throat and pre-separator was filled with appropriate solution (depending on type of fine particles being examined, see section 3.2 below) and covered up to be put in a rotating setup for 15 min in order to dissolve the excipients for chemical analysis. The impactor plates were filled with appropriate solution and put on a rotating table for 15 minutes at 50 rpm.

### 3.2. Liquid Chromatography

Chemical analyses of the impactor plates were done by using Liquid Chromatography, which is a widely used technique for analytical measurements of components in a sample mixture. The mixture, which consists of a solvent and the analytes, is passed with the help of a pump through a column filled with adsorbents of typically very fine particles (1.5-2 µm). Depending on the nature of each analyte, they will interact differently with the column, leading to a separation of the components once they exit the column. Depending on the analytes, elution times will be different and they can be separated from each other. By having an internal standard of known concentration in the mixture, the unknown analyte can be quantified. A schematic view of a chromatogram can be seen in Fig. 3.3. The BDP and LF components were in this work analyzed separately.

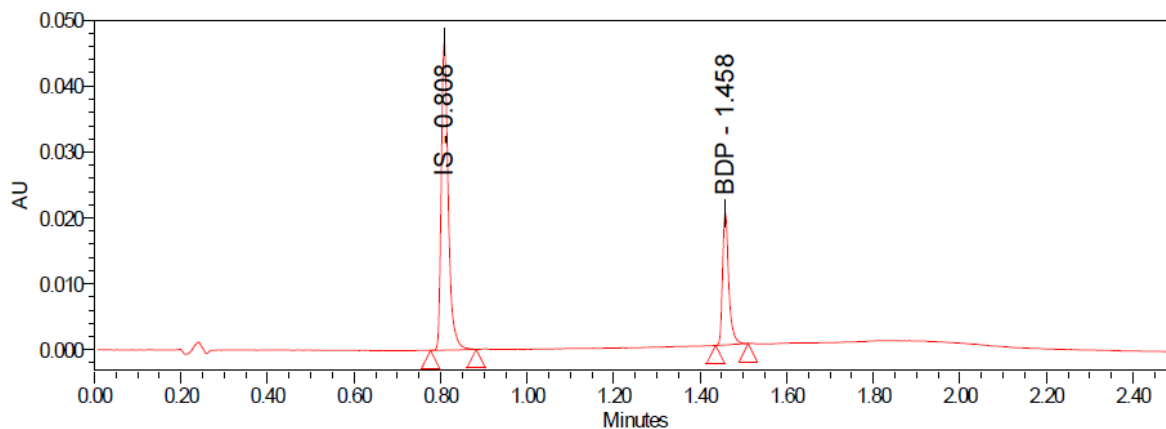


**Figure 3.3: A schematic view of a chromatogram acquired for one of the samples, where the BDP component was analyzed. The first peak resembles the internal standard and the second peak resembles the amount of BDP. The area beneath a peak corresponds to the amount and since the internal standard is known, the amount of BDP in each step can be calculated. This was done for each step of the NGI in order to get the PSD of the API.**

Chemical analysis of BDP was done by using a standard method relying on Liquid Chromatography (LC) coupled with an UV-detector. An internal standard (IS) solution was used for quantification of the BDP for each impactor plate. The IS consisted of 40 mg fluocinolone acetonide (reference substance) per 1000 ml of ethanol, which was used to dissolve the BDP in the different stages of the impactor. An amount of 20 ml was used at each step and when the BDP was dissolved completely, an amount of 0.5 ml from each step was transferred using a plastic pipette into an LC glass vial. Prior to this step the vials were filled with 0.7 ml buffert solution with a pH 3.2, consisting of 3.17 sodium dihydrogen and 0.23 g orthophosphoric acid per 1000 ml of de-ionized water. The vials were then analysed using Ultra Performance Liquid Chromatography (UPLC), giving the amount of BDP in each step of the NGI.

To assess the FPF of the LF component the same technique used for BDP could not be applied since lactose has no chromophores. Analysis of lactose intended for inhalation is overall vaguely described in literature. Some studies have done some attempts of doing so [17] but it has not been a major focus of the overall research. Thus, a part of this thesis was to find and evaluate such method.

The original idea was to try and analyze the LF using a LC-PAD method, which is based on reduction and oxidation potentials. But, due to malfunctioning instrument and long repair-time that idea had to be altered. Instead, an alternative method residing in mass-spectrometry was chosen.

To get the FPF of the lactose component a High-Pressure Liquid Chromatography) – system (HPLC) was used coupled with a MS detector. The principle behind MS is that the sample is vaporized and ionized, then sorted and counted through an electrical field, giving the amount of the analyte in the sample. Since this technique is not extensively used for this purpose, some method evaluation had to be done before the analysis of lactose in the formulations could start. Samples with known amount of lactose were made in order to find a linear detector region of the MS, as well as a comparison between LC-PAD and MS data which gave adequate correlations. The detection region finally used was set to 1 - 8 µg / ml.

Unlike the determination of BDP, where an internal standard could be used to quantify the amount of BDP in each LC vial, no such method could be applied for analyzing the amount of LF. Instead, an amount of 15 ml purified and de-ionized water was used to dissolve the lactose in each NGI-step (apart from the pre-separator, where a total of 30 ml of water was used). By knowing the exact amount of added water, the amount of lactose in each step could be calculated from the results of the measurement.

However, at first when running these samples the amount of lactose was too high and outside the linear detection region. Adjustments were made by diluting the throat-piece and pre-separator 100 times and impactor plates 1-5 10 times.

Since the mass-spectrometry were both more time consuming when running the HPLC-system (compared to the UPLC-system used for BDP analysis) and had a more limited access, it was decided to only take 1 replicate of the samples from the coated formulations and instead run all mixing times (apart for the 2 minute sample). To confirm that the mass-spectrometry method gave adequate results, the amount of powder loaded into the screenhaler was weighted before each run to see if reasonable amounts could be traced back.

However, for some data-points the results were flawed. For example, the detected amount of lactose was more than what was weighted in. Therefore, new replicates were taken for these time points, which gave results in agreement with the other data.

Once the data from the LC analysis was collected, an in-house developed excel template, based on statistical methods, was used to assess the FPF and MMAD values for the BDP and LF in each sample.

### 3.3 Laser diffraction measurements

The laser diffraction measurements were conducted using a Sympatec Helos instrument with two different setups, which will be described in the following sections.

#### 3.3.1 Sympatec RODOS

The RODOS setup is an automated dispersion unit, displayed in Fig. 3.4, which operates at air pressures ranging from 0.1 bar to 6 bar. It has a strong dispersion mechanism, created by using compressed air to push the sample powder through an injector.

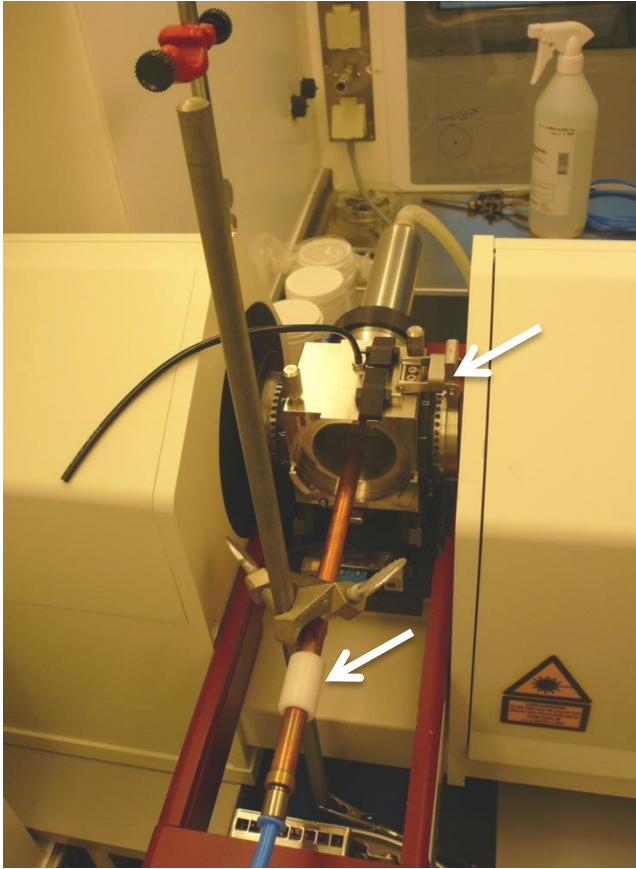
The powder was filled into a small glass vial and inserted into a chamber connected with a vacuum. A pressure of 4 bar was then applied and the powder was dispersed into an aerosol passing through the laser beam. This pressure is considered to fully disperse the sample powder. The feed rate of the glass vial into the chamber was set to 25 mm/s. 5 replicates were taken for every sample. All mixing times were investigated. A background reference measurement was taken prior to each new batch. The system was rinsed with lactose carriers between each batch in order to remove fine particles getting caught to the inner walls of the setup.



Figure 3.4: A schematic view of the RODOS setup [18]

#### 3.3.2 Sympatec Inhaler

The second setup of the LD system was an AstraZeneca in-house developed method, see Fig 3.5. The setup consisted of a metal tube, made from copper with an inner diameter of 8.4 mm, aligned towards the measuring chamber. The sample was put into this tube and flushed out through the laser beam using pressurized air. Two different air flows were investigated; 50 lpm and 100 lpm respectively.



**Figure 3.5: The Inhaler setup. The upper arrow points towards the measurement chamber. The lower arrow points towards the tube in which the powder was put into.**

All mixing times were investigated and 6 replicates were taken for each sample. Between every measurement the tube was flushed three times using pressurized air and for every third sample the tube was rinsed with lactose carriers, in order to remove possible excess particles adhering to the inner walls. A background measurement was taken prior to each new batch.

Whereas the settings applied in the RODOS system is considered to disperse the sample powder fully, the inhaler setup is more alike that of the NGI and the conditions thus more relevant to a patient inhalation. The employed air flow is within the same range as the NGI and the dispersion tube resembles the screenhaler-device used in the NGI

## 4. Results

In this chapter the results from all of the experimental work and measurements will be presented. They will be presented in the order of method they were acquired with, divided into formulations coated with MgSt followed by standard formulations. When present, the error bars in the graphs represent standard deviation amongst replicates. The raw data from the measurements are presented in Appendix I.

### 4.1 NGI

In the following section the data from the NGI measurements will be presented. As the different components (BDP and lactose) were analyzed separately they will be presented as such. Note that for all batches the total amount of added finer particles is always 8%. For example, 2% BDP in Fig. 4.1 refers to an analysis of the BDP component in a batch containing 2% BDP and 6% LF. Likewise, 2% LF in Fig. 4.7, refers to analysis of the lactose component in a batch containing 2% LF and 6% BDP.

Data are presented in terms of FPF and MMAD as a function of mixing time. An in-house developed excel template was used to determine these values by inserting the aerodynamic PSD data from the impactor measurements.

#### 4.1.1. Formulations with MgSt

*Results from BDP-measurements:*

Figs 4.1-4.4 show how the FPF of the BDP component for the coated formulations is influenced by the manufacturing process, in terms of different mixing times. The data shows an increase of FPF as mixing time increases, until it at a certain point reaches a maximum. Subsequently, the FPF declines as the mixing time increases further. This is consistent for all batches and the maximum of the FPF is obtained for the 30 minute sample of the mixing process.

The ratio between BDP and LF influences the value of the maximum FPF; the highest FPF is for the batch with the lowest amount of BDP. As can be seen in Fig. 4.5 the maximum FPF is steadily declining the more BDP that the formulation contains. Furthermore, the larger amount of BDP, the less is the difference between maxima and minima points, resulting in a more flat curvature.



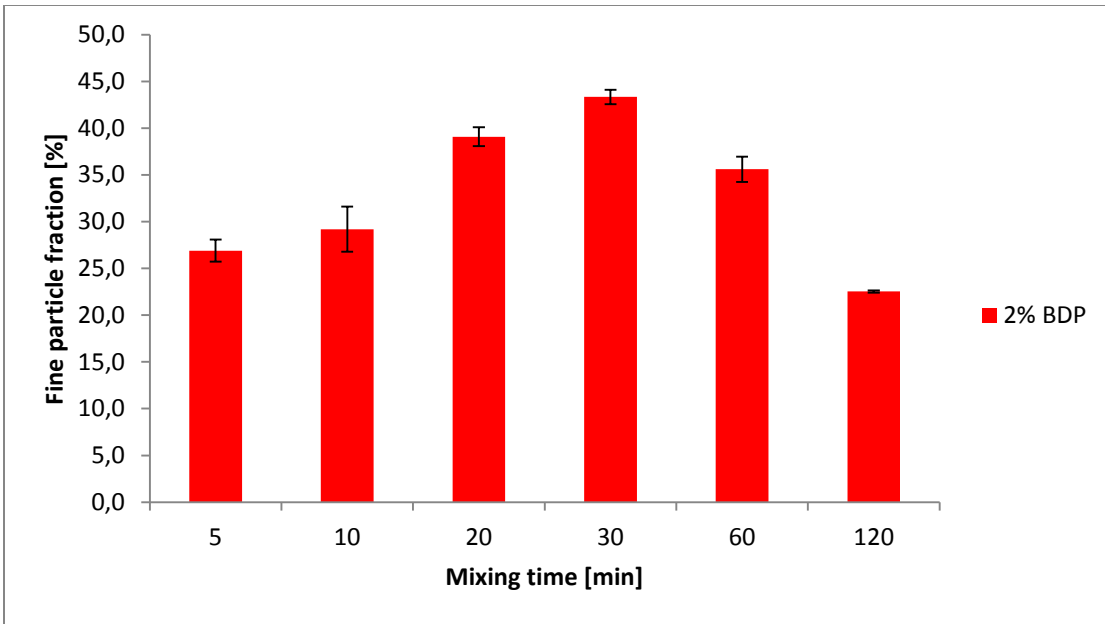


Figure 4.1: Fine Particle Fraction of BDP obtained from impactor analysis of formulation containing 2% BDP and 6% LF, as a function of mixing time. The values represent mean values of 2 replicates and the error bars shows the standard deviation.

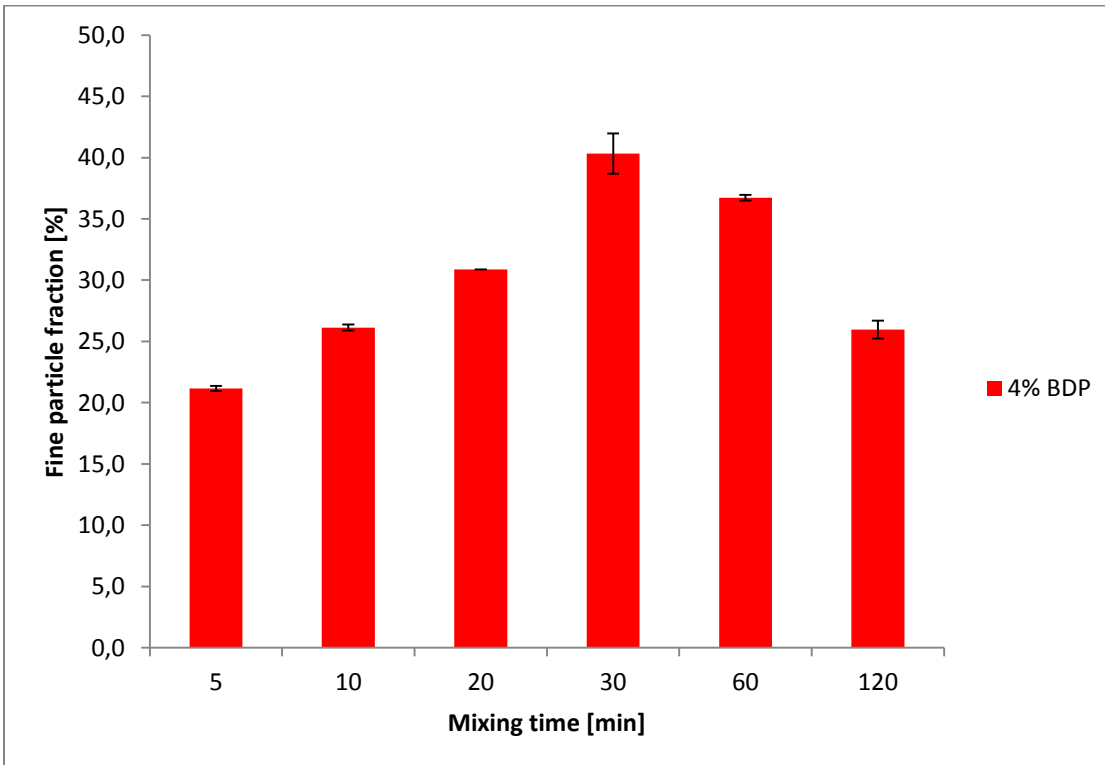


Figure 4.2: Fine Particle Fraction of BDP obtained from impactor analysis of formulation containing 4% BDP and 4% LF, as a function of mixing time. The values represent mean values of 2 replicates and the error bars shows the standard deviation.

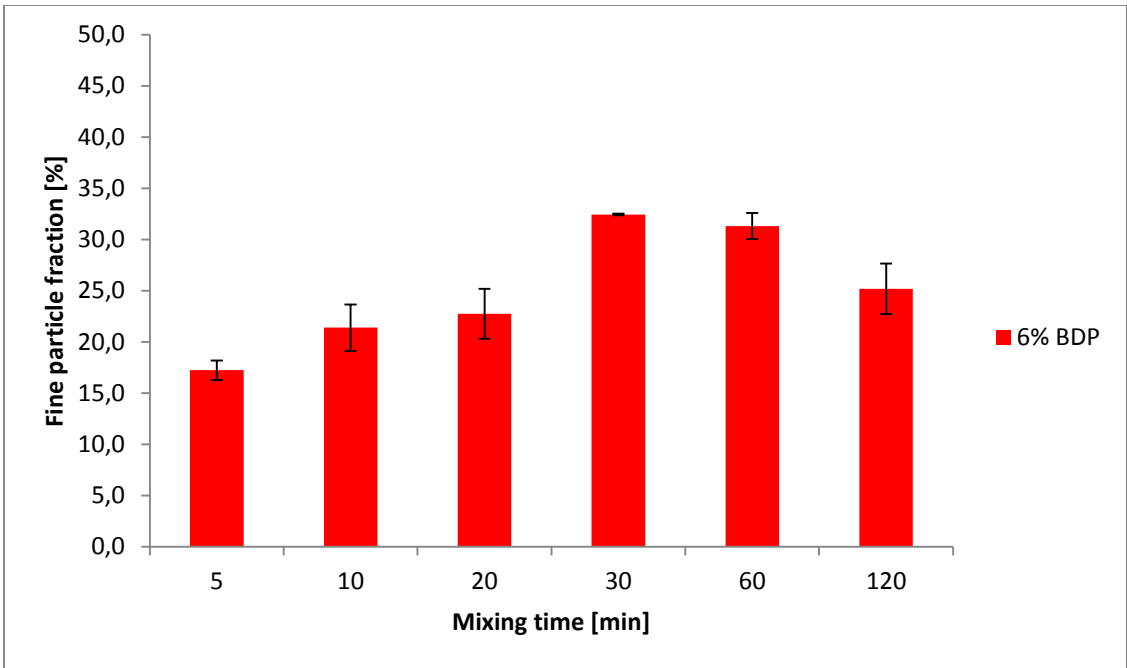


Figure 4.3: Fine Particle Fraction of BDP obtained from impactor analysis of formulation containing 6% BDP and 2% LF, as a function of mixing time. The values represent mean values of 2 replicates and the error bars shows the standard deviation.

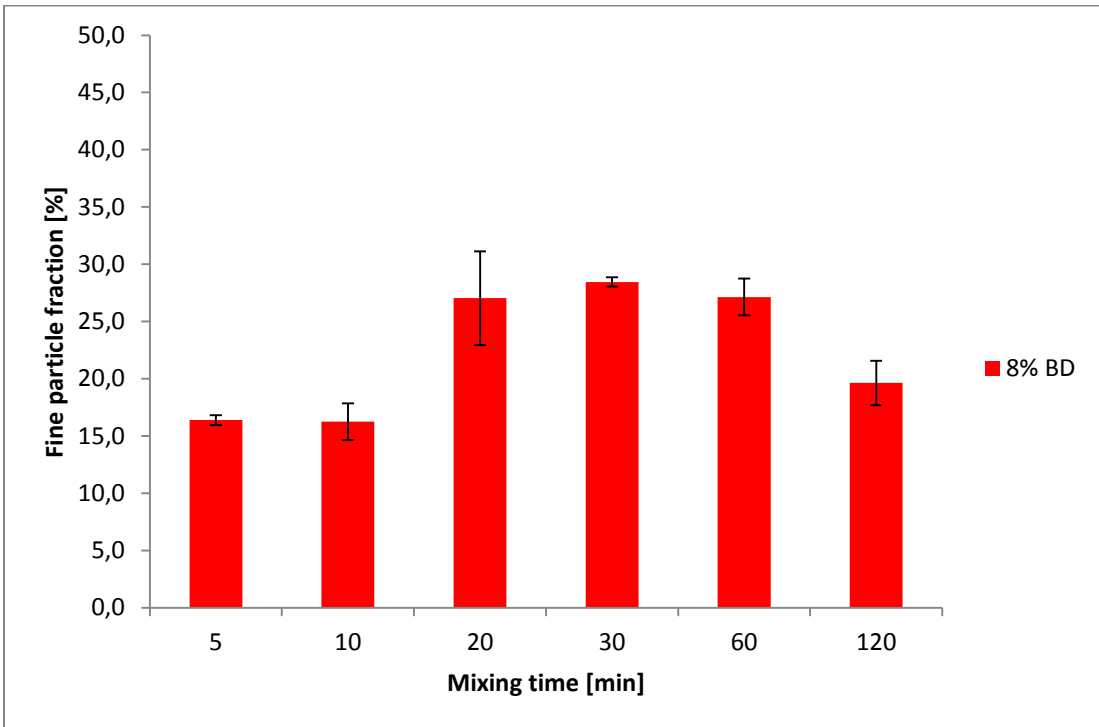


Figure 4.4: Fine Particle Fraction of BDP obtained from impactor analysis of formulation containing 8% BDP and 0% LF, as a function of mixing time. The values represent mean values of 2 replicates and the error bars shows the standard deviation.

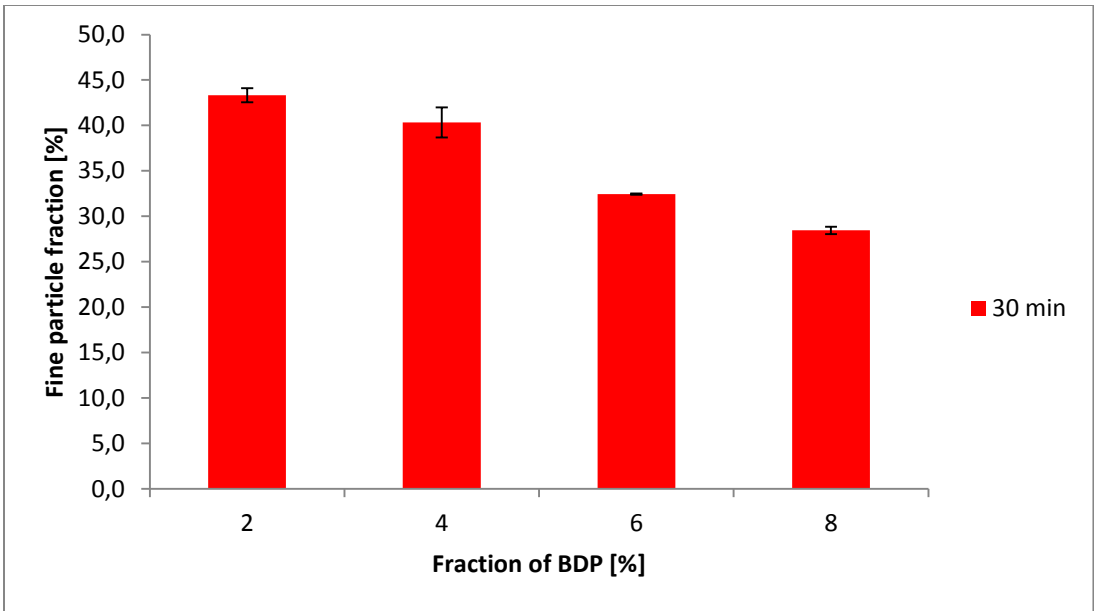


Figure 4.5: Fine Particle Fraction of the BDP component obtained from impactor analysis of the 30 minute samples, as a function of concentration of BPD. The values represent mean values of 2 replicates and the error bars shows the standard deviation.

In Fig. 4.6 the MMAD of BDP is plotted as a function of mixing time. It can be found that the value of MMAD is the lowest where the FPF is the highest.

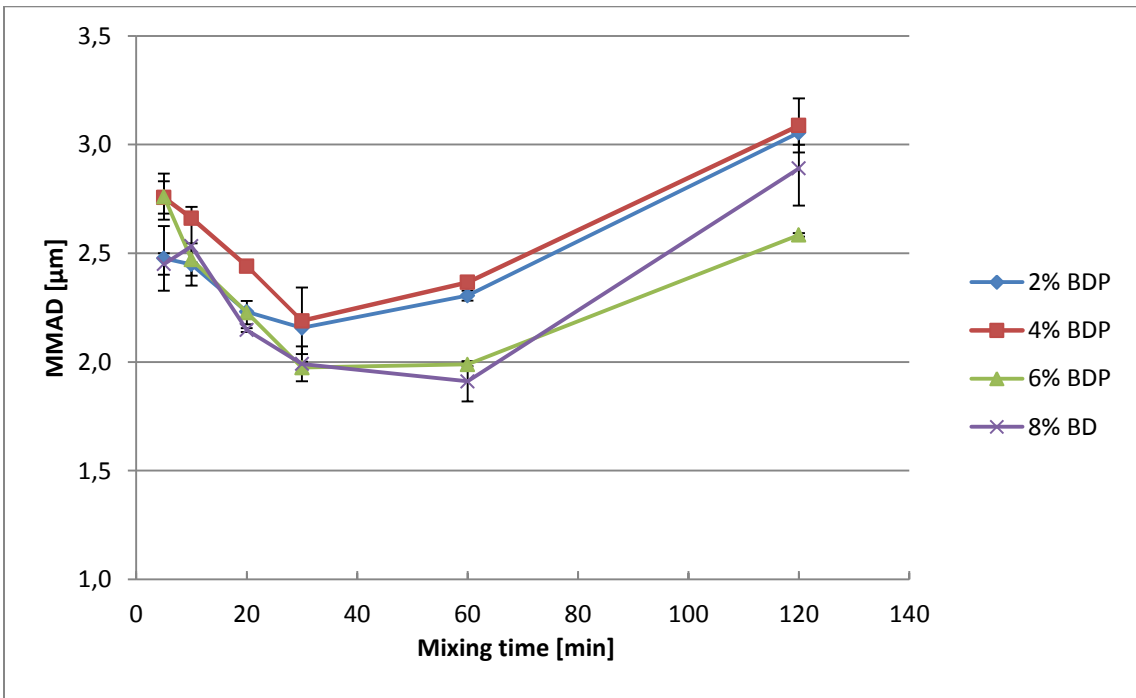


Figure 4.6: Mass Median Aerodynamic Diameter of BDP as a function of mixing time. The values represent mean values of 2 replicates and the error bars shows the standard deviation.

*Results from lactose measurements:*

Figs 4.7 - 4.10 show how the FPF of the lactose varies for different mixing times. Note that since the lactose includes the carriers as well, the FPF results are much lower than that of BDP. The maximum value of the Y-axis is the total amount of added LF.

Compared to the curvature of BDP, the LF curves are much flatter and it is not as easy to distinguish a maximum value in FPF. However, for the batch containing 8% LF there seems to be a decrease of FPF as mixing time increases, except for the 120 minute point, which show an increase.

No error bars are presented as only one replicate was taken, as stated in section 3.2.

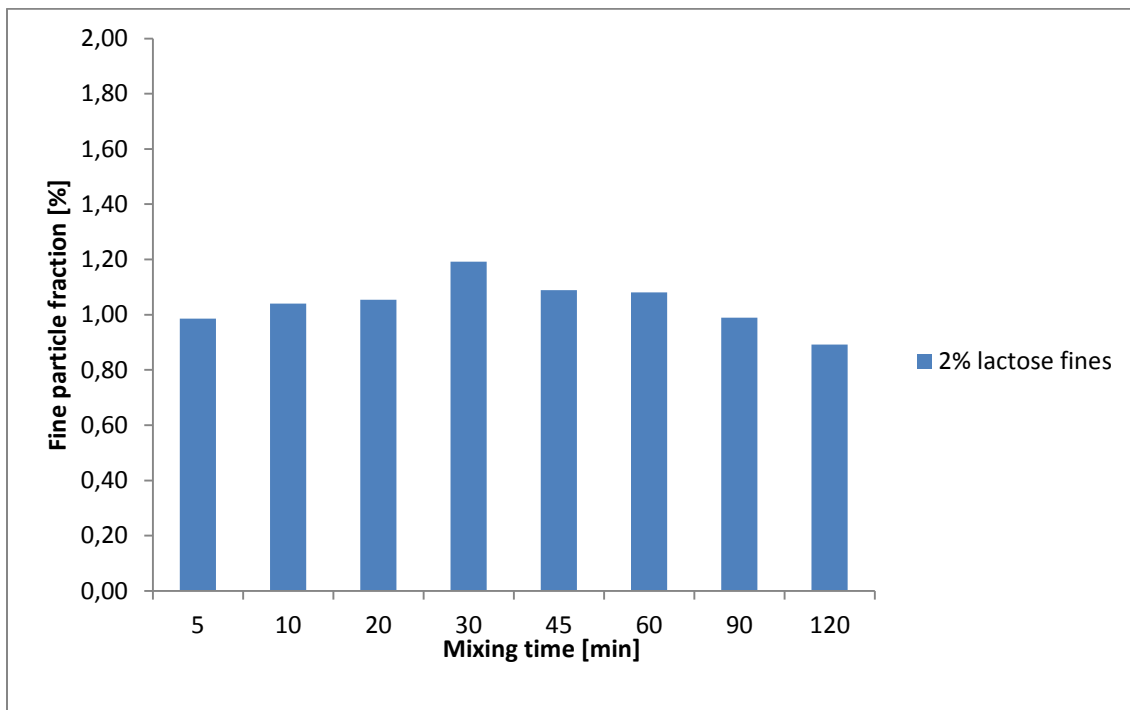


**Figure 4.7: Fine Particle Fraction of lactose obtained from impactor analysis of formulation containing 2% LF and 6% BDP, as a function of mixing time.**

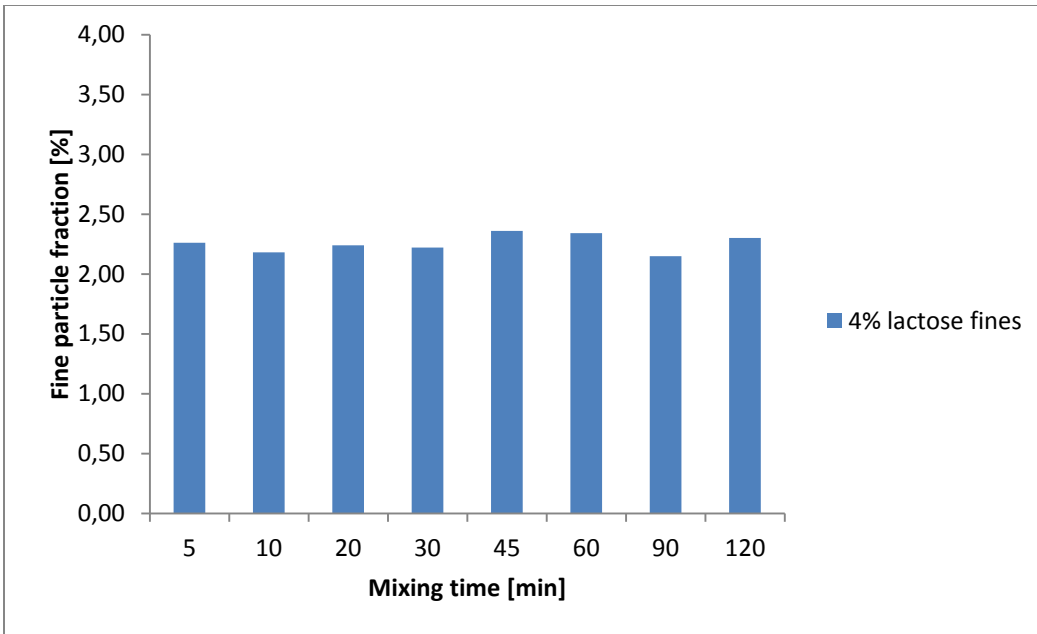


Figure 4.8: Fine Particle Fraction of lactose obtained from impactor analysis of formulation containing 4% LF and 4% BDP, as a function of mixing time.

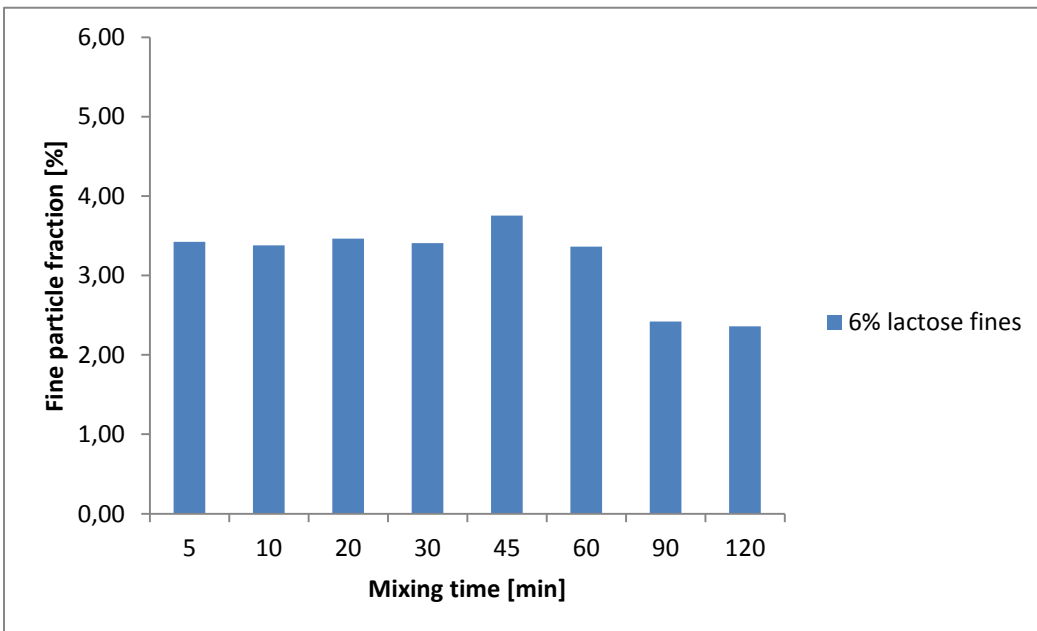


Figure 4.9: Fine Particle Fraction of lactose obtained from impactor analysis of formulation containing 6% LF and 2% BDP, as a function of mixing time.

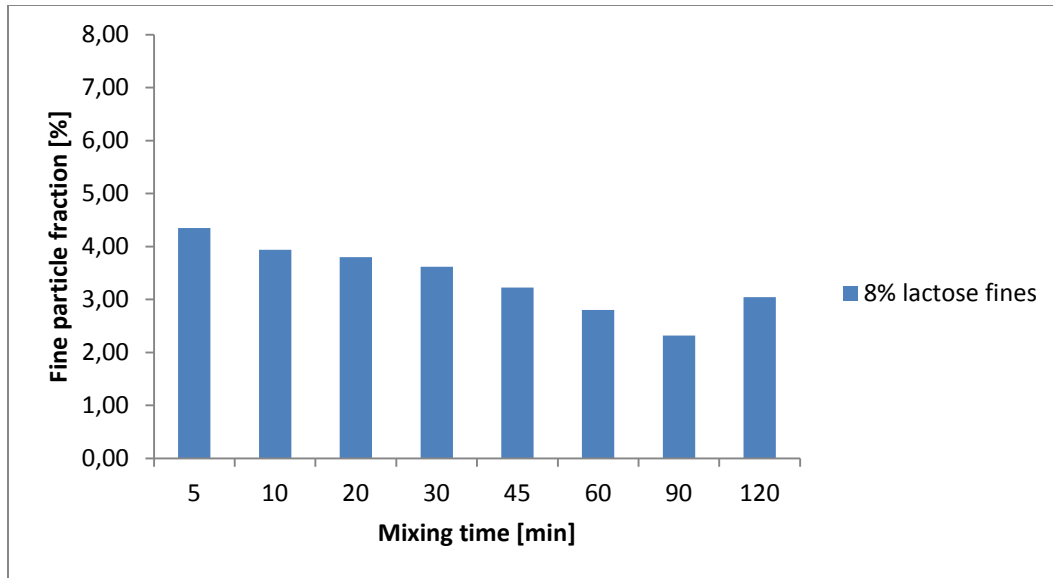


Figure 4.10: Fine Particle Fraction of lactose obtained from impactor analysis of formulation containing 8% LF and 0% BDP, as a function of mixing time.

In Fig. 4.11 the MMAD of the fine lactose component is plotted against mixing time. It is consistently higher than that of BDP. Note that the MMAD evaluation is more difficult for LF, since the carrier particles influences the MMAD evaluation within the excel template. This result in some samples having values above the validated range of MMAD determination.

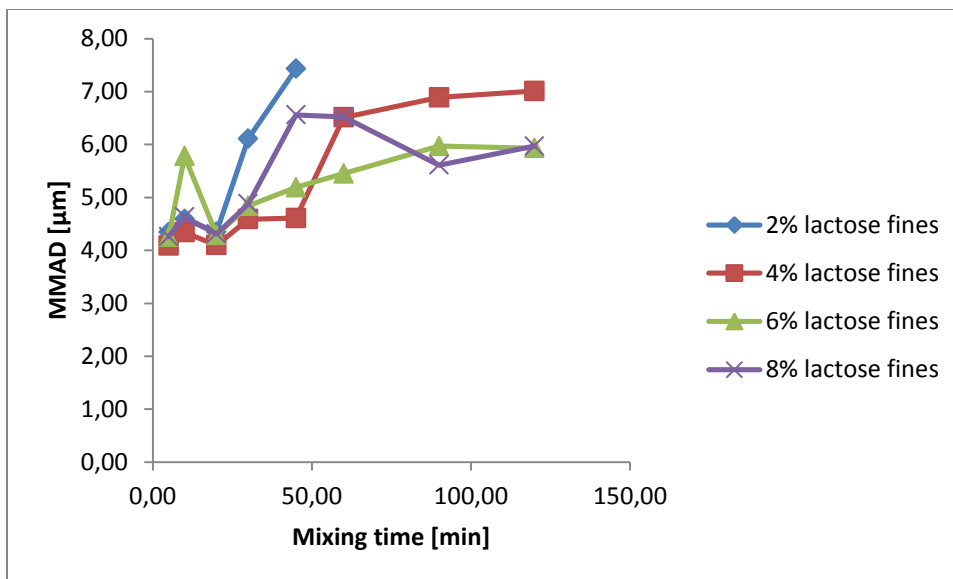


Figure 4.11: Mass Median Aerodynamic Diameter as a function of mixing time for lactose. The values following the 45 minute sample of the batch containing 2% LF are omitted, due to high values above the validated range for MMAD determination.

### 4.1.2 Standard formulations

In this section the results from the second series of mixing, referred to as standard formulations, will be presented. A narrowed amount of batches were manufactured, leaving out the relationships of 2 + 6 and 6 + 2 between the LF and BDP.

*Results from BDP-measurements:*

Overall, the values of FPF are much lower for these formulations compared to the coated batches. Furthermore, the mixing time seem to have less influence on the FPF as well, as the difference in maxima and minima points is much lower than before. However, the batch with 4% BDP and 4% LF has a higher FPF than the batch with 8% BDP and 0% LF. It is hard to determine any clear maximum point for both batches, but the batch with 8% BDP seems to have the maximum shifted towards higher mixing times. Though, that might be due to errors that lie within the measurement technique.

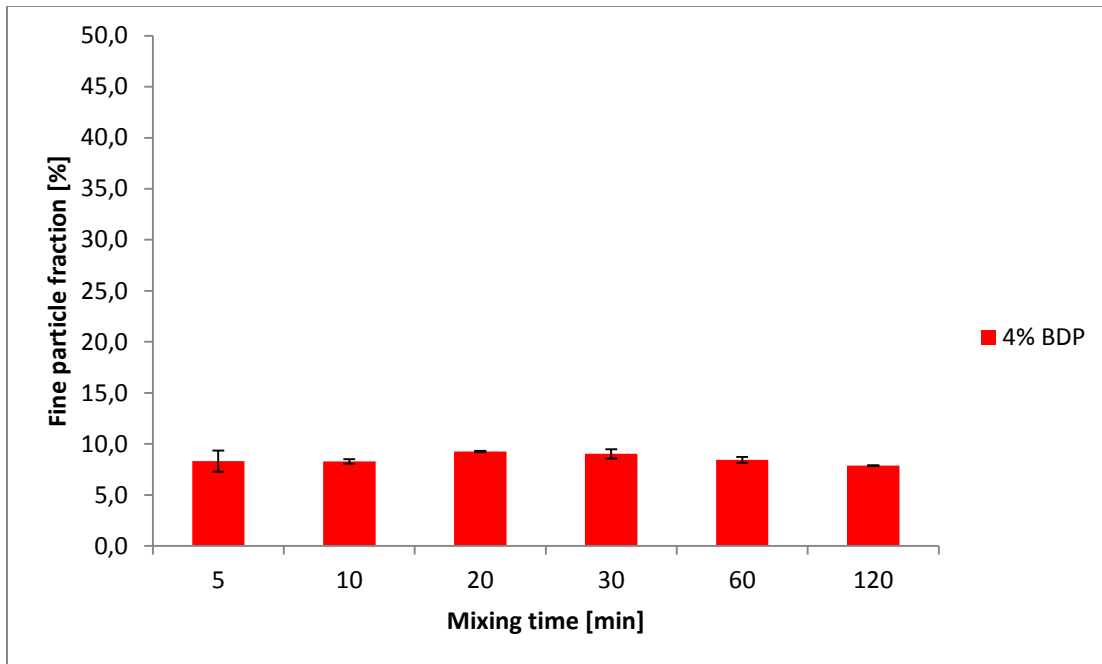


Figure 4.12: Fine Particle Fraction of BDP obtained from impactor analysis of formulation containing 4% BDP and 4% LF, as a function of mixing time. The values represent mean values of 2 replicates and the error bars shows the standard deviation.

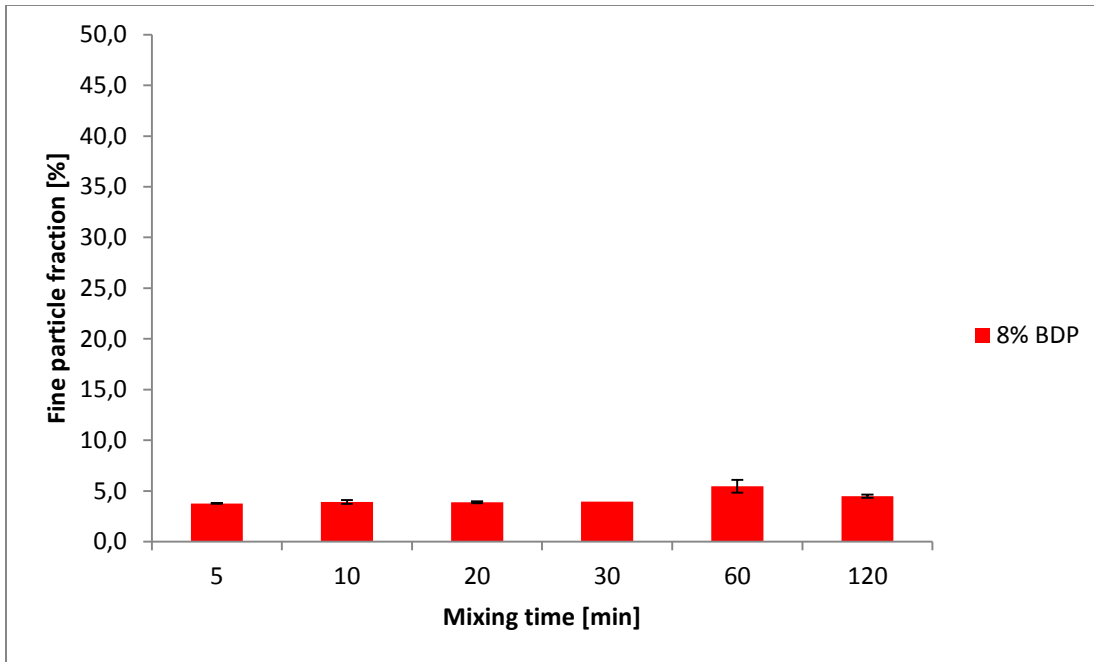


Figure 4.13: Fine Particle Fraction of BDP obtained from impactor analysis of formulation containing 8% BDP and 0% LF, as a function of mixing time. The values represent mean values of 2 replicates and the error bars shows the standard deviation.

Regarding the MMAD values, shown in Fig. 4.14, the 8% BDP seems to have a minimum at 60 min, which would correlate to a maximum of FPF at the same time point. The 4% BDP is showing a steady increase of MMAD over time. Both batches have a consistently higher MMAD compared to the coated formulations, for all mixing times.

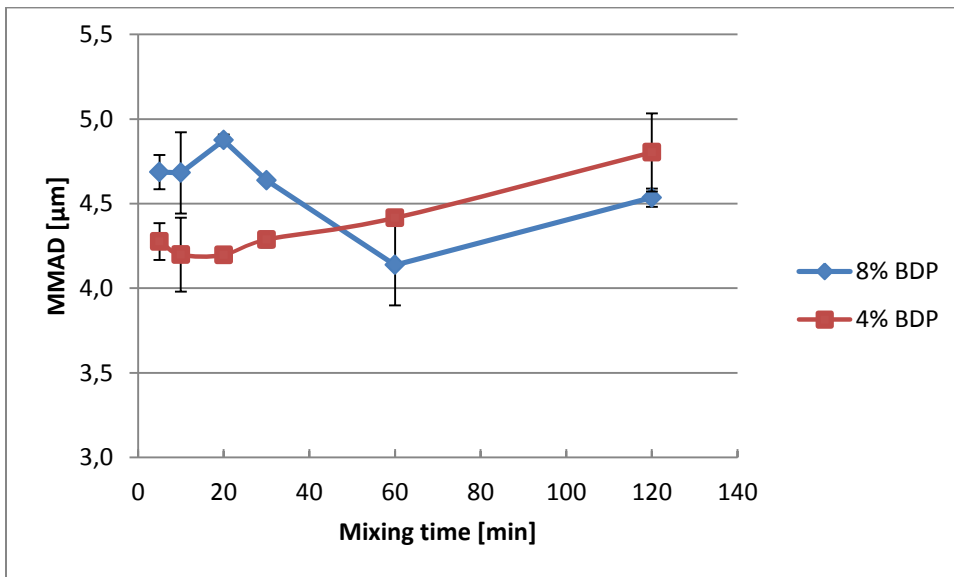
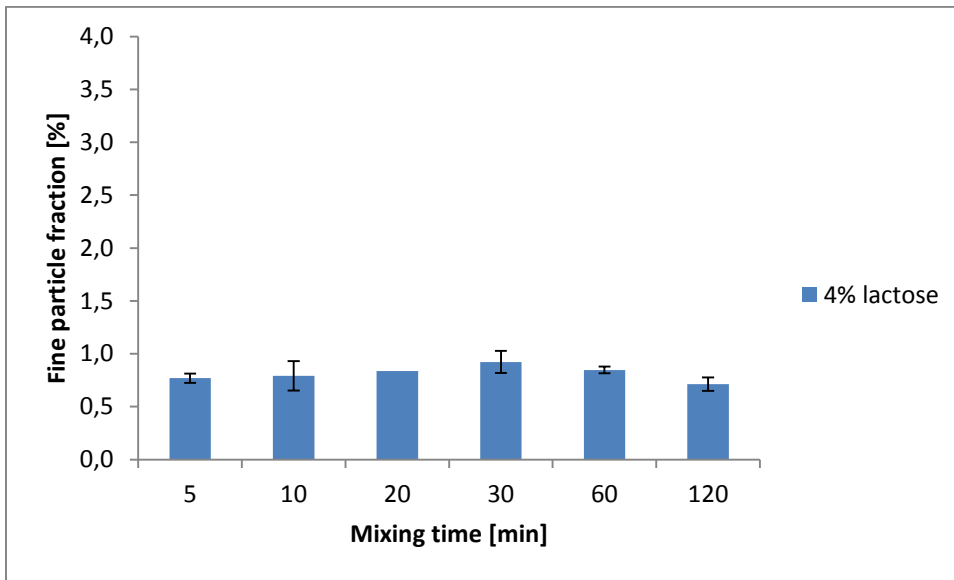


Figure 4.14: Mass Median Aerodynamic Diameter of BDP as a function of mixing time. The values represent mean values of 2 replicates and the error bars shows the standard deviation.



*Results from lactose measurements:*

As well as for the BDP, the FPF of lactose are lower for the uncoated formulations, see Figs 4.15-4.16. For the batch containing 4% LF and 4% BDP, the flat curvature however remains, as is the case of the decreasing curve for 8% LF. The 120 minute sample of 8% LF was unfortunately damaged during the manufacturing process, making a comparison between the coated and the standard formulations more troublesome.



**Figure 4.15: Fine Particle Fraction of lactose as a function of mixing time for batch containing 4% LF and 4% BDP. Note that the 20 min bar represents only one sample, due to the other replicate having an unrealistic value of over 5 % which is more than 100% of the added LF. Therefore, that point was omitted from the figure. The values represent mean values of 2 replicates and the error bars shows the standard deviation.**

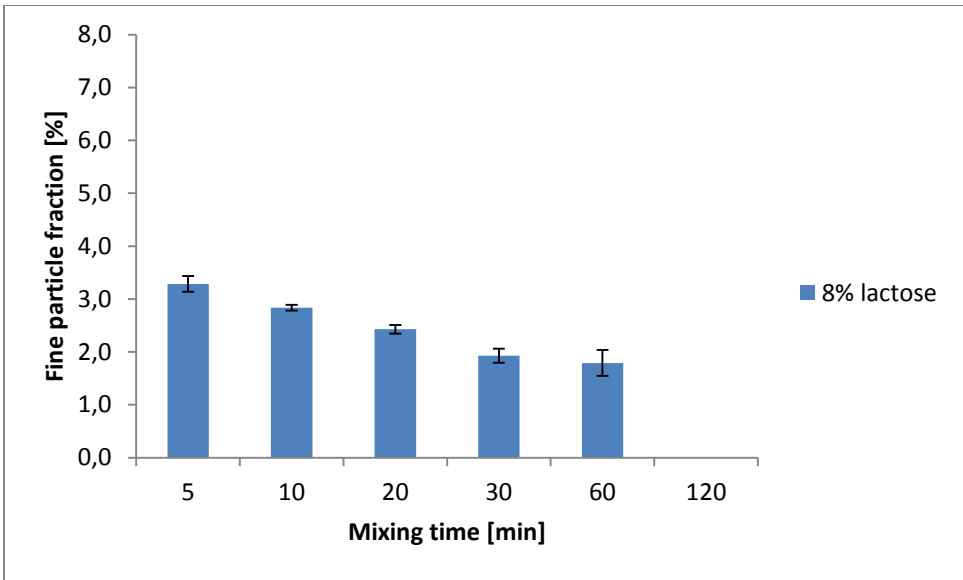


Figure 4.16: Fine Particle Fraction of lactose obtained from impactor analysis of formulation containing 8% LF and 0% BDP, as a function of mixing time. The values represent mean values of 2 replicates and the error bars shows the standard deviation.

The lactose MMAD values, which can be seen in Fig. 4.17, approaches the limit where the evaluations are no longer valid. The graph should only be interpreted as the MMAD for LF is larger for the standard formulations than for the coated formulations as well as not being influenced much by the mixing process.

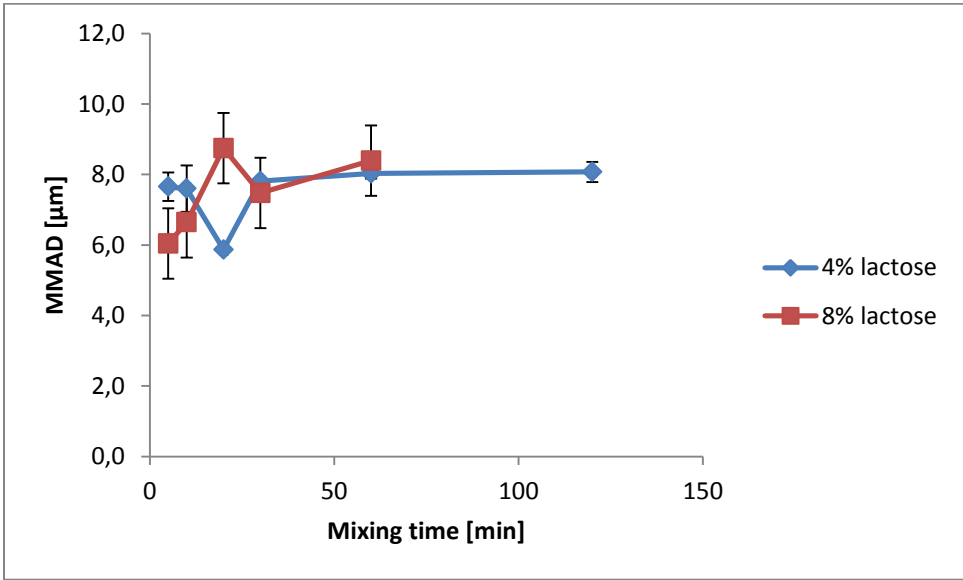


Figure 4.17: Mass Median Aerodynamic Diameter as a function of mixing time for lactose. The values represent mean values of 2 replicates and the error bars shows the standard deviation.

## 4.2 Laser diffraction

In the following section the results from the different laser diffraction setups will be presented. As two different set ups were used they will be presented separately, starting with the RODOS setup followed by the Inhaler setup. The results will be presented as  $F_5$  and FPmode. Since laser diffraction cannot distinguish between different materials, the results will be including both the lactose and BDP components combined.

### 4.2.1. Sympatec RODOS

The Sympatec RODOS setup can in this work be considered as a maximum dispersion reference for the formulations, as the dispersion pressure is significantly higher compared to both the NGI and Sympatec Inhaler setup.

#### *Coated formulations*

In Fig. 4.18,  $F_5$  is presented for all batches. As was the case for the NGI, a maximum point can be seen for almost all formulations, with the 8% LF batch as an exception. However, the maxima occur much earlier into the mixing process, as well as the decrease in  $F_5$  is greater than for the FPF of the NGI curves. The batch containing the highest amount of BDP (8% BDP and 0% LF) shows the highest value of  $F_5$  and as the amount of BDP decreases, so does the fraction  $<5 \mu\text{m}$ .

Regarding the 8% LF batch, no maxima point is seen and  $F_5$  decreases as the mixing time increases. However, surprisingly for all batches is that into 120 minutes of the mixing process they all seem to gather at the same point, giving approximately the same value. If this is due to some physical principle or simply just a coincidence can only be speculated based on these data.

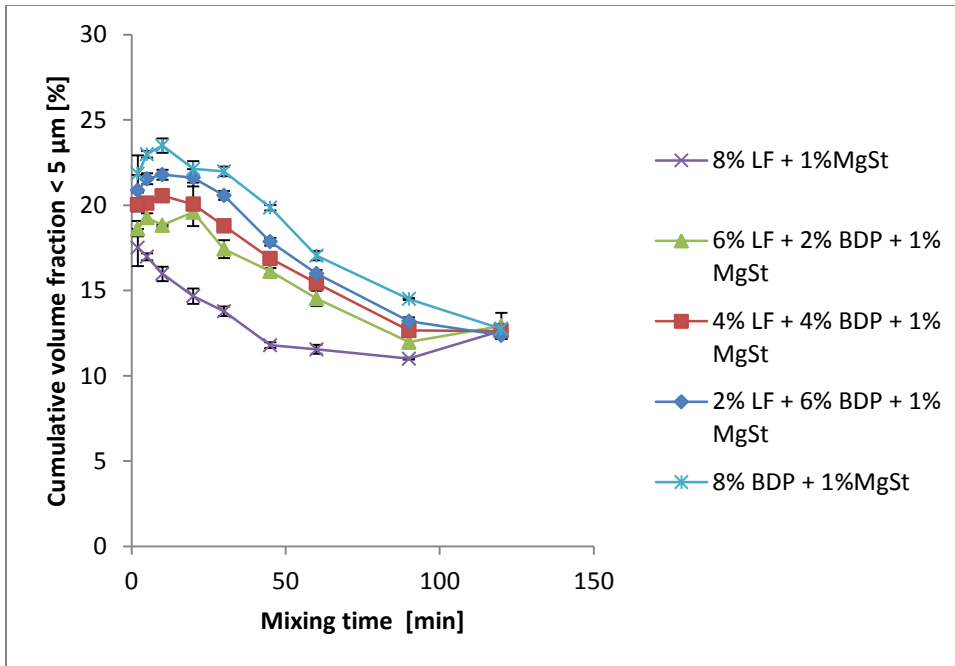


Figure 4.18: Cumulative volume fraction < 5  $\mu\text{m}$  for formulations coated with MgSt, assessed with Sympatec RODOS at 4 bar dispersing pressure. The values represent mean values of 5 replicates and the error bars shows the standard deviation.

Regarding the FPmode, see Fig.4.19, there are some things to be noticed. Batches with the highest amount of BDP (8% and 6% respectively) and the 8% LF batch, are both rather flat and aren't influenced much by the mixing process.

However, the 2%BDP / 6% LF batch has a similar curvature as the same batch measured with the NGI, with a minima point slightly shifted towards an earlier mixing time.

The curvature for 4% BDP / 4% LF are at the beginning flat, with an increase at 60 minutes into the mixing process.

It can be noted that the values on the Y-axis are higher than that of the added total amount of fines. This is due to the fact that the mathematical calculations and simplifications leads to an overestimation of finer particles within the formulations, as stated in section 1.2.

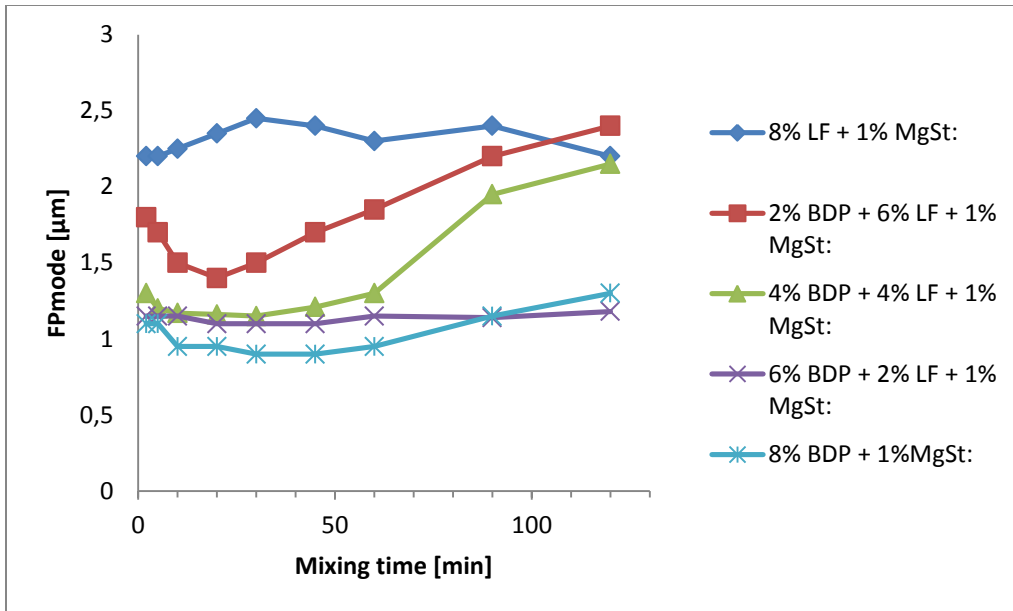


Figure 4.19: Fine Particle mode for formulations coated with MgSt, assessed with the Sympatec RODOS at 4 bar dispersing pressure. The values represent mean values of 5 replicates.

#### Standard formulations

In Fig. 4.20 the  $F_5$  for standard formulations measured in RODOS at 4 bar is presented. However, these data are likely to be faulty, as it was discovered that the measurement times exceeded the normal measurement times greatly (10s instead of 0.5s). This was seen as a build-up effect, where the first replicate showed normal measuring times but as the measurements progressed, the measurement time increased. This might be due to finer particles adhering to the inner walls of the setup, which after sub-sequent measurements starts to liberate and thus disturbs the measurement. It was seen that the measurement time decreased to normal values after rinsing the system. This was clearly seen after the 20 minute sample of the 8% LF formulation. After this point the measurement time went up and cannot be considered trustworthy.

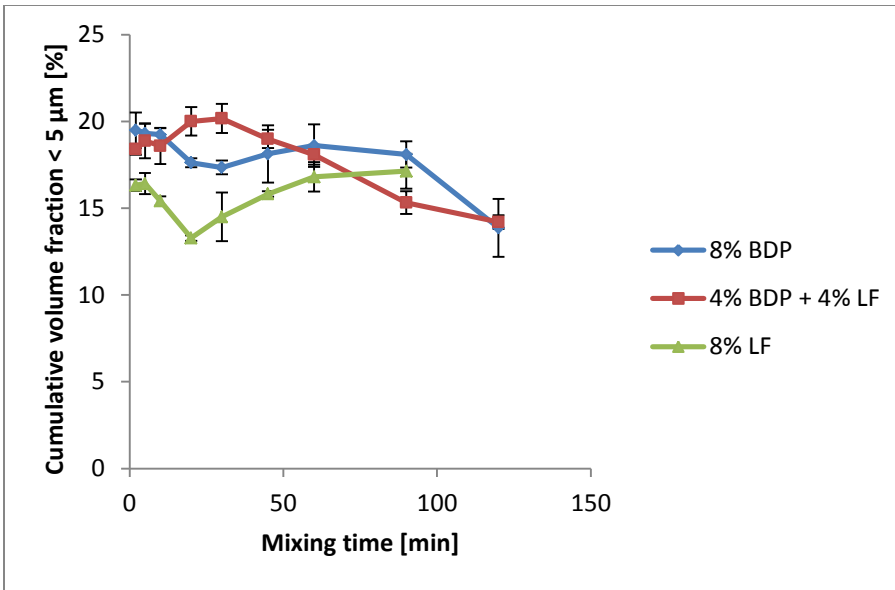


Figure 4.20: Cumulative volume fraction < 5 μm for standard formulations, assessed with Sympatec RODOS at 4 bar dispersing pressure. The values represent mean values of 5 replicates and the error bars shows the standard deviation.

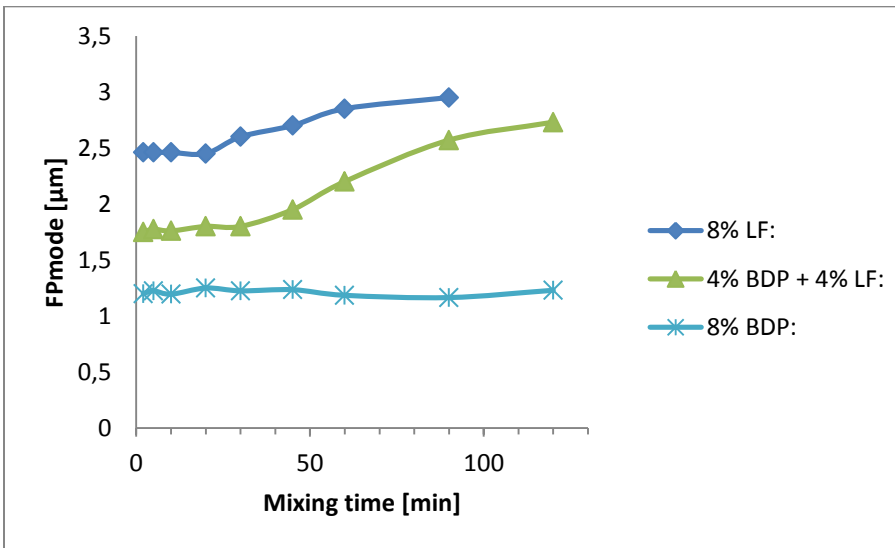


Figure 4.21: Fine Particle mode for standard formulations, assessed with the Sympatec RODOS at 4 bar dispersing pressure. The values represent mean values of 5 replicates.

### 4.2.2. Sympatec Inhaler

The Sympatec Inhaler instrument is a more patient relevant set up than RODOS, as the air flow are more alike the ones in a general DPI.

#### Coated formulations

In Fig. 4.22 and 4.23 the  $F_5$  is presented for 50 lpm and 100 lpm, respectively. The standard deviations are rather large for all batches, but common for both graphs is the behavior of respective formulation. For all batches except 8% LF, they follow, more or less, the same curvature as for the NGI results with a maxima point in the mixing process. The 8% LF batch seems to show a decline in  $F_5$  as mixing time increases.

Fig. 4.22 shows a lower  $F_5$  for all batches, as is expected when a lower dispersion flow is used.

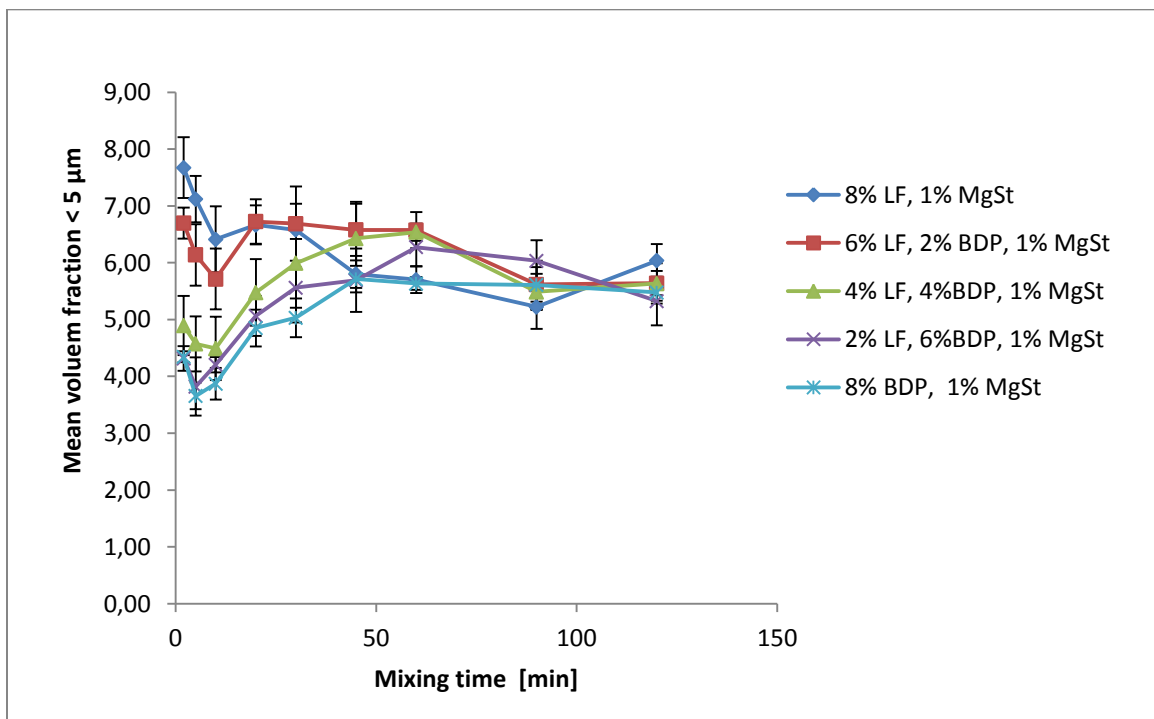


Figure 4.22: Cumulative volume fraction < 5  $\mu\text{m}$  for formulations coated with MgSt, assessed using Sympatec Inhaler at 50 lpm. The values represent mean values of 6 replicates and the error bars shows the standard deviation.

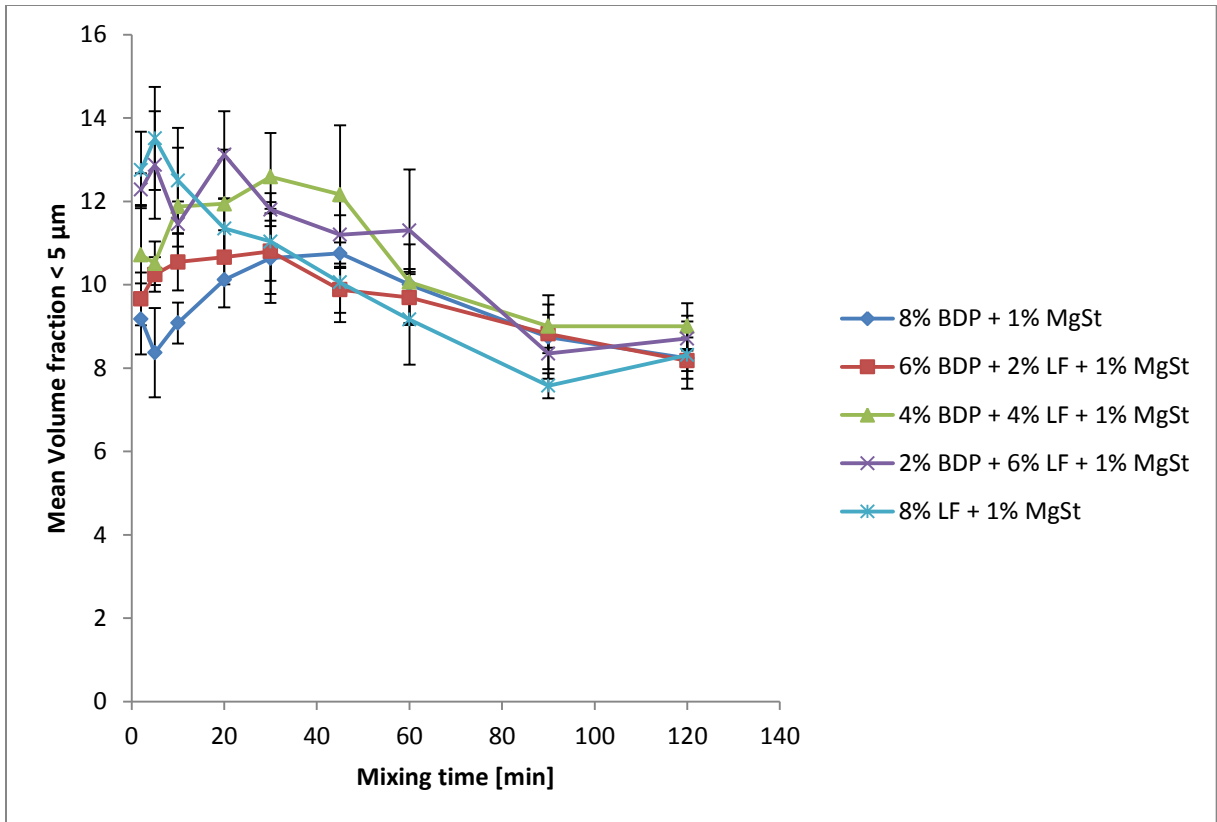


Figure 4.23: Cumulative volume fraction < 5 μm for formulations coated with MgSt assessed using Sympatec Inhaler at 100 lpm. The values represent mean values of 6 replicates and the error bars shows the standard deviation.

Considering the FPmode, Fig. 4.24 presents the result from the measurements done with a flow of 50 lpm. All batches, except 8% BDP, shows a sudden increase of particle size in the beginning of the mixing process, but as the mixing time increases they all flattens out at approximately the same value. The behavior of the 8% BDP batch is more or less the same, but with a not as sudden increase in the beginning.

By increasing the air flow to 100 lpm, the particle size of the FPmode decreases as can be seen in Fig. 4.25. The end points of the relative concentrations (8% BDP + 0% LF and 0% BDP + 8% LF) shows a rather flat curvature, while the other batches have the same look (more or less) as the NGI curves, with a minima point somewhere in the mixing process.



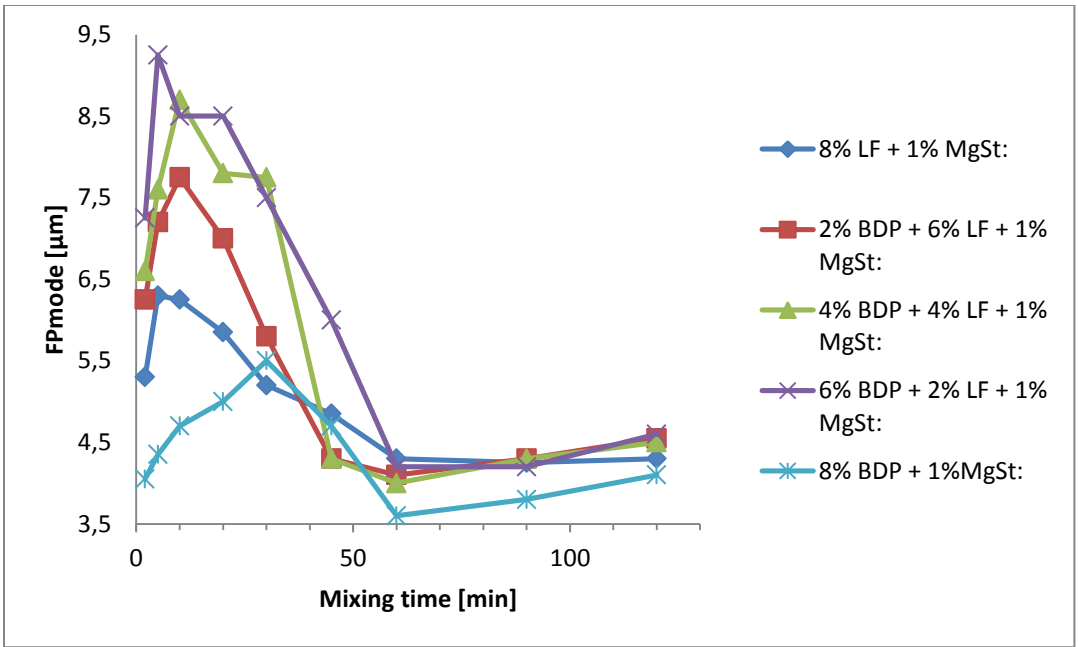


Figure 4.24: Fine Particle mode for formulations coated with MgSt assessed with the Sympatec Inhaler setup at 50 lpm. The values represent mean values of 6 replicates.

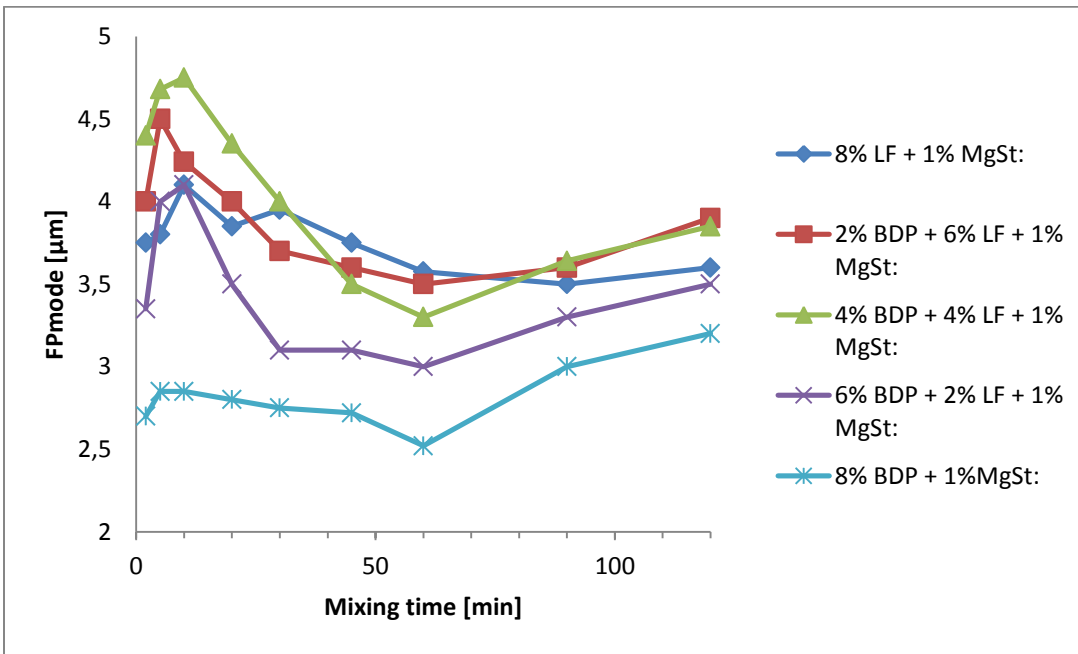


Figure 4.25: Fine Particle mode for formulations coated with MgSt assessed with the Sympatec Inhaler setup at 100 lpm. The values represent mean values of 6 replicates.

Standard formulations

The standard formulations show a rather flat curvature considering the  $F_5$ , as presented in Fig. 4.26 and 4.27. A small decrease in the beginning of the mixing process can be seen for 4% BDP + 4% LF and 8% BDP. The air pressure does not seem to influence the appearances of the curves, apart from giving a higher fraction  $<5 \mu\text{m}$  for the higher air flow.

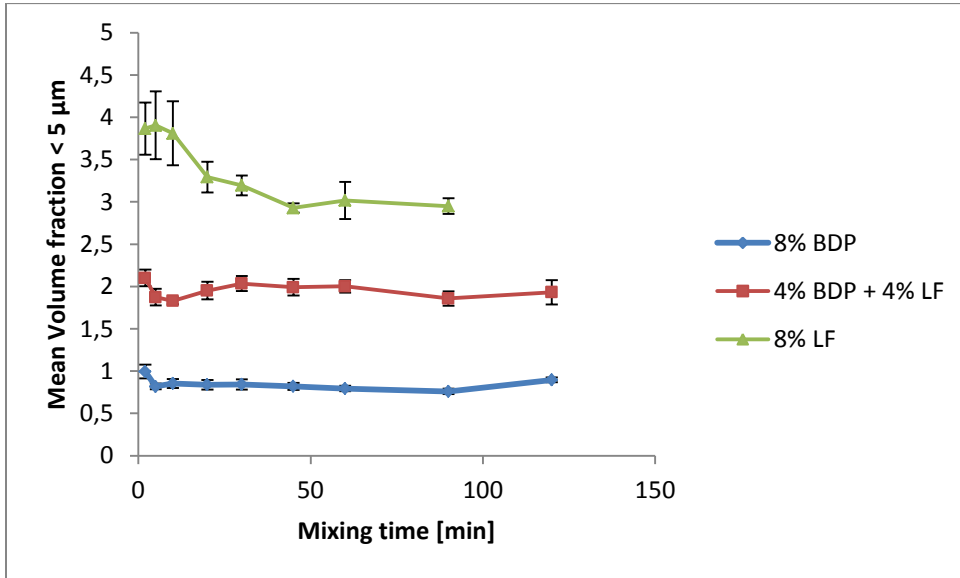


Figure 4.25: Cumulative volume fraction  $< 5 \mu\text{m}$  for standard formulations, assessed with the Sympatec Inhaler setup at 50 lpm. The values represent mean values of 6 replicates and the error bars shows the standard deviation.

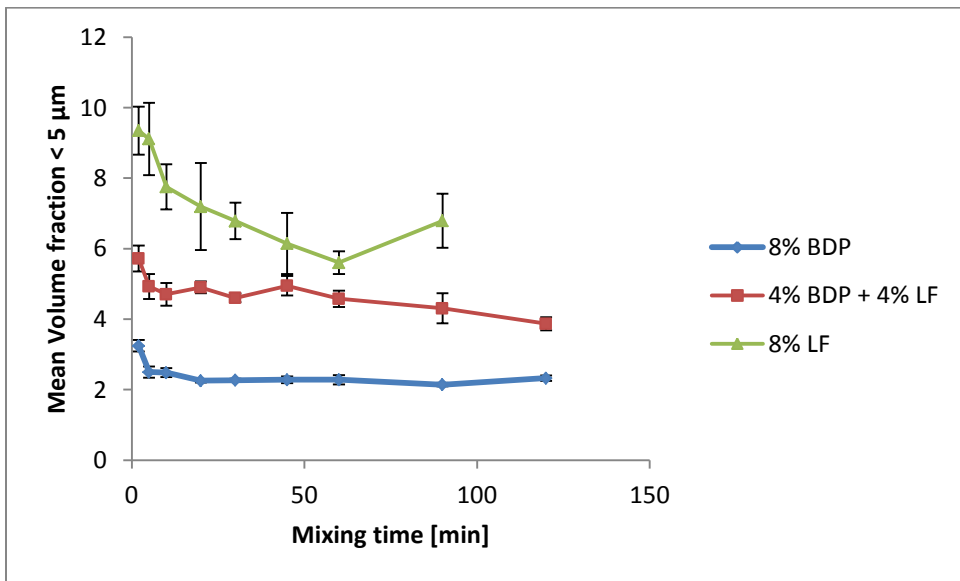


Figure 4.26: Cumulative volume fraction  $< 5 \mu\text{m}$  for standard formulations, assessed with the Sympatec Inhaler setup at 100 lpm. The values represent mean values of 6 replicates and the error bars shows the standard deviation.

As it goes for the FPmode of the standard formulations, these curves are as well rather flat and the particle sizes are larger for the lower air pressure. Note that no data from the 8% BDP could be obtained as no FPmode could be distinguished from the PSD.

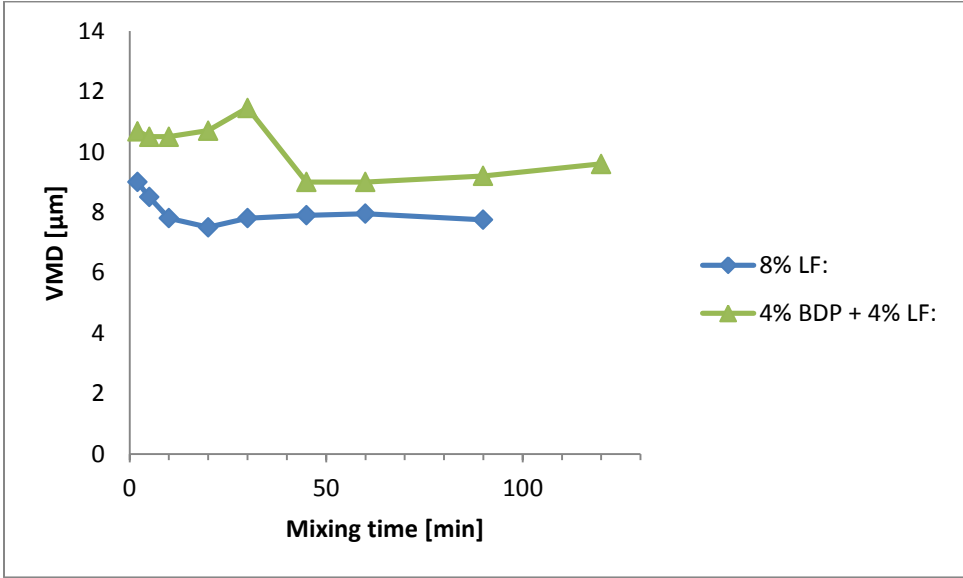


Figure 4.27: Fine Particle mode for standard formulations assessed with the Sympatec Inhaler setup at 50 lpm. The values represent mean values of 6 replicates.

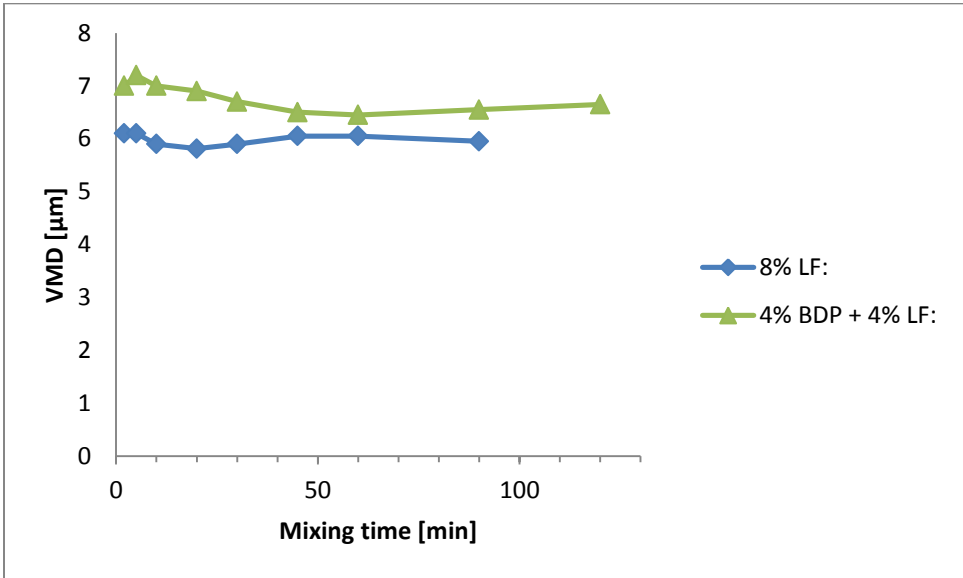


Figure 2.28: Fine Particle mode for standard formulations assessed with the Sympatec Inhaler setup at 50 lpm. The values represent mean values of 6 replicates.

### 4.3 Relaxation effect of formulations.

When analyzing the FPF of the BDP component in the coated formulations a, to some degree, unexpected effect was observed. The initial measurements displayed a maximum FPF of the BDP at 30 minutes of mixing, which was consistent for all formulations. The 45 min samples were thus analyzed to see if there would be a shift in the maximum FPF. Along with these measurements, the 20 and 30 minute samples of coated formulations with 8% BDP were analyzed anew in order to confirm that they would give the same results as previously measurements. However, the FPF was higher than previously, showing that the FPF had increased over time. These results are displayed in Fig. 4.29.

A speculative explanation to this can be that electrostatic forces induced upon mixing equilibrates over time, thus allowing for a less strong attraction between API and carrier which would results in a better dispersion, thus a higher FPF. However, the time limit of this work prohibited further investigation on this matter and therefor these results will not be considered further when discussing the results.

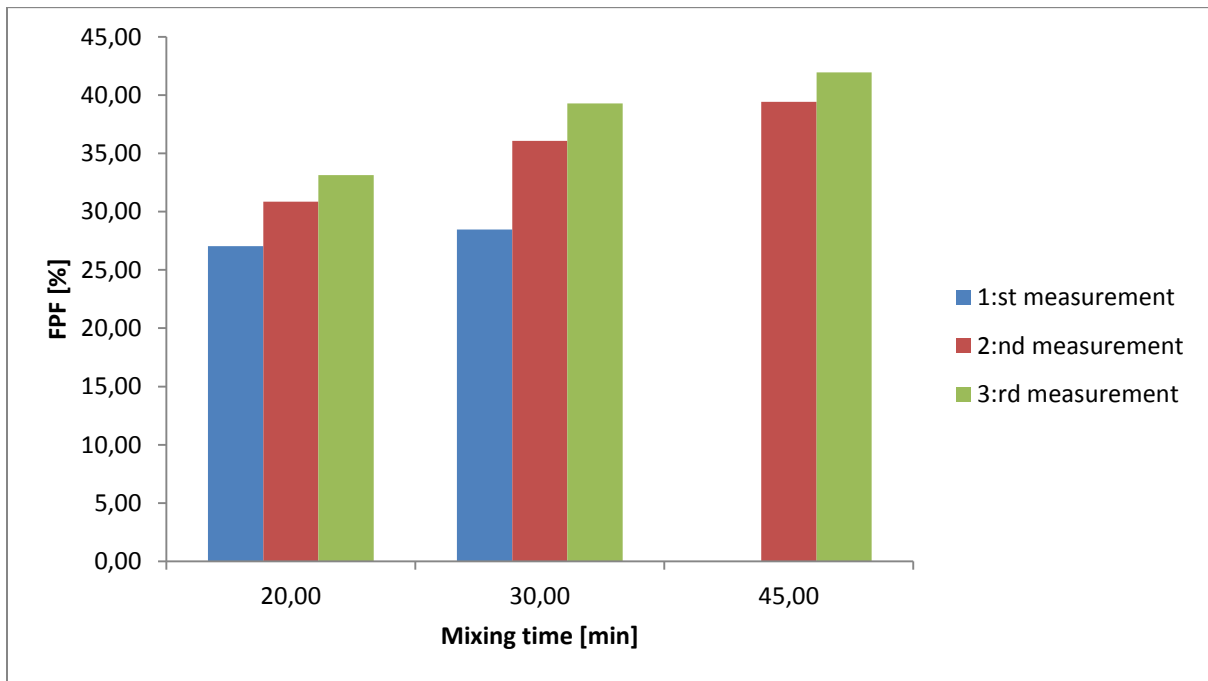


Figure 4.29: Effect of storage time for coated formulation with 8% BDP. The FPF was assessed using the NGI and the measurements were made at different times after manufacturing. The first result is from the measurements presented in 4.1, the second measurements were made approximately 3 weeks after the first measurement and the third measurements was made approximately a month after that. No data from the 45 minute sample were acquired in the first measurement series.

#### 4.4 Effect of intrinsic fines.

When analyzing the lactose components of the formulations, it was unknown how much of an effect the intrinsic fines would have on the final performance. Therefore, lactose NGI analyses were made from the batches where no LF were added, i.e. the 8% BDP formulations. Both the coated and the standard batch were analyzed and two different mixing times (5 and 30 minutes) were chosen. The results are presented in Fig. 4.30.

Regarding the coated formulations, the amount of LF is low for both samples, with a small decrease for the longer mixing time. For the standard formulations, the amount of LF seems to increase as the mixing time increases, indicating that LF are produced during mixing. A sample of pure carrier was also measured and the result lies within the same reach of the 5 minute samples. The difference might be within the error margins as the method of lactose analysis was flawless.

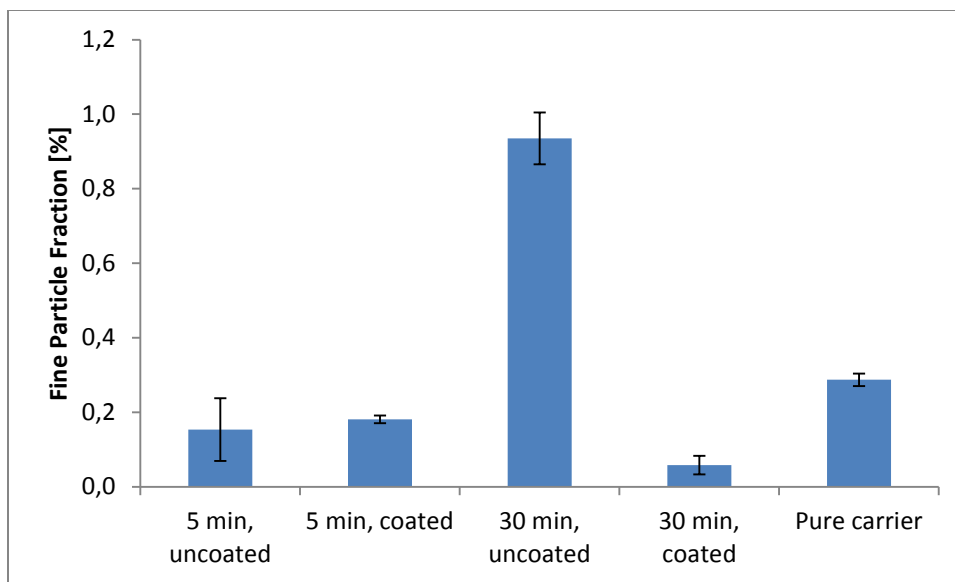


Figure 4.30: A comparison of the intrinsic LF within 8% BDP formulations. The bars represent a mean value of 2 replicates and the error bars shows the standard deviation.

## 4.5 Images from scanning electron microscopy

To further understand the structure and distribution of finer particles in the formulations, morphological images were acquired using scanning electron microscopy (SEM). The batches that were analyzed were the 4% BDP + 4% LF of both the coated and the standard formulations. The results can be seen in Fig. 4.31-4.33. Note that these images are not necessarily representative of the formulations as a whole, but more as a qualitative way of understanding the arrangement of particles.

### *Coated formulations*

Fig. 4.31-4.33 shows the resulting SEM images for the coated formulation from samples of 10, 60 and 120 minutes of mixing. It can be seen that in the earlier mixing stages there are more particles or agglomerates on the carriers and for the 120 min sample there seems to be fewer particles or agglomerates on the carriers. A possible explanation to this is that the particles are either pressed onto the carriers or they might tumble off the carriers in the mixing progress.

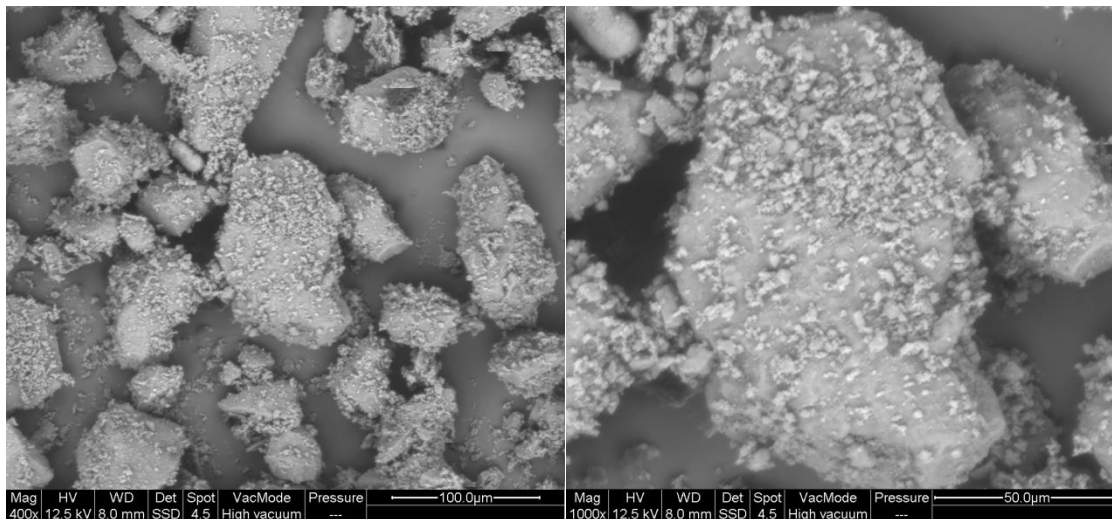


**Figure 4.31: SEM images acquired from the 4% BDP + 4% LF for the coated formulation, taken at 10 minutes of mixing.**

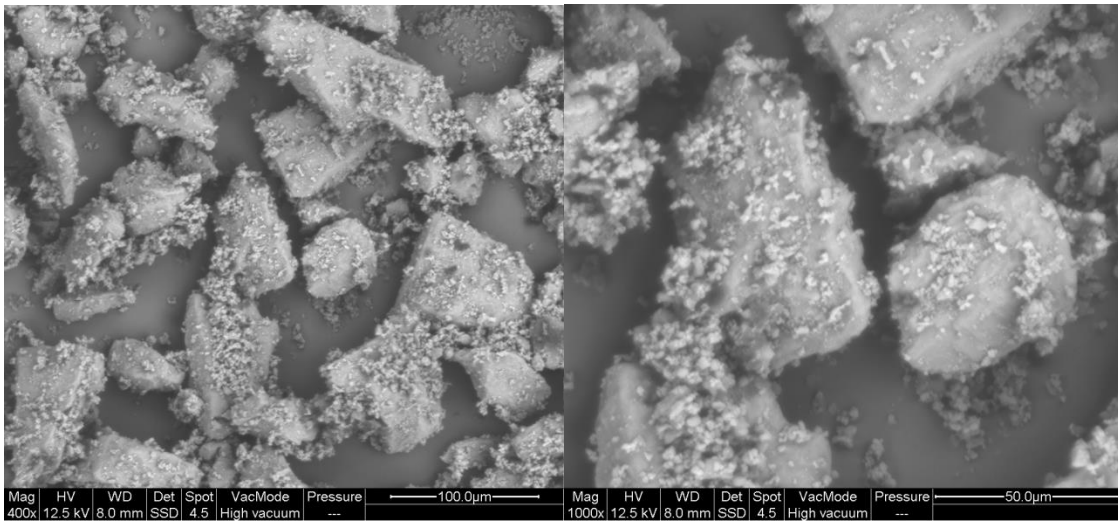


Figure 4.32: SEM images acquired from the 4% BPD + 4% LF for the coated formulation, taken at 60 minutes of mixing.

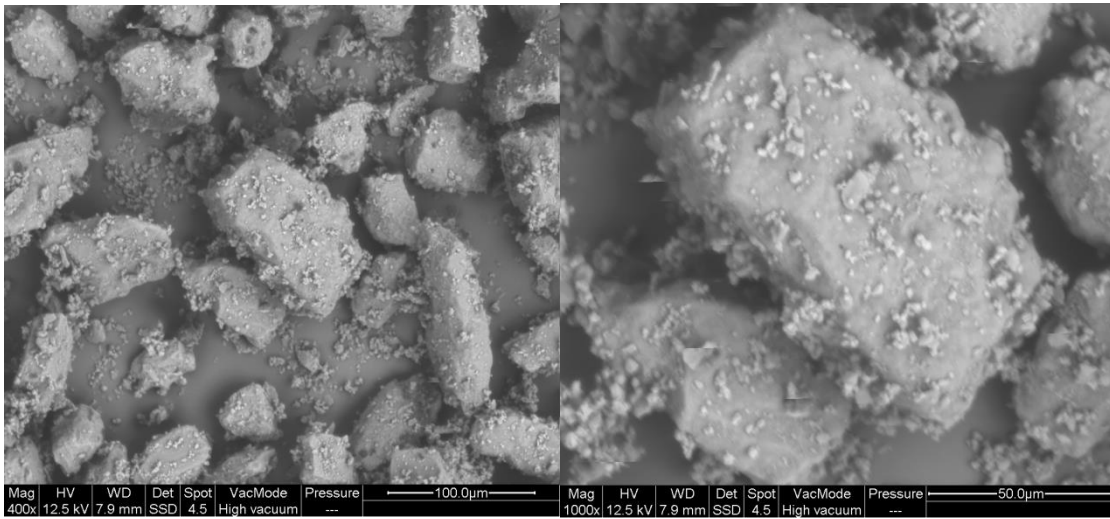
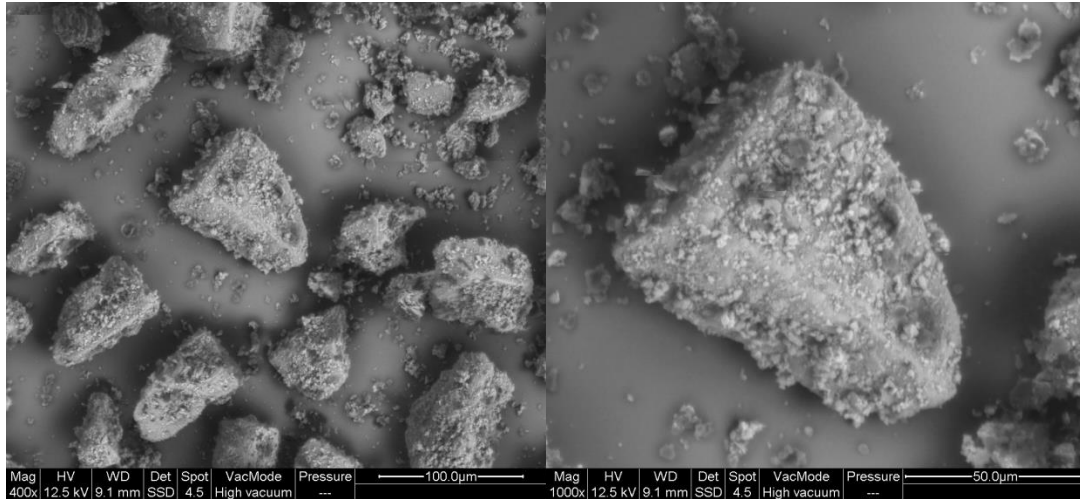


Figure 4.33: SEM images acquired from the 4% BPD + 4% LF for the coated formulation, taken at 120 minutes of mixing.

*Standard formulations*

Fig. 4.34-4.35 shows the resulting SEM images for the standard formulation from samples of 10 and 60 minutes of mixing. One difference that can be observed is that in the beginning of the mixing there seems to be more particles/agglomerates coated on the carriers.



**Figure 4.34: SEM images acquired from the 4% BPD + 4% LF for the standard formulation, taken from 10 minutes of mixing**

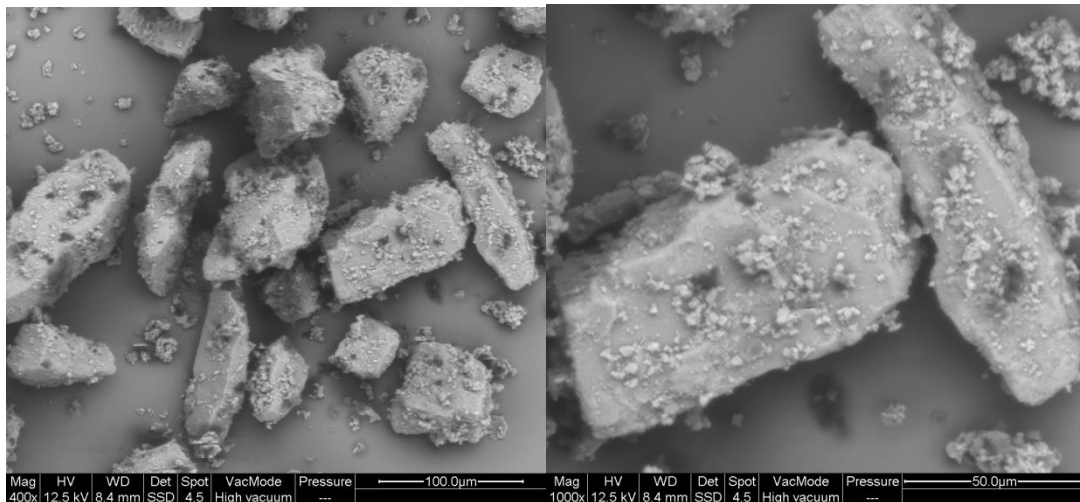


**Figure 4.35: SEM images acquired from the 4% BPD + 4% LF for the standard formulation, taken from 60 minutes of mixing**



## **5. Discussion**

In the following chapter the results will be discussed and evaluated. The discussion will be divided into two main parts, where the first one will consider the observed dispersion properties of the formulations, with a main focus evaluating the data assessed from the NGI. The second part focuses on correlating data from NGI to that obtained by LD.

### **5.1 Behavior of the adhesive mixtures**

This section will consider and discuss the nature and behavior of the manufactured formulations based on the obtained results from the NGI. The observed effects will be discussed one by one. It should be noted that previous research in this area can not necessarily be aligned to this study as there are many variables that can change the results. For example, this work used a rather simple dispersion device, where other studies employed more advanced inhalers. Furthermore, different APIs behave differently and it is not unlikely to believe that LF will behave in another way if mixed with other APIs.

#### **5.1.1 Effect of coating agent**

As described in chapter 1 the adhesive forces between carriers and excipients in an adhesive mixture can be reduced by introducing a so called coating agent. For this study MgSt was used and it is clear that it influences the dispersability of the powder greatly. Regarding the BDP, FPF is significantly higher for the coated formulations, see Fig. 5.1. The same goes for the LF, see Fig. 5.2, although this effect have not been shown before. This is in agreement with the stated theory described in section 1.1, that a FCA reduces adhesive forces within an adhesive mixture. Naturally, when the forces between particles are weakened the dispersability of the powder mixture increases, resulting in a higher FPF profile for the coated formulations.

Another observation that can be made is that the mixing time is critical for coated formulations whereas the mixing time seems to be less important for standard formulations. The strong and non-linear influence of mixing time is alone an interesting observation and will be discussed in the subsequent section.

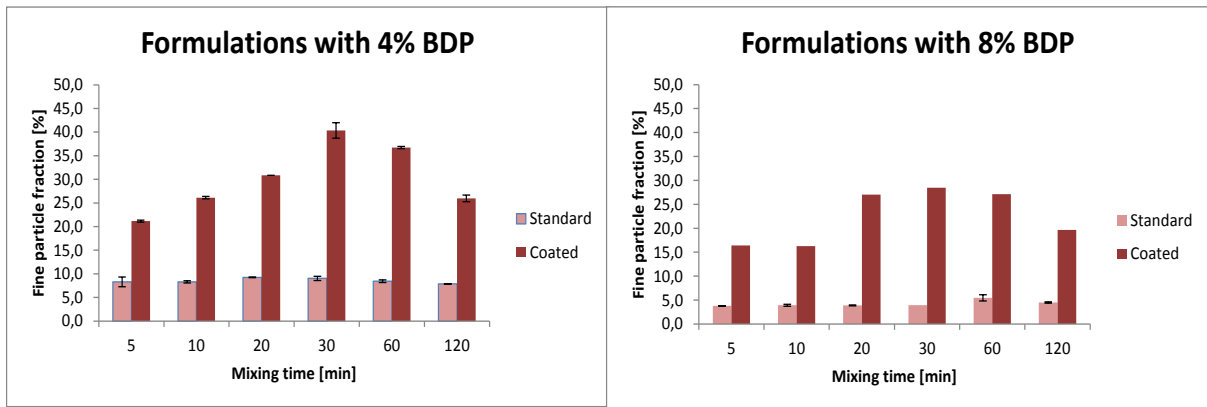


Figure 5.1: Comparison between the FPF profiles of the BDP component in 4% respective 8% concentration for coated and standard formulations. It is clear that the FPF of the coated formulations is consistently higher for all batches.

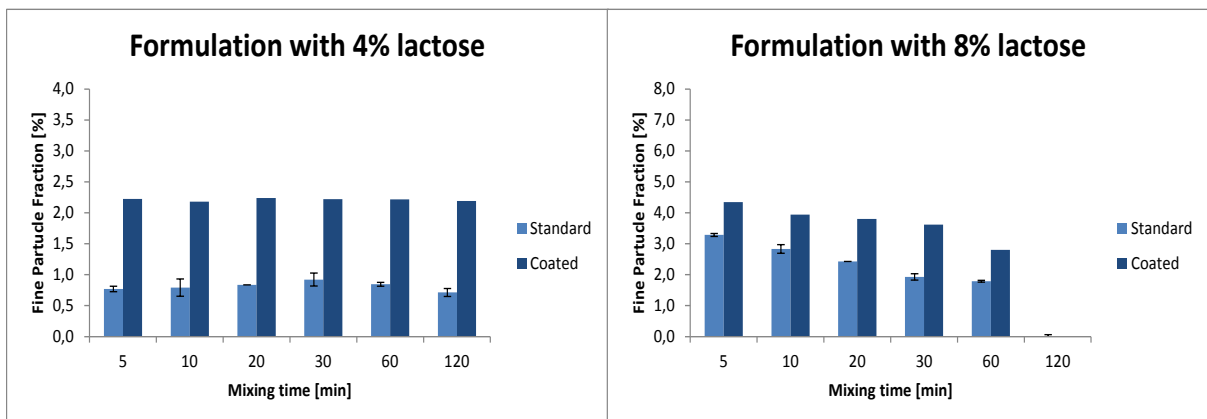


Figure 5.2: Comparison between the FPF profiles of the LF component in 4% respective 8% concentration for coated and standard formulations. It is clear that the FPF of the coated formulations is consistently higher for all batches.

### 5.1.2 Influence of different mixing times

As mentioned in the previous section, the coated formulations display a rather critical impact from the mixing process, in terms of different mixing times. As regards the standard formulations no such clear effect can be seen.

Starting with the BDP analysis, the appearance of the FPF curves, see section 4.1 or Fig 5.1, displays an initial increase. At a certain point the curve shifts and starts to decrease instead, as the mixing time go on. As this appearance is more or less absent for the standard formulations, it indicates that the coating of the carriers plays an important role within the process.

When preparing the manufacturing of the formulations, the raw material of BDP was introduced in the form of apparent agglomerates. These were then distributed in the powder mixture by a slow pre-mixing step. When the full speed of the mixing blades (800 rpm) was set, it is not unlikely to believe that these agglomerates started to break up into smaller parts due to the shear forces induced by the mixing blades along with collisions with the carriers.

Such de-agglomeration has also been observed by Nguyen et al [19], which further fortifies this reasoning. As the size of the BDP agglomerates decreases, it is possible to that they start to adhere to the layer of MgSt on the carriers. Considering that the FPF increased as the mixing progressed, the BDP must somehow be able to disperse more easily upon inhalation.

A possible explanation to this can be that the BDP (particles/agglomerates) are getting more and more evenly distributed onto the layer of MgSt on the carrier particles. As the MgSt works to reduce adhesive forces it is likely that a higher FPF is achieved when BDP and MgSt interact. This can be done either by the adhesion of BDP particles onto the coated carriers, or that the MgSt adheres to and lubricates the fine BDP particles.

As the mixing goes on it is observed that at a certain point, the dispersibility of the powder is reduced. One explanation can be that the particles/agglomerates that have adhered to the carriers are getting more and more compressed into the carriers. At a certain time point, the rate of BDP (particles/agglomerates) adhering to the carriers is surpassed by the rate of BDP affected by these press-on forces, which results in the shift and decrease of the FPF curve. Another explanation could be that longer mixing might break down clusters of particles that are easily dispersed during inhalation, thus lowering the FPF profile.

The rather flat FPF-profile achieved for the standard formulations shows that without the coating with MgSt, the BDP is less able to disperse from the carriers. This is expected as the carriers coated with MgSt have a lower surface energy and friction than the uncoated carrier [7]. Furthermore, the effect of different mixing time seems to be less crucial for the standard formulations.

The reasoning above has yet to include the effect of the added LF. As goes for this component, the analysis is not as straight forward as for the case of BDP. The NGI data are given in FPF of total amount of lactose, not just FPF of the added LF. To be able to compare the FPF of BDP and added LF, a conversation of the FPF of lactose has to be made. This is simply done by dividing the FPF by the concentration of LF, see eq. 5.1.

$$FPF_{LF} = \frac{FPF_{Total\ Lactose}}{\text{Amount of extrinsic LF} / \text{Total amount of lactose}} \quad (\text{eq. 5.1})$$

In Figure 5.3 - 5.5 this conversation has been done for coated formulations including both BDP and LF. As can be seen, the FPF of the LF is consistently higher than that of the BDP.

The curvature for the BDP is almost the same for all formulations, with differing values in FPF. But, as goes for the FPF of LF, this is not the case. The formulation with the highest amount of LF, i.e. 6%, is showing a rather flat appearance at the start of the mixing process, but as the BDP reaches its maximum, so does the LF starts to decline. For the case of 4% BDP +4% LF, the LF curve is rather flat during the whole mixing process. For the 6% BDP + 2 % LF the LF seems to follow the BDP curve. However, if this is due to the formulations themselves or within the uncertainty of the measurement method is yet unknown.

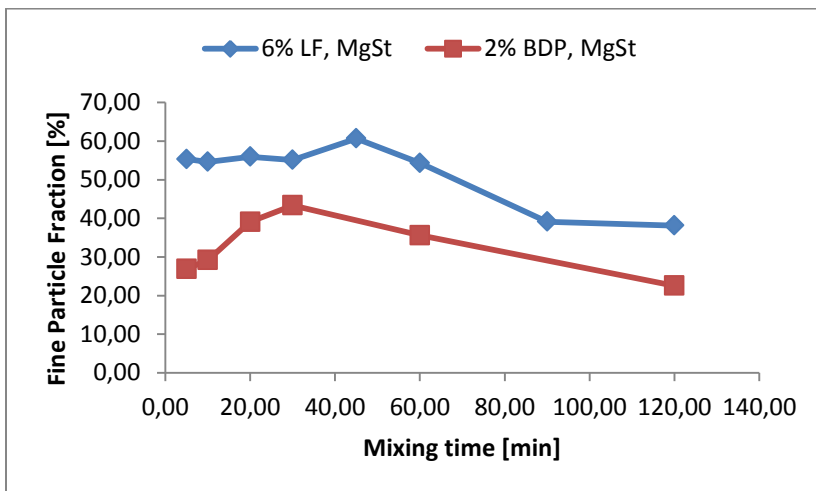


Figure 5.3: Fine Particle Fraction for coated formulation containing 6% LF and 2% BDP as a function of mixing time.

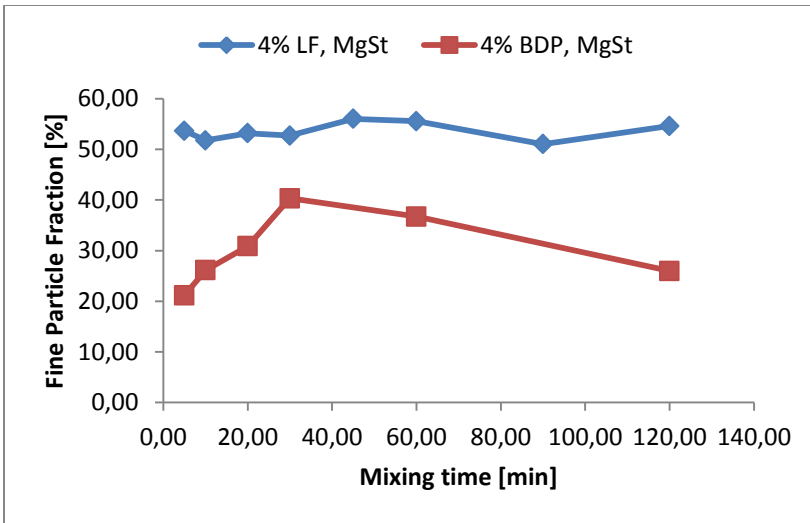


Figure 5.4 Fine Particle Fraction for coated formulation containing 4% LF and 4% BDP as a function of mixing time.

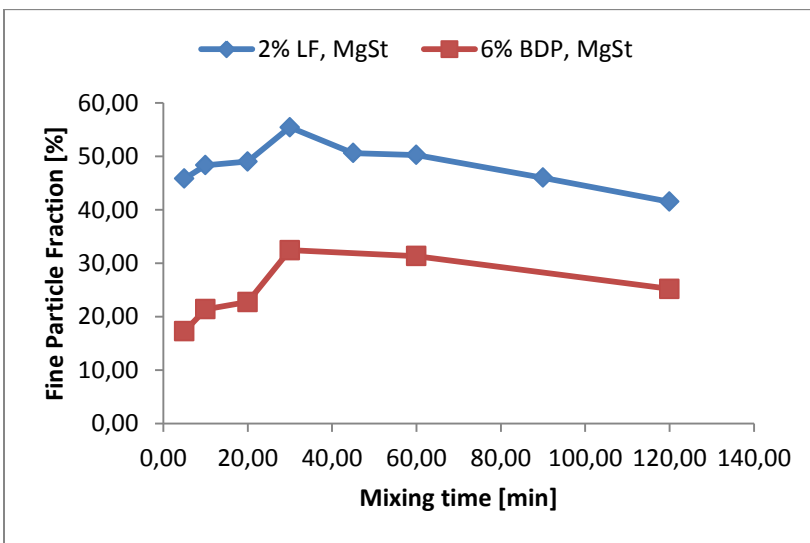


Figure 5.5 Fine Particle Fraction for coated formulation containing 2% LF and 6% BDP as a function of mixing time.

The batches with 8% LF are not showing a maximum FPF, as a line with a negative slope is observed as the mixing time is increased. This indicates that the BDP and LF are otherwise interacting with each other, since the absence of BDP possibly leads to the LF being pressed onto the carriers directly from the start of the mixing.

### 5.1.2.1 Mathematical modeling of FPF of BDP

To further understand the FPF behavior of the BDP, data can be fitted to a descriptive mathematical equation, from which for example rate constants for the process can be estimated. Based on the FPF profile versus mixing time of the BDP component for coated formulations, it is clear that that an initial increase is taking place ( $y_1$ ) followed by a decaying segment ( $y_2$ ). This can be described by two different equations, where the combination of the two gives the FPF, displayed in eq. 5.2- 5.4.

$$y_1 = A + \frac{B}{1 + e^{-k_1 t}} \quad (\text{eq. 5.2})$$

$$y_2 = e^{-k_2 t} \quad (\text{eq. 5.3})$$

$$FPF = y_1 * y_2 \quad (\text{eq. 5.4})$$

A and B are constants relating to the FPF level,  $k_1$  and  $k_2$  are the rate-constants for the coating respective pressing, or “caking”, processes.

**Table 5.1:** Calculated constants from equations 5.2-5.4

	A	B	$K_1$ [ $\text{min}^{-1}$ ]	$K_2$ [ $\text{min}^{-1}$ ]	$R^2$
2% BDP	-27.9	91.7	0.07	0.008	0.94
4% BDP	-43.4	115.5	0.05	0.009	0.94
6% BDP	-44.1	111.0	0.04	0.008	0.88
8% BDP	-45.7	108.5	0.04	0.010	0.90

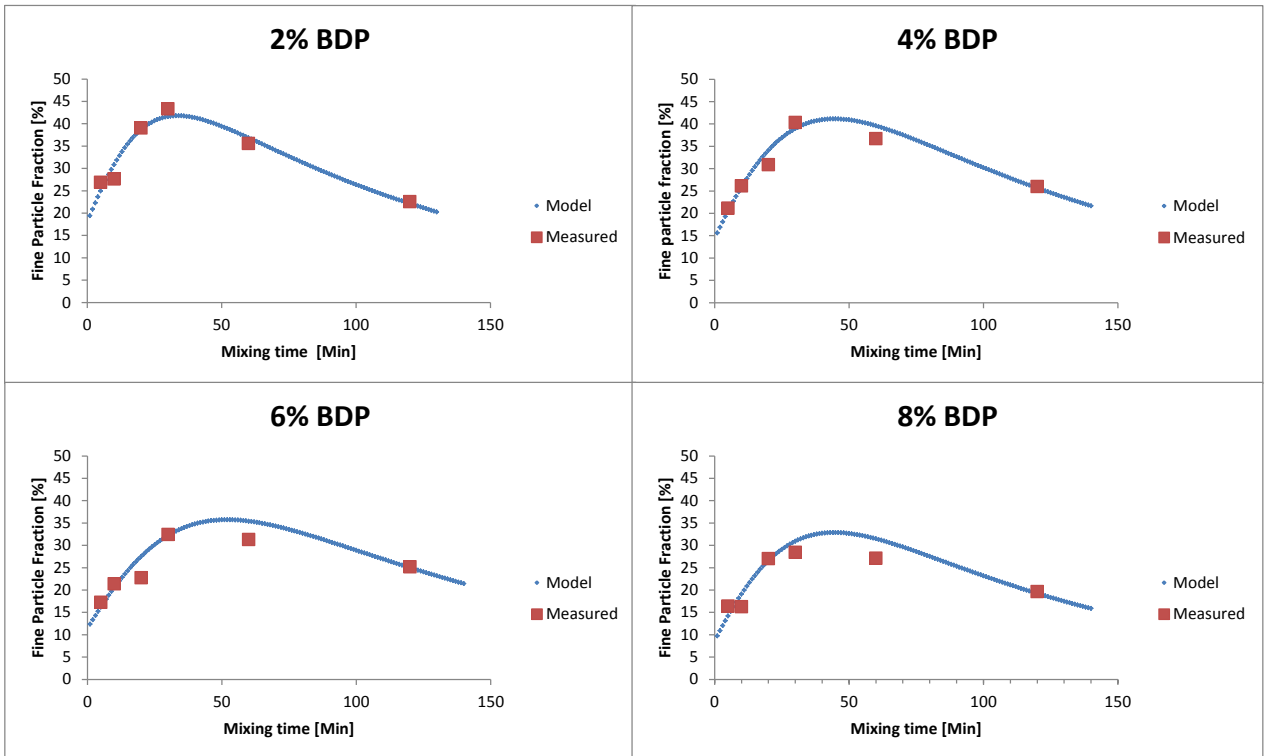


**Figure 5.6: Mathematical modeling for FPF values of coated formulations, as regards the BDP component. The dots represent the assessed data and the line represents values acquired from the equation.**

As can be seen in Fig 5.6, the mathematical model fits the FPF-values rather well, as displayed by the  $R^2$  values close to 1 given in table 5.1. More data-points should possibly give a better fitting.

However, the rate constants for the mathematical models were roughly the same for all formulations.  $k_1$  was consistently larger than  $k_2$ , indicating that the coating step is faster than the caking process. For further understanding of the formulations it would be favourable if more time points could be obtained. The calculated constants can be seen in table 5.1.

### 5.1.3. Effect of different concentrations between BDP and LF

When considering the relative concentration between BDP and LF it is quite obvious that LF have an influence on the FPF of BDP. A clear pattern is seen that the formulations with the lowest amount of BDP, and thus highest amount of LF, results in the highest FPF of BDP, see Fig. 5.7. This is somewhat contradictory to a previous study reviewed by Jones et al [3] which suggested that the optimum relationship between the API and LF should be 1:1. However, that study employed another type of API than the one used in this thesis as well as larger LF. Even though those results cannot be directly compared with the results in this thesis, it displays the difficulties of studying adhesive mixtures as there are many different factors that can alter the results.

In Fig. 5.7 the FPF for each formulation at 30 minutes of mixing is plotted against the concentration of BDP.

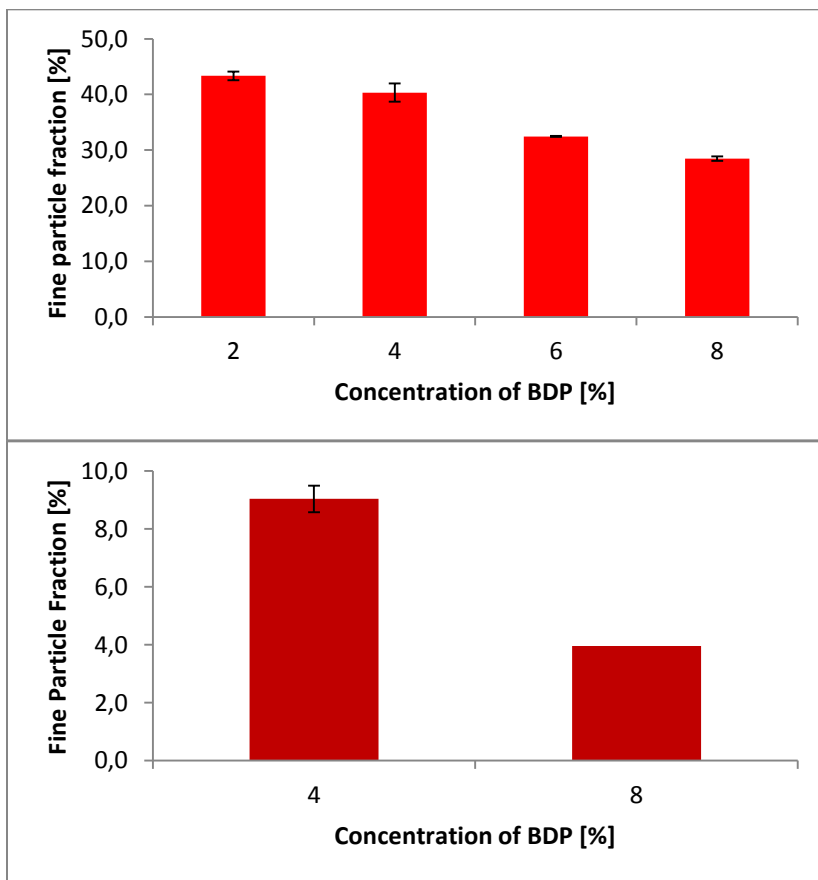


Figure 5.7: How the FPF is affected by concentration of BDP, taken from 30 minutes into mixing process. The upper image displays coated formulations and the lower displays standard formulations. The values represent mean values of 2 replicates and the error bars shows the standard deviations.



This can be explained by the fact that LF gives a higher FPF than the BDP for all formulations. Amongst the theories proposed to explain the effect of LF is the formation of agglomerates. Assuming that this takes place during mixing, a co-agglomerate of BDP and LF will likely give a FPF value somewhere in between that of the FPF of LF and BDP separately. This could also tell something about the adhesive forces interacting in such clusters; the more LF the less stable clusters, as an increased LF concentration gives a higher FPF.

#### **5.1.4 Formation of agglomerates**

As stated in previous section there are indications that the BDP and LF interact when mixed together. This would be in agreement with the theory stated in chapter 1 (that agglomerates of BDP and LF are built up during the mixing process). Regarding the MMAD values of BDP they are considerably larger than the size of a single particle, which supports the theory of formation of agglomerates. As a combination of BDP and LF resulted in a FPF value somewhere in between, it is likely to believe that co-aggregates are forming during mixing. Another interpretation of the data is that including LF into the formulations forms larger clusters. If these clusters would be equally parted BDP as LF, the MMAD should show the same value, which is not the case.

However, the MMAD evaluation of LF is not to be entirely relied on as the PSD includes the carriers, which may lead to a skewed distribution that the excel template cannot account for [5]. It is also seen (Figure 4.6) that the less BDP the higher MMAD for BDP, which is consistent with co-aggregate formation taking into account that LF have a larger particle size.

An observation made from the FPmode results from Inhaler setup (Figure 4.24 and 4.25) is that there are agglomerates present in the beginning of the mixing stage, but as the air flow increases from 50 lpm to 100 lpm, the values of FPmode is decreased, indicating a breakage of these agglomerates. This must mean that there are agglomerates within the powder mixtures strong enough to withstand a flow of 50 lpm. When the flow increases it is enough to partially break down these clusters, resulting in lower FPmode. Not only being in agreement with the theory on formation of agglomerates, it would also give an indication on how strong the agglomerates are.

When analyzing SEM images taken at different time points, it can be seen that in the beginning of the mixing process there are particles, or agglomerates, on the surfaces of the carriers.

Even though these images only give a qualitative picture of the powders, it can be seen that at 10 and 60 minutes there are agglomerates or particles adhered to the carriers.

For the 120 minute sample the amount of agglomerates/clusters seems to be less, either because they have broken down, or have been pressed onto the carriers as a result of over mixing.

## 5.2. Comparison between NGI and Laser Diffraction

This section will be devoted to finding out how well the NGI data fits the data assessed by laser diffraction (LD). It has been observed in previous studies that the used instrument overestimates the amount of finer particles when analyzing adhesive mixtures [15]. To adjust for this overestimation a calibration curve can be generated. This can be done by measuring a known weight concentration of fines and carrier using the RODOS setup. As the RODOS setup disperses the powder mixture fully, each component is being analyzed separately. In a previous Master thesis [18] such calibration curve was generated using the same batch of LF and carrier as used in this work. A calibration curve was also acquired for an API referred to as AZD8683. With AZD8683 having the same density as BDP and a similar particle size distribution, it can be assumed that they will scatter the light similarly; therefore it is considered that this calibration curve can be used for BDP as well. The calibration curves, shown in Fig 5.8, give the relation for much of signal < 5 μm a certain amount of fines corresponds to. Eq. 5.5 and 5.6 describes this overestimation effect:

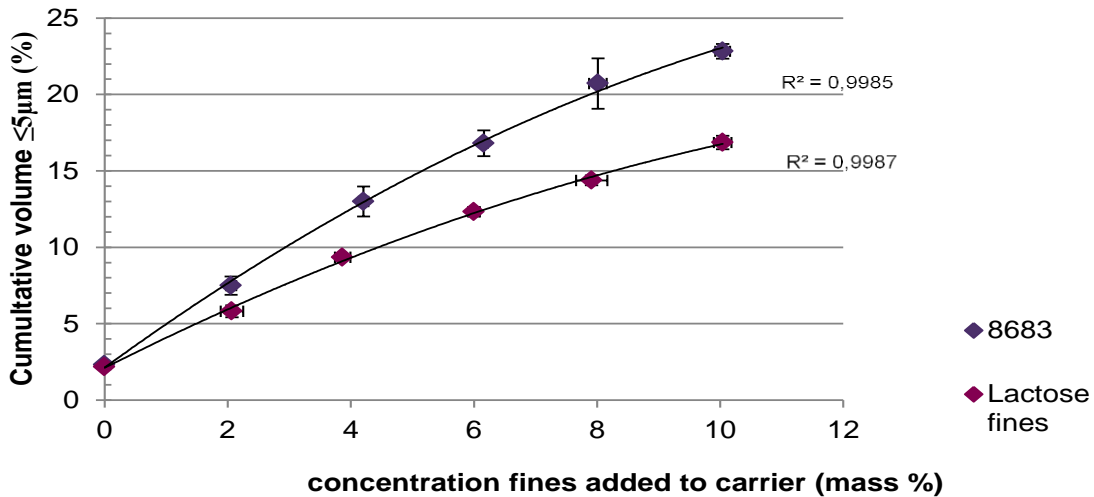


Figure 5.8: Calibration curves showing how much the Sympatec instruments overestimates the amount of particles < 5 μm. The values represent mean values of 3 replicates. The horizontal error bars represents the standard deviation of the weight in amount. The vertical error bars represent the standard deviation from the measurement [18]

$$F(< 5\mu m)_{SV003+fine\ lactose} = 2.11 + 2.03X - 0.056X^2 \quad (\text{eq. 5.5})$$

$$F(< 5\mu m)_{SV003+Micronised\ AZD8683} = 2.13 + 2.93X - 0.084X^2 \quad (\text{eq. 5.6})$$

These equations can be used to transform the FPF data from NGI for both BDP and LF into values corresponding to LD measurements.

It is assumed that the MgSt has little influence on the measurements regarding  $F_5$ . This is believed to be valid because MgSt is seen to form a layer around the carriers, giving little contribution to the  $F_5$ . As the MMAD analysis of the LF is rather inconclusive there is no point in trying to correlate MMAD assessed by the NGI with FPmode. As displayed in the RODOS setup (Fig. 4.18) a higher amount of BDP gives a higher  $F_5$ . This can be explained by the fact that LF contains a part of particles larger than  $5\ \mu\text{m}$  which is not taken into account in the data-evaluation of the instrument.

As the air flow used in the NGI measurements (77 lpm) differed from the Inhaler setup (50 and 100 lpm) a mean value was taken from the inhaler data in order to see if that gave a better correlation.

The comparison between the NGI and LD data will be done by extracting the coefficient of determination, denoted  $R^2$ . It is a statistical coefficient that explains how much of the variability of a factor is caused or explained by its relationship to another factor. In Fig. 5.9 the translated NGI values are plotted on the x-axis and the LD data are plotted on the Y-axis. The responding  $R^2$  are rather close to 1, which should indicate a good correlation. In general, the higher the  $R^2$ , the better the model fits the data. The  $R^2$  can have values between 0 and 1. For other plots such as Fig 5.9 see Appendix II.

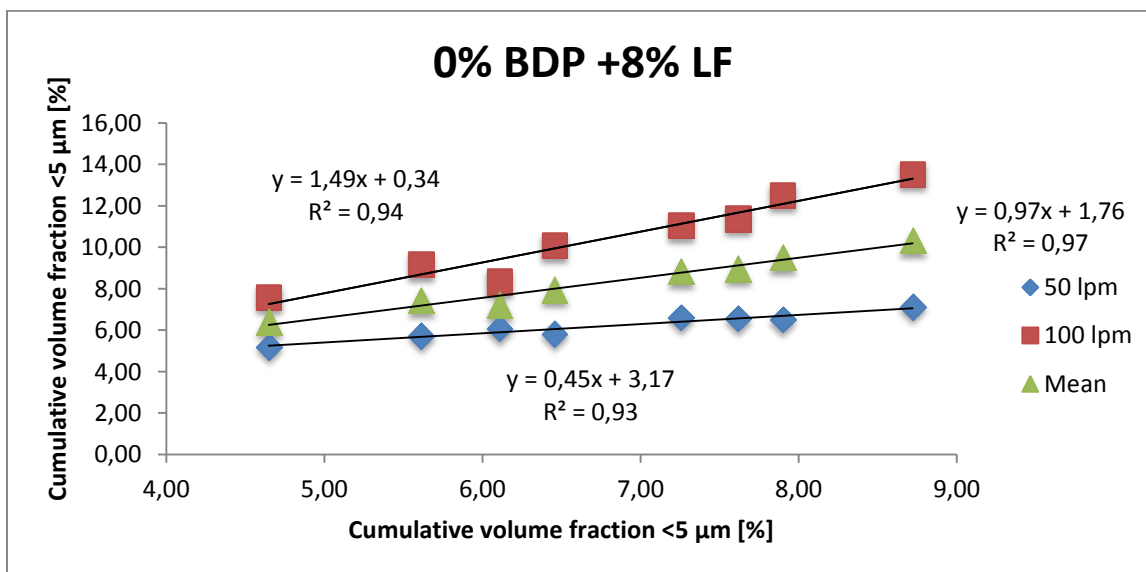


Figure 5.9: Correlation between Sympatec Inhaler and NGI for coated formulation containing 0% BDP and 8% added LF. The correlation is very good as  $R^2$  approaches 1.

In the following sections different plots will be given where the NGI data has been translated into corresponding LD values, starting with the coated formulations.

*Coated formulations*

The calculated  $R^2$  values for the coated formulations are displayed in table 5.2. It can be seen that formulations including only one type of added fines, i.e. 8 % BDP + 0% LF and 0% BDP + 8% LF, shows highest  $R^2$  values. However, the values assessed by the Inhaler setup had a rather high relative standard deviation (RSD) between replicates, inducing an uncertainty into the correlations.

**Table 5.2:**  $R^2$  for correlation between NGI and LD data, for the 1% MgSt coated formulations.

Formulation	$R^2$ , 50 lpm	$R^2$ , 100 lpm	$R^2$ , Mean
8% BDP + 0% LF + 1% MgSt	0.46	0.79	0.93
6% BDP + 2% LF + 1% MgSt	0.19	0.01	0.05
4% BDP + 4% LF + 1% MgSt	0.87	0.05	0.56
2% BDP + 6% LF + 1% MgSt	0.00	0.73	0.84
0% BDP + 8% LF + 1% MgSt	0.93	0.97	0.94

By instead plotting the values as a function of mixing time, the behavior of each formulation can be investigated. This is done in Fig. 5.10 and 5.11.

Starting with Fig. 5.10 with the formulation containing 8 % BDP, 0% LF and 1% MgSt, the 100 lpm and NGI data seems to have similar curvature ( $R^2 = 0.79$ , see table 5.2) whereas the 50 lpm data does not follow the NGI data at all. The formulation containing 8% LF at the air flow of 50 gives a rather similar curve to the translated NGI data, as well for 100 lpm ( $R^2 = 0.93$  and  $R^2=0.97$ , respectively).

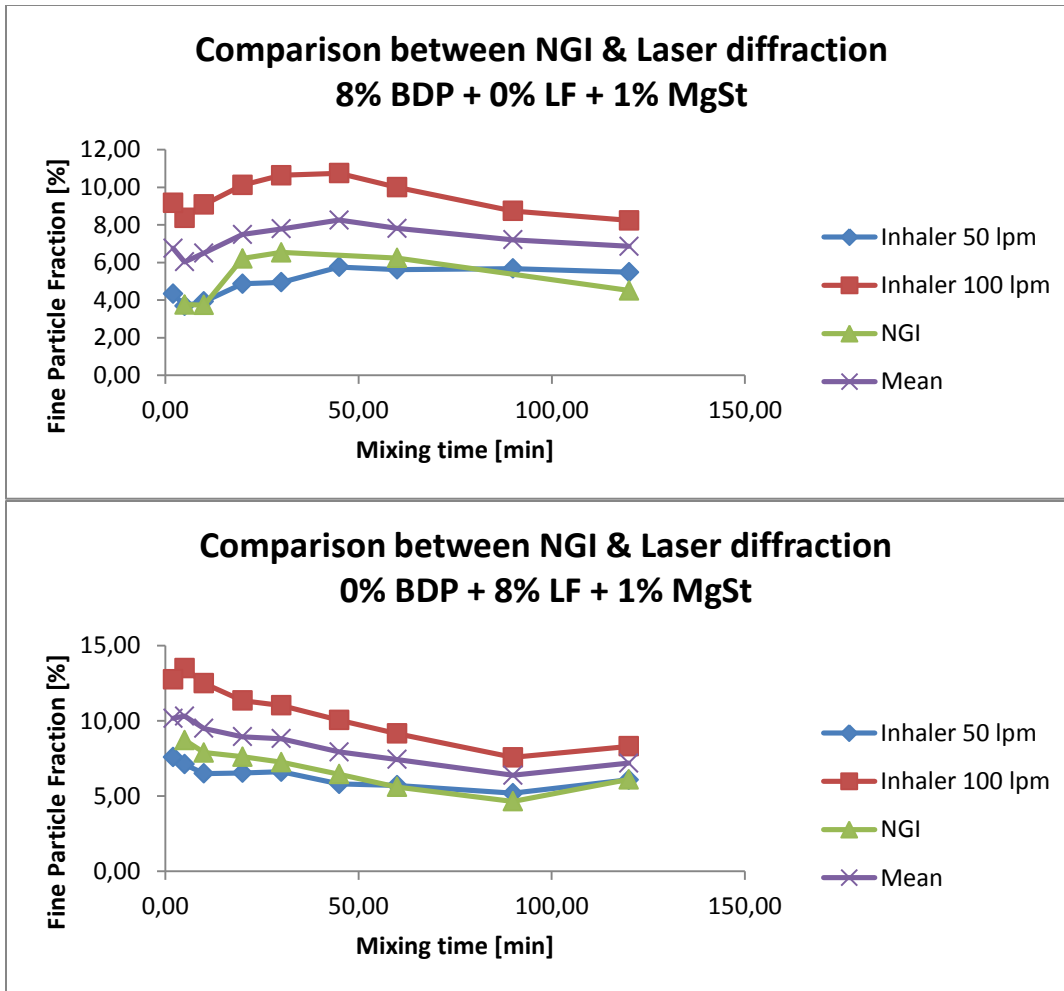


Figure 5.10: Comparison between Sympatec Inhaler and NGI for formulations containing 8% BDP + 0% LF and 0% BDP + 8%LF.

When continuing with the rest of the coated formulations there are both bad and good correlation results, as seen in table 5.2. It seems that the higher amount of BDP, the worse is the correlation. In Fig 5.11, the formulation with 6% BDP and 2 % LF displays both rather poor correlation as well as poor curve-fitting as the  $R^2$  values are close to 0. However, even though the correlations are rather bad the curvatures are in some cases very alike. For example, the mean value curvature for formulation 4% BDP + 4% LF is almost the same as the NGI data, even if  $R^2 = 0.56$ . This shows that behavior of a formulation can be predicted by the usage of LD and that the poor correlation value is just due to the very flat curves.

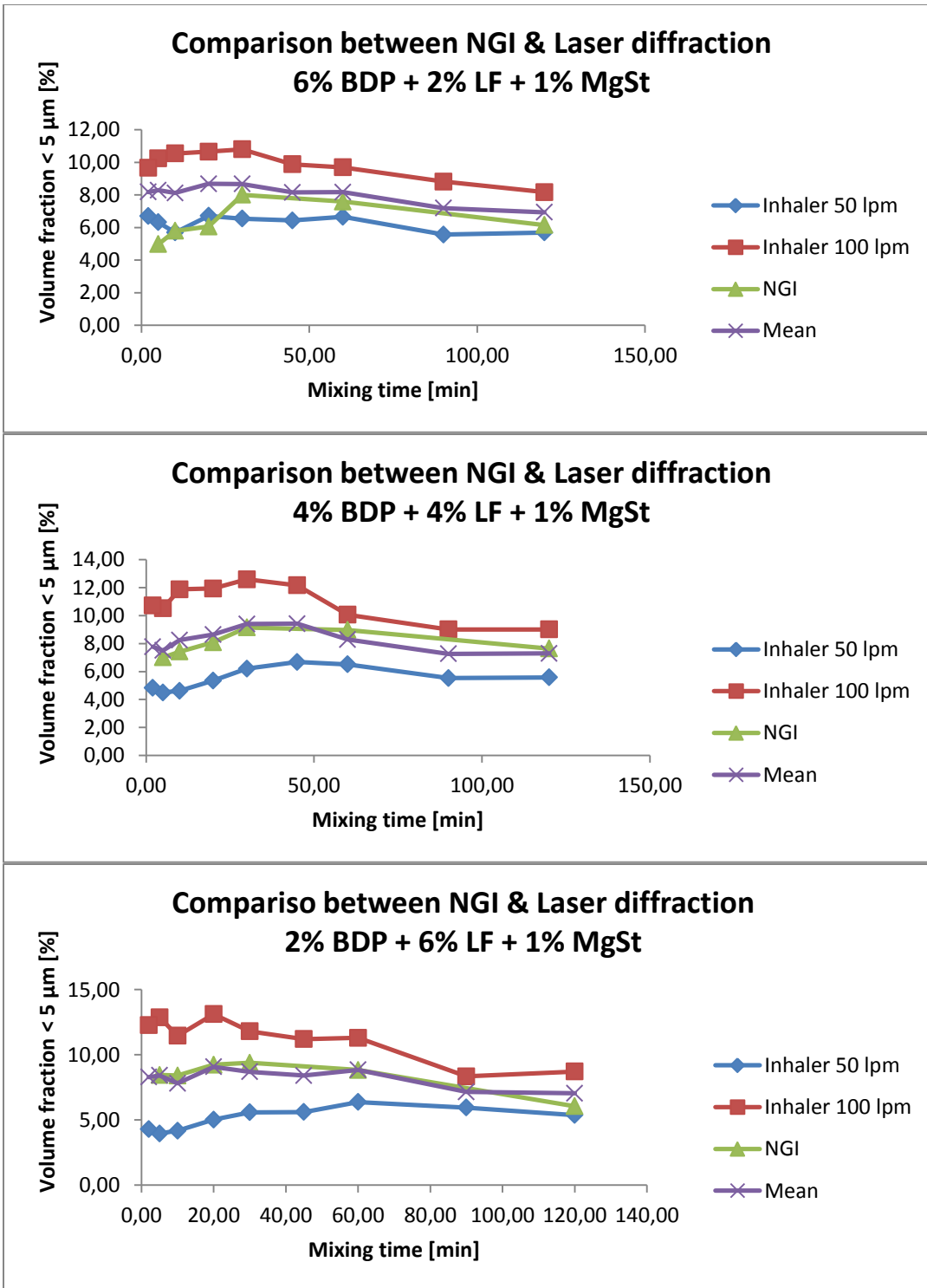


Figure 5.11: Comparison between Sympatec Inhaler and NGI for formulations containing 6% BDP + 2% LF, 4% BDP + 4%LF and 2% BDP + 6% LF.

### Standard Formulations

As for the standard formulations, the batch with only lactose correlates really well, as displayed by the  $R^2$  values shown in table 5.3. However, for formulations with added BDP the correlations are worse (highest  $R^2=0.46$ ), indicating that the BDP is more cohesive than lactose and that the dispersion of BDP is more dependent on the setup than lactose.

**Table 5.3:**  $R^2$  for correlation between NGI and LD data, for the standard formulations.

Formulation	$R^2$ , 50 lpm	$R^2$ , 100 lpm	$R^2$ , Mean
8% BDP + 0% LF	0.11	0.16	0.23
4% BDP + 4% LF	0.46	0.21	0.36
0% BDP + 8% LF	0.93	0.95	0.92

As can be seen in Fig. 5.12 the appearance of the curves are rather flat, which make a comparison between NGI and LD rather inconclusive

To conclude this section it is clear that the formulations with both LF and BDP show a poorer correlation between LD and NGI than formulations with only one component of fines. But, even if the  $R^2$  sometime is rather poor the appearance of the curves can be very similar, indicating that it is possible to screen a formulation using LD.

However, the calibration curve used was made for another API with another PSD than the BDP. To further investigate if there is a possible way of screening formulations using these LD setups, a calibration curve originating from BDP should be made as well as applying more similarly dispersion setups, as regards the flow used as well as the dispersion devices. Optimum would be if the same device could be used in both setups as it seems that the formulations are rather dependent on the exact dispersion conditions and settings that are used.

To be able to correct for the contribution from the LF in a screening of a formulation, the analysis of lactose in the NGI needs to be better understood. Further investigations are needed to see if the LF behaves in the same way as here reported or differently, when combined with another API. The more knowledge gained about the behavior of LF, the easier it will be to correct for it in LD measurements.

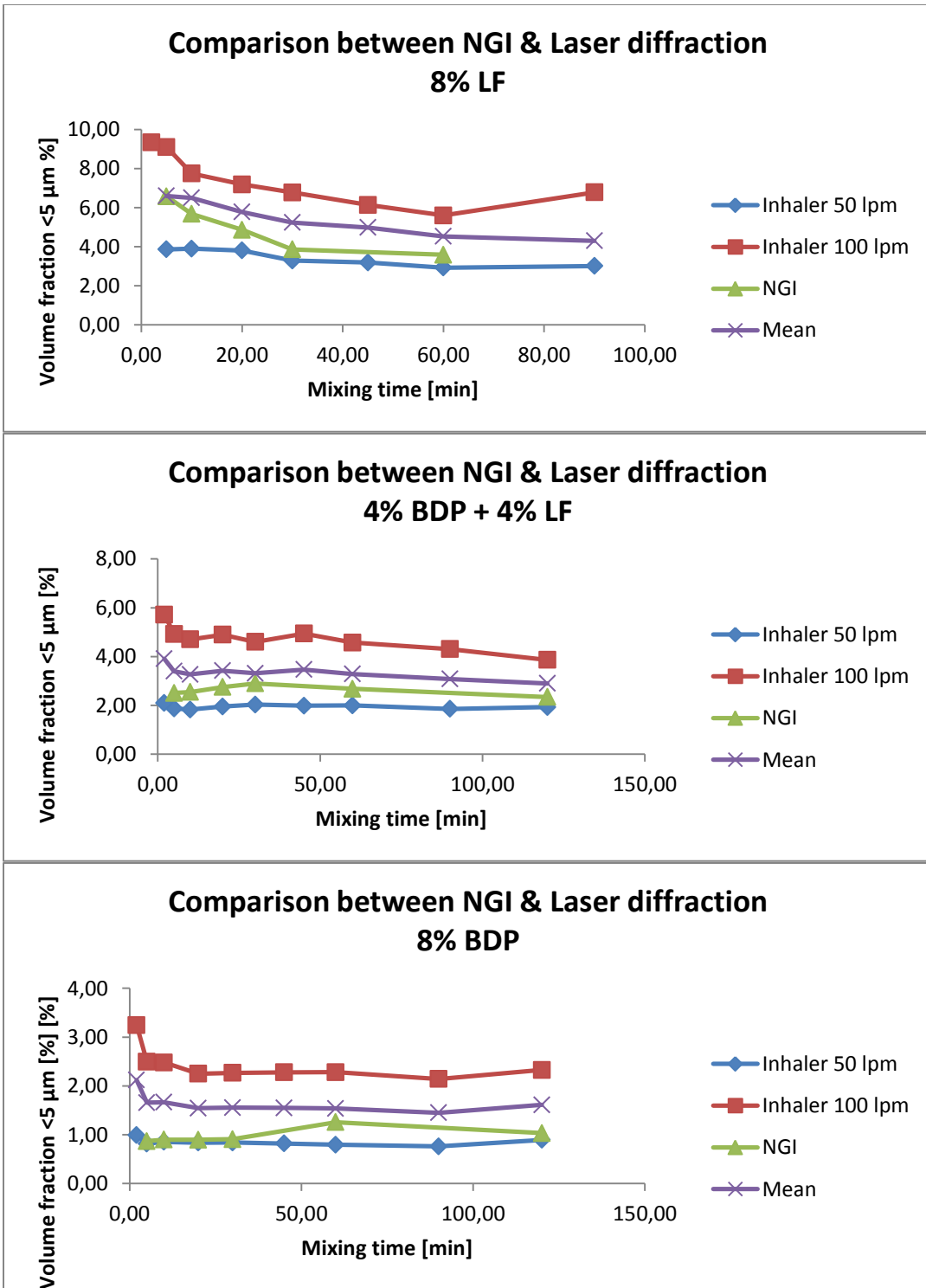


Figure 5.12: Comparison between Sympatec Inhaler and NGI for formulations containing 6% BDP + 2% LF, 4% BDP + 4%LF and 2% BDP + 6% LF.



## 6. Conclusions and further work.

The following chapter will give a conclusion of this work, followed by suggestions on what can be done in future studies.

### 6.1 Conclusions

In this thesis, adhesive mixtures intended for inhalation were manufactured using a high shear mixer. Two different sets of formulations were produced, one with the addition of a coating agent, MgSt, and the other without such component. Lactose monohydrate was used as carrier. The API used was BDP, a glucocorticoid with anti-inflammatory properties. Furthermore, fine particle lactose were added and the total amount of added fines was kept constant, at 8 wt%, for all batches, whereas the relative weight concentration between lactose fines and BDP was varied systematically. Several samples were taken throughout the mixing process at different time points.

To assess the particle size distribution of the manufactured batches, two different measurement techniques were used, first one was the NGI and the other being based on laser diffraction.

NGI was used to assess the FPF and MMAD of BDP and LF. The analysis of BDP is rather straight forwards, but the analysis of LF needs more tuning and evaluation to be as fully reliable. For the manufactured formulations it was found that:

- MgSt significantly increases FPF
- Mixing time is critical for MgSt formulations
  - Initial increase in FPF
  - Overmixing reduces FPF
- Mixing time is less important for standard formulations
- LF yields higher FPF than BDP
- LF and BDP interact with each other, possibly forming agglomerates which would lie in agreement with the suggested theory found in literature.

The second part of this thesis was to see how well the data assessed from the NGI fitted with the data from the LD. A comparison between NGI and LD was done, where the obtained FPF of both BDP and LF was translated into corresponding values of the LD measurement system. It was found that:

- Formulations with only LF shows best correlation
- Coated formulations correlates better than standard formulations
- Poor correlation does not mean poor fitting.

- Possible to correct for LF, but correlation depends on flow and setup of the two systems.

## 6.2 Further work

This thesis has approached the behaviour of LF within an adhesive mixture by manufacturing several formulations with varying concentration between LF and API. One of the conclusions drawn from the data was that the BDP and LF interact with each other, possibly forming agglomerates. To further strengthen this reasoning it would be favourable if the surface structure of the powder could be established more thoroughly than by SEM analysis. One technique that could be used for this purpose is Time Of Flight – Secondary Ion Mass Spectroscopy (TOF-SIMS).

To further address the behaviour of LF the analysis method used for lactose is in need of improvement, to be as reproducible as the BDP method. It would be favourable if the influences of the carriers could be reduced, as a single bounce between impactor stages could drastically change the measurement data. Optimum would have been to be able to use some sort of internal standard, e.g. glucose or an isotope of lactose, depending on the measurement technique. The LC-PAD method should be investigated further alongside with the MS to further improve the quality of data.

As regards the correlation between NGI and laser diffraction data, the curvature of the translated data seems to fit LD data rather well. As the LF seems to behave rather differently in different formulations, it will be hard to establish a general method to correct for LF in LD measurements. However, it would be favourable if the dispersion settings would be more similar. In the NGI the sample was sucked out from the dispersion device, whereas in the LD it was flushed out. It would also be favourable if the applied air flow was the same for both instruments as it has been shown that the dispersion is rather dependent on the airflow used. Another thing to do is to measure another calibration curve, based on BDP instead of AZD8684.

To get a broader understanding of the behaviour of the lactose fines there are several other things that can be addressed. This thesis has investigated how the LF interact with a specific type of API. It is however not obvious how it will behave together with another type of API. It can also be investigated how the particle size of the LF will effect the system, as previous studies has indicated that this matters as well as the total concentration of finer particles and relative concentration between API/LF.

Other type of investigations that can be made is to manufacture using another type of mixer process, for example a tumbler mixer which will give a more gentle mixing

process. The high shear mixer is a rather intensive process and the LF might interact and mix differently if subjected to another type of mixing.

## 7. References

1. Pilcer, G. and Amighi, K., *Formulation strategy and use of excipients in pulmonary drug delivery*, Internal Journal of Pharmaceutics, Volume 392, 2010.
2. Hinds, W.C., *Aerosol Technology: Properties, Behavior and Measurement of airborne particles*, 2<sup>nd</sup> Ed. 1999
3. Jones, M., *An investigation into the Dispersion Mechanisms of Ternary Dry Powder Inhaler Formulations by the Quantification of Interparticulate Forces*, Final PhD thesis, University of Bath, 2006.
4. Aulton, M.E., *Pharmaceutics – The science of dosage form design*, Elsevier, 2002.
5. Kinnunen, H.M., *Active sites, agglomerates or increased cohesion? Investigations into the mechanisms of how lactose fines improve dry powder inhaler performance*, Final PhD thesis, University of Bath, 2012.
6. Willets, J., *Investigation into the Effects of High Shear Blending and Storage on Powders for Inhalation*, Final PhD Thesis, University Of Birmingham, 2011.
7. Morton, D. Begat, P. Green, M. Price, R. Staniforth, John. Whittock, A. Young, P., *The study of force control additives in creating high performance dry powder inhaler formulations*, Respiratory Drug Delivery VIII, University of Bath, 2002.
8. Jones, M.D. and Price, R., *The influence of Fine Excipient Particles on the Performance of Carrier-Based Dry Powder Inhalation Formulations*, Pharmaceutical Research, Vol.23, No. 8, 2006.
9. Shur, J. Harris, H. Jones, M.D., Kaerger, JS. Price, R. *The role of Fines in the Modification of the Fluidization and Dispersion Mechanism within Dry Powder Inhaler Formulations*, Pharmaceutical Research, Vol.25, No. 7, 2008.
10. Dickhoff, B.H.J. de Boer, AH. Lambregts, D. Frijlink, HW. *The effect of carrier surface treatment on drug particle detachment from crystalline carriers in adhesive mixtures for inhalation*, Internal Journal of Pharmaceutics 327, 2006.
11. Kinnunen, H.M., Hebbink, G., Peters, H. Huck, D. Makein, L. Price, R. *Extrinsic lactose fines improve dry powder inhaler formulation performance of a cohesive batch of budesonide via agglomerate formation and consequential co-deposition*, Internal Journal of Pharmaceutics 478, 2014.
12. <http://www.mspcorp.com/pharmaceutical/model-170-next-generation-impactor>  
assessed 2015-03-28
13. <http://www.copleyscientific.com/products>  
assessed 2015-03-28
14. Sympatec Homepage, <https://www.sympatec.com/EN/LaserDiffraction/LaserDiffraction.html>  
assessed 2015-03-28
15. – Thalberg. K. Berg, E. Fransson, M. *Modeling dispersion of dry powders for inhalation. The concepts of total fines, cohesive energy and interaction parameters*, Internal Journal of Pharmaceutics 427, 2012.

16. <http://www.pharmaceuticalonline.com/doc/high-shear-granulator-p1-6-0001>  
assessed 2015-03-28

17. Guchardi, R. Frei, M. John, E. Kaerger, G. *Influence of fine lactose and magnesium stearate on low dose dry powder inhaler formulations*, Internal Journal of Pharmaceutics 348, 2007.

18. Tran. J, *Dry Particle sizing of Pharmaceutical formulations using laser diffraction*, Master of Science Thesis, Gothenburg University and AstraZeneca, Pharmdev, 2013.

19. Nguyen, D. Rasmusson, A. Niklasson Björn, I. Thalberg, K. *Mechanistic time scales in adhesive mixing investigated by dry particle sizing*, Eur. J. Pharm. Sci. 69 (2015), 19-25.

# Appendix I – Raw data from measurements

## Data from NGI

Table A. Raw data from NGI measurements of 8% BDP + 0% LF.

8% BDP + 0% LF									
		Coated with 1% MgSt				Standard			
		BDP		LF		BDP		LF	
min		FPF	MMAD	FPF	MMAD	FPF	MMAD	FPF	MMAD
5	Mean	26,9	2,58	-	-	3,8	4,7	v	-
	SD	1,2	0,1	-	-	0,0	0,1	-	-
10	Mean	29,2	2,44	-	-	3,9	4,7	-	-
	SD	2,4	0,0	-	-	0,2	0,2	-	-
20	Mean	39,1	2,23	-	-	3,9	4,9	-	-
	SD	1,0	0,0	-	-	0,1	0,0	-	-
30	Mean	43,3	2,15	-	-	4,0	4,6	-	-
	SD	0,8	0,0	-	-	-	-	-	-
45	Mean	-	-	-	-	-	-	-	-
	SD	-	-	-	-	-	-	-	-
60	Mean	35,6	2,32	-	-	5,5	4,1	-	-
	SD	1,3	0,0	-	-	0,6	0,2	-	-
90	Mean	-	-	-	-	-	-	-	-
	SD	-	-	-	-	-	-	-	-
120	Mean	22,5	3,09	-	-	4,5	4,5	-	-
	SD	0,1	0,0	-	-	0,1	0,1	-	-

**Table B.** Raw data from NGI measurements of 6% BDP + 2% LF.

6% BDP + 2% LF									
		Coated with 1% MgSt				Standard			
		BDP		LF		BDP		LF	
min		FPF	MMAD	FPF	MMAD	FPF	MMAD	FPF	MMAD
<b>5</b>	Mean	26,9	2,58	0,99	4,34	-	-	-	-
	SD	1,2	0,1	-	-	-	-	-	-
<b>10</b>	Mean	29,2	2,44	1,04	4,59	-	-	-	-
	SD	2,4	0,0	-	-	-	-	-	-
<b>20</b>	Mean	39,1	2,23	1,05	4,35	-	-	-	-
	SD	1,0	0,0	-	-	-	-	-	-
<b>30</b>	Mean	43,3	2,15	1,19	6,11	-	-	-	-
	SD	0,8	0,0	-	-	-	-	-	-
<b>45</b>	Mean	-	-	0,94	7,43	-	-	-	-
	SD	-	-	-	-	-	-	-	-
<b>60</b>	Mean	35,6	2,32	1,08	12,15	-	-	-	-
	SD	1,3	0,0	-	-	-	-	-	-
<b>90</b>	Mean	-	-	0,99	28,23	-	-	-	-
	SD	-	-	-	-	-	-	-	-
<b>120</b>	Mean	22,5	3,09	0,89	10,28	-	-	-	-
	SD	0,1	0,0	-	-	-	-	-	-

**Table C.** Raw data from NGI measurements of 4% BDP + 4% LF.

<b>4% BDP + 4% LF</b>									
		<b>Coated with 1% MgSt</b>				<b>Standard</b>			
		BDP		LF		BDP		LF	
<b>min</b>		FPF	MMAD	FPF	MMAD	FPF	MMAD	FPF	MMAD
<b>5</b>	Mean	21,2	2,8	2,23	3,90	8,3	4,3	3,3	6,0
	SD	0,2	0,1	-	-	1,0	0,1	0,1	0,1
<b>10</b>	Mean	26,1	2,7	2,18	4,34	8,3	4,2	2,8	6,6
	SD	0,2	0,0	-	-	0,2	0,2	0,1	0,2
<b>20</b>	Mean	30,9	2,4	2,24	4,10	9,3	4,2	2,4	8,7
	SD	0,0	0,0	-	-	0,1	0,0	0,1	3,1
<b>30</b>	Mean	40,3	2,2	2,22	4,59	9,0	4,3	1,9	7,5
	SD	1,6	0,2	-	-	0,5	0,0	0,1	0,3
<b>45</b>	Mean	-	-	2,18	6,09	-	-	-	-
	SD	-	-	-	-	-	-	-	-
<b>60</b>	Mean	36,7	2,4	2,22	4,84	8,4	4,4	1,8	8,4
	SD	0,2	0,0	-	-	0,3	0,0	0,1	2,0
<b>90</b>	Mean	-	-	2,15	6,89	-	-	-	-
	SD	-	-	-	-	-	-	-	-
<b>120</b>	Mean	26,0	3,1	2,19	5,13	7,9	4,8	-	-
	SD	3,0	0,1	-	-	0,0	0,2	-	-



**Table D.** Raw data from NGI measurements of 2% BDP + 6% LF.

2% BDP + 6% LF									
		Coated with 1% MgSt				Standard			
		BDP		LF		BDP		LF	
min		FPF	MMAD	FPF	MMAD	FPF	MMAD	FPF	MMAD
<b>5</b>	Mean	26,9	2,58	3,42	4,25	-	-	-	-
	SD	1,2	0,1	-	-	-	-	-	-
<b>10</b>	Mean	29,2	2,44	3,38	5,78	-	-	-	-
	SD	2,4	0,0	-	-	-	-	-	-
<b>20</b>	Mean	39,1	2,23	3,46	4,29	-	-	-	-
	SD	1,0	0,0	-	-	-	-	-	-
<b>30</b>	Mean	43,3	2,15	3,41	4,84	-	-	-	-
	SD	0,8	0,0	-	-	-	-	-	-
<b>45</b>	Mean	-	-	3,75	5,19	-	-	-	-
	SD	-	-	-	-	-	-	-	-
<b>60</b>	Mean	35,6	2,32	3,36	5,45	-	-	-	-
	SD	1,3	0,0	-	-	-	-	-	-
<b>90</b>	Mean	-	-	2,42	5,97	-	-	-	-
	SD	-	-	-	-	-	-	-	-
<b>120</b>	Mean	22,5	3,09	2,36	5,93	-	-	-	-
	SD	0,1	0,0	-	-	-	-	-	-

**Table E.** Raw data from NGI measurements of 0% BDP + 8% LF.

<b>0% BDP + 8% LF</b>									
		<b>Coated with 1% MgSt</b>				<b>Standard</b>			
		<b>BDP</b>		<b>LF</b>		<b>BDP</b>		<b>LF</b>	
<b>min</b>		<b>FPF</b>	<b>MMAD</b>	<b>FPF</b>	<b>MMAD</b>	<b>FPF</b>	<b>MMAD</b>	<b>FPF</b>	<b>MMAD</b>
<b>5</b>	Mean	-	-	4,35	4,26	-	-	3,3	6,0
	SD	-	-	-	-	-	-	0,1	0,1
<b>10</b>	Mean	-	-	3,94	4,63	-	-	2,8	6,6
	SD	-	-	-	-	-	-	0,1	0,2
<b>20</b>	Mean	-	-	3,80	4,31	-	-	2,4	8,7
	SD	-	-	-	-	-	-	0,1	3,1
<b>30</b>	Mean	-	-	3,62	4,88	-	-	1,9	7,5
	SD	-	-	-	-	-	-	0,1	0,3
<b>45</b>	Mean	-	-	3,22	6,56	-	-	-	-
	SD	-	-	-	-	-	-	-	-
<b>60</b>	Mean	-	-	2,80	6,52	-	-	1,8	8,4
	SD	-	-	-	-	-	-	0,1	2,0
<b>90</b>	Mean	-	-	2,32	5,61	-	-	-	-
	SD	-	-	-	-	-	-	-	-
<b>120</b>	Mean	-	-	3,05	5,97	-	-	-	-
	SD	-	-	-	-	-	-	-	-

## Data from Sympatec inhaler - coated formulations

**Table F.** Raw data from Sympatec inhaler measurements of 0% BDP + 8% LF.

Min	0% BDP + 8% LF + 1% MgSt							
	Inhaler - 50 lpm				Inhaler – 100 lpm			
	F <sub>5</sub>	SD	RSD	FPmode	F <sub>5</sub>	SD	RSD	FPmode
2	6,09	0,30	4,90	5,3	8,31	0,81	9,70	3,75
5	5,19	0,43	8,26	6,3	7,58	0,30	3,96	3,8
10	5,72	0,26	4,59	6,25	9,17	1,09	11,85	4,1
20	5,81	0,27	4,64	5,85	10,06	0,96	9,51	3,85
30	6,62	0,14	2,18	5,2	11,04	0,94	8,55	3,95
45	6,55	0,22	3,29	4,85	11,35	0,71	6,23	3,75
60	6,51	0,59	9,11	4,3	12,50	1,26	10,10	3,575
90	7,12	0,46	6,41	4,25	13,51	1,24	9,15	3,5
120	7,60	0,56	7,40	4,3	12,75	0,92	7,20	3,6

**Table G.** Raw data from Sympatec inhaler measurements of 2% BDP + 6% LF.

Min	2% BDP + 6% LF + 1% MgSt							
	Inhaler - 50 lpm				Inhaler – 100 lpm			
	F <sub>5</sub>	SD	RSD	FPmode	F <sub>5</sub>	SD	RSD	FPmode
2	5,38	0,46	8,56	6,25	8,71	0,55	6,28	4
5	5,95	0,33	5,53	7,2	8,35	0,37	4,48	4,5
10	6,38	0,25	3,84	7,75	11,30	1,46	12,92	4,24
20	5,61	0,58	10,37	7	11,20	0,80	7,18	4
30	5,58	0,39	7,00	5,8	11,80	0,40	3,35	3,7
45	5,03	0,38	7,56	4,3	13,12	1,05	7,97	3,6
60	4,17	0,12	2,87	4,1	11,46	0,54	4,70	3,5
90	3,96	0,43	10,90	4,3	12,88	1,29	10,02	3,6
120	4,29	0,23	5,43	4,55	12,28	0,39	3,17	3,9

**Table H.** Raw data from Sympatec inhaler measurements of 4% BDP + 4% LF.

Min	4% BDP + 4% LF + 1% MgSt							
	Inhaler - 50 lpm				Inhaler – 100 lpm			
	F <sub>5</sub>	SD	RSD	FPmode	F <sub>5</sub>	SD	RSD	FPmode
2	5,58	0,37	6,59	6,6	9,01	0,55	6,12	4,4
5	5,53	0,33	6,01	7,6	9,01	0,52	5,76	4,68
10	6,51	0,15	2,34	8,7	10,06	0,31	3,09	4,75
20	6,68	0,22	3,33	7,8	12,17	1,66	13,63	4,35
30	6,21	1,01	16,19	7,75	12,59	1,05	8,36	4
45	5,35	0,56	10,47	4,3	11,94	1,30	10,89	3,5
60	4,61	0,53	11,46	4	11,88	1,41	11,90	3,3
90	4,49	0,50	11,04	4,3	10,52	0,52	4,97	3,64
120	4,82	0,55	11,43	4,5	10,72	1,19	11,14	3,85

**Table I.** Raw data from Sympatec inhaler measurements of 2% BDP + 6% LF.

6% BDP + 2% LF + 1% MgSt								
Min	Inhaler - 50 lpm				Inhaler – 100 lpm			
	F <sub>5</sub>	SD	RSD	FPmode	F <sub>5</sub>	SD	RSD	FPmode
2	5,70	0,18	3,19	7,25	8,18	0,24	2,99	3,35
5	5,57	0,31	5,57	9,25	8,82	0,46	5,19	4
10	6,66	0,27	4,09	8,5	9,69	0,61	6,31	4,1
20	6,44	0,34	5,25	8,5	9,88	0,55	5,57	3,5
30	6,55	0,62	9,48	7,5	10,80	1,02	9,45	3,1
45	6,71	0,44	6,53	6	10,66	0,65	6,11	3,1
60	5,70	0,60	10,46	4,2	10,54	0,68	6,42	3
90	6,33	0,30	4,75	4,2	10,25	0,41	4,02	3,3
120	6,71	0,31	4,55	4,6	9,66	0,63	6,56	3,5

**Table J.** Raw data from Sympatec inhaler measurements of 0% BDP + 8% LF.

8% BDP + 0% LF + 1% MgSt								
Min	Inhaler - 50 lpm				Inhaler – 100 lpm			
	F <sub>5</sub>	SD	RSD	FPmode	F <sub>5</sub>	SD	RSD	FPmode
2	5,48	0,16	2,98	4,05	8,24	0,49	5,99	2,7
5	5,68	0,44	7,66	4,35	8,75	1,00	11,46	2,85
10	5,63	0,13	2,23	4,7	10,00	0,97	9,70	2,85
20	5,77	0,21	3,72	5	10,75	0,92	8,55	2,8
30	4,95	0,31	6,22	5,5	10,64	1,07	10,09	2,75
45	4,87	0,36	7,38	4,7	10,12	0,66	6,54	2,72
60	3,92	0,28	7,02	3,6	9,08	0,49	5,41	2,52
90	3,70	0,23	6,27	3,8	8,37	1,07	12,81	3
120	4,34	0,11	2,48	4,1	9,18	0,85	9,28	3,2

## Data from Sympatec inhaler - standard formulations

**Table K.** Raw data from Sympatec inhaler measurements of 0% BDP + 8% LF.

Min	0% BDP + 8% LF +0% MgSt Inhaler - 50 lpm				Inhaler – 100 lpm			
	F <sub>5</sub>	SD	RSD	FPmode	F <sub>5</sub>	SD	RSD	FPmode
2	2,95	0,09	3,17	9	6,79	0,77	11,33	6,1
5	3,02	0,22	7,23	8,5	5,60	0,32	5,72	6,1
10	2,93	0,05	1,84	7,8	6,14	0,87	14,13	5,9
20	3,20	0,12	3,65	7,5	6,78	0,52	7,61	5,81
30	3,29	0,18	5,49	7,8	7,19	1,24	17,21	5,9
45	3,81	0,38	9,90	7,9	7,75	0,64	8,28	6,05
60	3,91	0,40	10,27	7,95	9,11	1,02	11,24	6,05
90	3,87	0,31	7,98	7,75	9,35	0,68	7,28	5,95
120	2,95	0,09	3,17	9	6,79	0,77	11,33	6,1

**Table L.** Raw data from Sympatec inhaler measurements of 4% BDP + 4% LF.

Min	4% BDP + 4% LF +0% MgSt Inhaler - 50 lpm				Inhaler – 100 lpm			
	F <sub>5</sub>	SD	RSD	FPmode	F <sub>5</sub>	SD	RSD	FPmode
2	1,93	0,14	7,45	10,68	3,87	0,19	4,84	7
5	1,86	0,08	4,55	10,5	4,31	0,43	9,93	7,2
10	2,00	0,07	3,68	10,5	4,58	0,23	5,12	7
20	1,99	0,10	4,93	10,7	4,95	0,28	5,58	6,9
30	2,03	0,09	4,38	11,45	4,60	0,13	2,72	6,7
45	1,95	0,10	5,35	9	4,90	0,17	3,39	6,5
60	1,83	0,04	2,13	9	4,71	0,32	6,83	6,45
90	1,87	0,10	5,30	9,2	4,93	0,36	7,27	6,55
120	2,10	0,10	4,70	9,6	5,72	0,37	6,42	6,65

**Table M.** Raw data from Sympatec inhaler measurements of 8% BDP + 0% LF.

Min	8% BDP + 0% LF +0% MgSt Inhaler - 50 lpm				Inhaler – 100 lpm			
	F <sub>5</sub>	SD	RSD	FPmode	F <sub>5</sub>	SD	RSD	FPmode
2	0,90	0,03	3,02	-	2,33	0,08	3,27	-
5	0,76	0,03	4,36	-	2,14	0,05	2,26	-
10	0,79	0,03	4,04	-	2,28	0,13	5,72	-
20	0,82	0,04	5,17	-	2,28	0,10	4,32	-
30	0,84	0,06	7,15	-	2,27	0,05	2,00	-
45	0,84	0,06	6,67	-	2,25	0,05	2,05	-
60	0,85	0,05	6,28	-	2,48	0,13	5,12	-
90	0,82	0,03	4,27	-	2,50	0,16	6,32	-
120	0,99	0,08	8,10	-	3,25	0,16	5,08	-

## Data from Sympatec RODOS – 4 bar

**Table N.** Raw data from Sympatec RODOS measurements of 0% BDP + 8% LF.

Min	0% BDP + 8% LF							
	Coated with 1% MgSt				Standard			
	F <sub>5</sub>	SD	RSD	FPmode	F <sub>5</sub>	SD	RSD	FPmode
2	12,65	0,76	6,00	2,2	17,13	1,00	5,84	2,46
5	11,01	0,37	3,37	2,2	16,80	0,84	5,03	2,46
10	11,55	0,46	3,95	2,25	15,82	0,16	1,03	2,46
20	11,79	0,19	1,61	2,35	14,50	1,40	9,66	2,45
30	13,78	0,53	3,83	2,45	13,28	0,15	1,13	2,6
45	14,67	0,30	2,06	2,4	15,41	0,27	1,72	2,7
60	15,97	0,07	0,44	2,3	16,42	0,61	3,73	2,85
90	16,98	0,26	1,53	2,4	16,33	0,33	2,02	2,95
120	17,52	0,45	2,58	2,2	17,13	1,00	5,84	2,46

**Table O.** Raw data from Sympatec RODOS measurements of 2% BDP + 6% LF.

Min	2% BDP + 6% LF							
	Coated with 1% MgSt				Standard			
	F <sub>5</sub>	SD	RSD	FPmode	F <sub>5</sub>	SD	RSD	FPmode
2	12,93	0,19	1,49	1,8	-	-	-	-
5	11,98	0,12	1,03	1,7	-	-	-	-
10	14,54	0,14	0,99	1,5	-	-	-	-
20	16,13	0,15	0,95	1,4	-	-	-	-
30	17,43	0,15	0,87	1,5	-	-	-	-
45	19,59	1,28	6,52	1,7	-	-	-	-
60	18,83	0,24	1,29	1,85	-	-	-	-
90	19,27	0,22	1,12	2,2	-	-	-	-
120	18,62	0,38	2,02	2,4	-	-	-	-

**Table P.** Raw data from Sympatec RODOS measurements of 4% BDP + 4% LF.

Min	4% BDP + 4% LF							
	Coated with 1% MgSt				Standard			
	F <sub>5</sub>	SD	RSD	FPmode	F <sub>5</sub>	SD	RSD	FPmode
2	12,63	0,17	1,37	1,3	14,20	0,39	2,75	1,75
5	12,66	0,21	1,64	1,2	15,32	0,66	4,29	1,775
10	15,43	0,11	0,69	1,17	18,08	0,57	3,16	1,76
20	16,88	0,28	1,64	1,16	18,99	0,52	2,75	1,8
30	18,79	0,18	0,94	1,15	20,16	0,84	4,15	1,8
45	20,06	0,14	0,68	1,21	20,00	0,82	4,12	1,95
60	20,55	0,16	0,80	1,3	18,59	1,04	5,61	2,2
90	20,12	0,13	0,64	1,95	18,88	1,00	5,32	2,57
120	20,02	0,41	2,04	2,15	18,40	0,31	1,70	2,73

**Table Q.** Raw data from Sympatec RODOS measurements of 6% BDP + 2% LF.

6% BDP + 2% LF								
Min	Coated with 1% MgSt				Standard			
	F <sub>5</sub>	SD	RSD	FPmode	F <sub>5</sub>	SD	RSD	FPmode
2	12,38	0,22	1,80	1,15	-	-	-	-
5	13,20	0,22	1,67	1,15	-	-	-	-
10	15,99	0,22	1,37	1,15	-	-	-	-
20	17,86	0,22	1,23	1,1	-	-	-	-
30	20,57	0,27	1,31	1,1	-	-	-	-
45	21,61	0,51	2,36	1,1	-	-	-	-
60	21,79	0,29	1,33	1,15	-	-	-	-
90	21,55	0,32	1,48	1,14	-	-	-	-
120	20,86	0,91	4,36	1,18	-	-	-	-

**Table R.** Raw data from Sympatec RODOS measurements of 8% BDP + 0% LF.

8% BDP + 0% LF								
Min	Coated with 1% MgSt				Standard			
	F <sub>5</sub>	SD	RSD	FPmode	F <sub>5</sub>	SD	RSD	FPmode
2	12,76	0,19	1,46	1,1	13,87	1,67	12,03	1,2
5	14,50	0,05	0,37	1,1	18,10	0,76	4,21	1,225
10	17,04	0,27	1,59	0,95	18,61	1,22	6,58	1,195
20	19,85	0,17	0,84	0,95	18,13	1,64	9,07	1,25
30	21,98	0,28	1,27	0,9	17,35	0,39	2,27	1,225
45	22,12	0,46	2,07	0,9	17,62	0,26	1,48	1,235
60	23,49	0,42	1,80	0,95	19,23	0,38	1,96	1,185
90	22,99	0,20	0,88	1,15	19,31	0,56	2,89	1,165
120	21,84	1,09	5,00	1,3	19,49	1,02	5,26	1,23

## Appendix II – Correlation plots

### Coated formulations

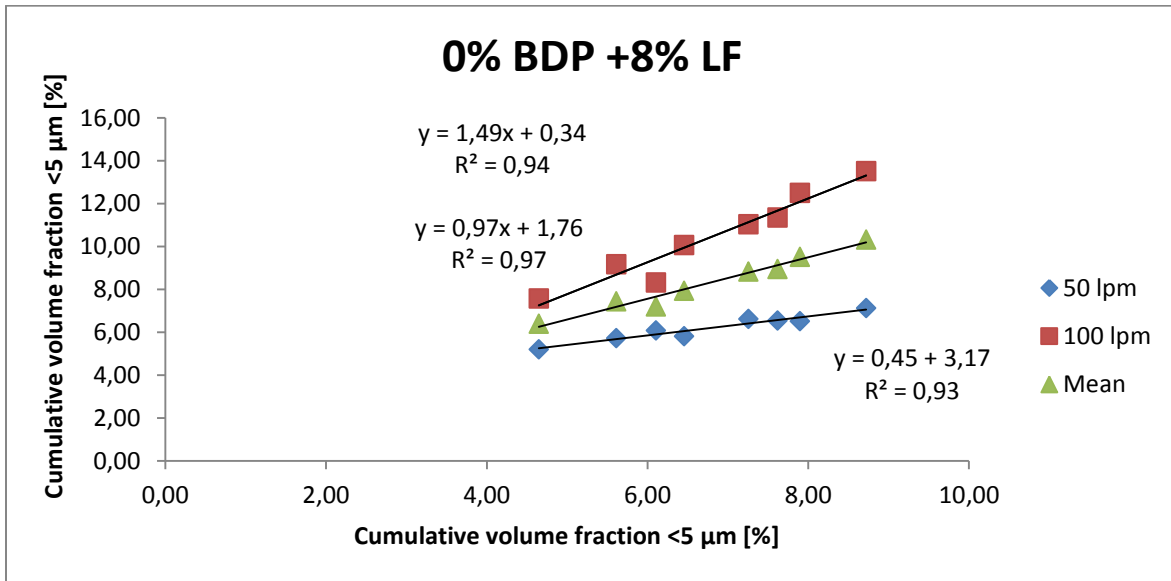


Figure A: Correlation between Sympatec Inhaler and NGI for coated formulation containing 0% BDP and 8% added LF.

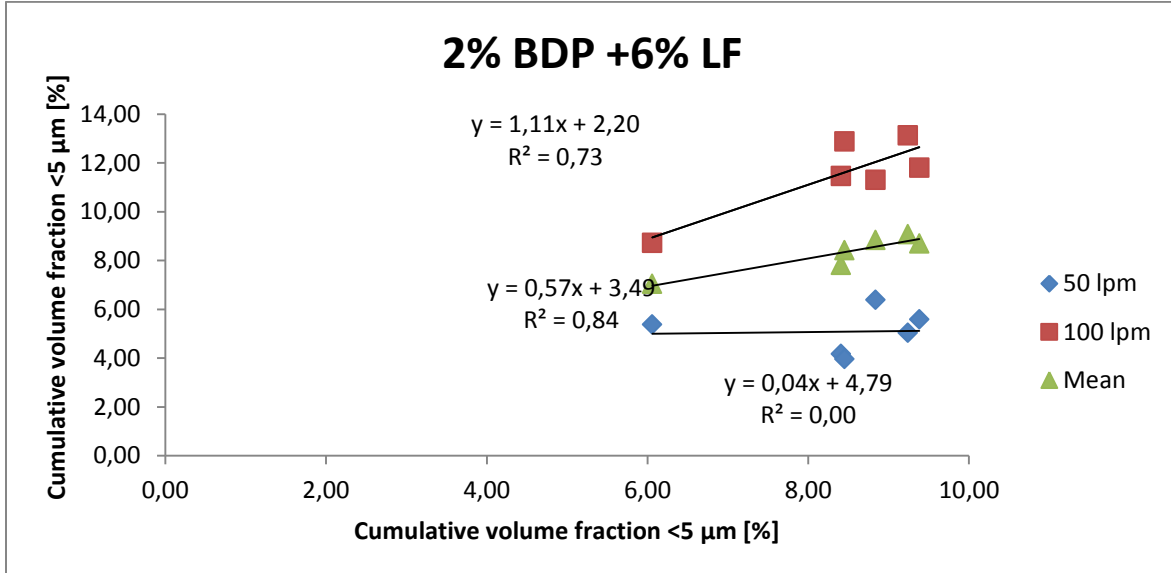


Figure B: Correlation between Sympatec Inhaler and NGI for coated formulation containing 2% BDP and 6% added LF.



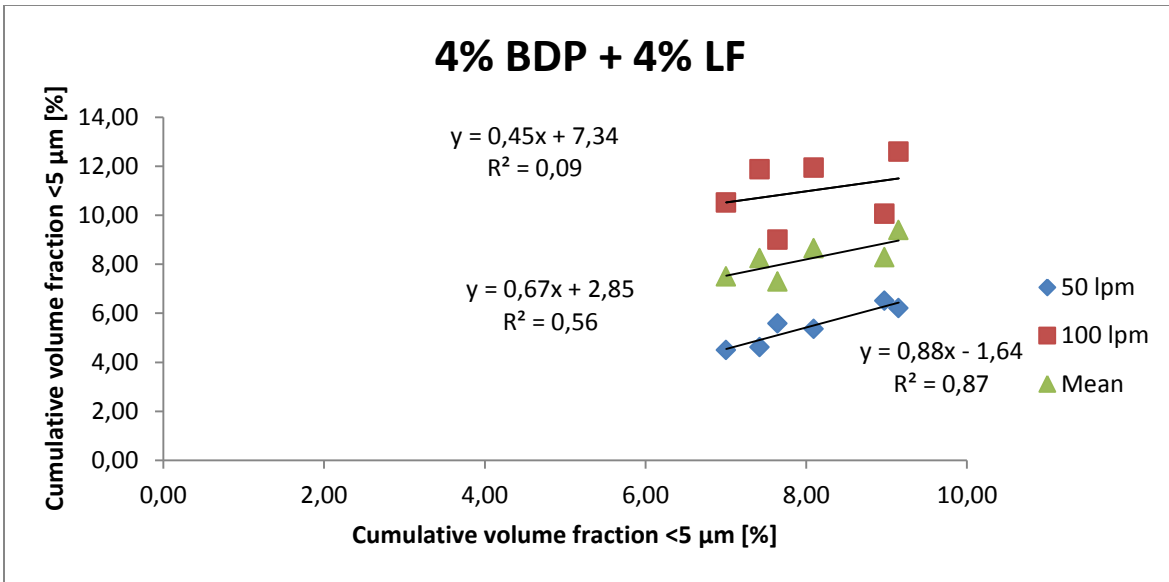


Figure C: Correlation between Sympatec Inhaler and NGI for coated formulation containing 4% BDP and 4% added LF.

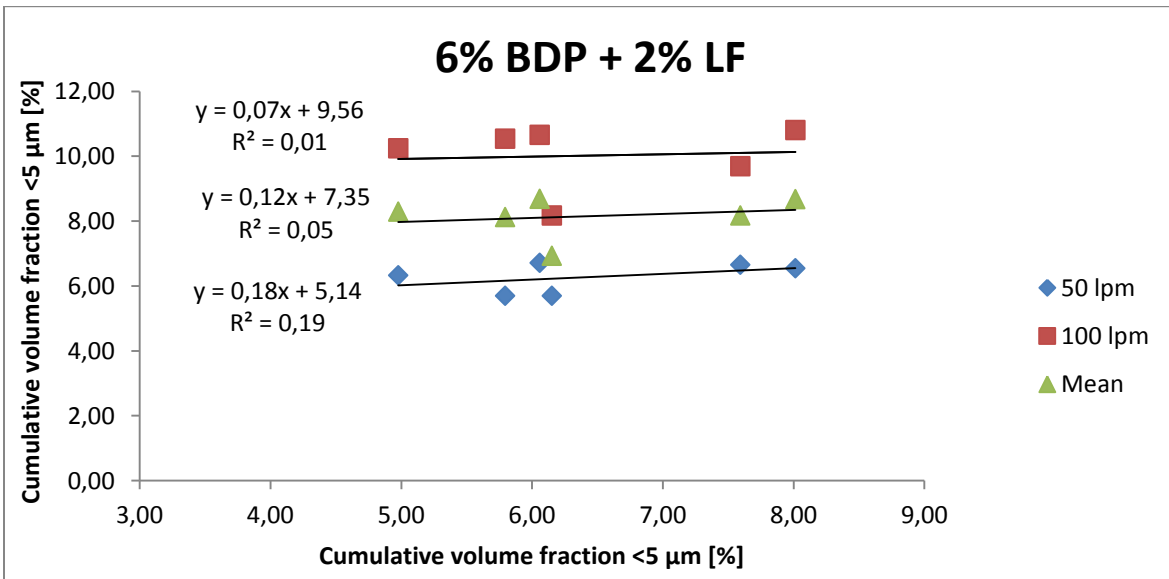


Figure D: Correlation between Sympatec Inhaler and NGI for coated formulation containing 6% BDP and 2% added LF.

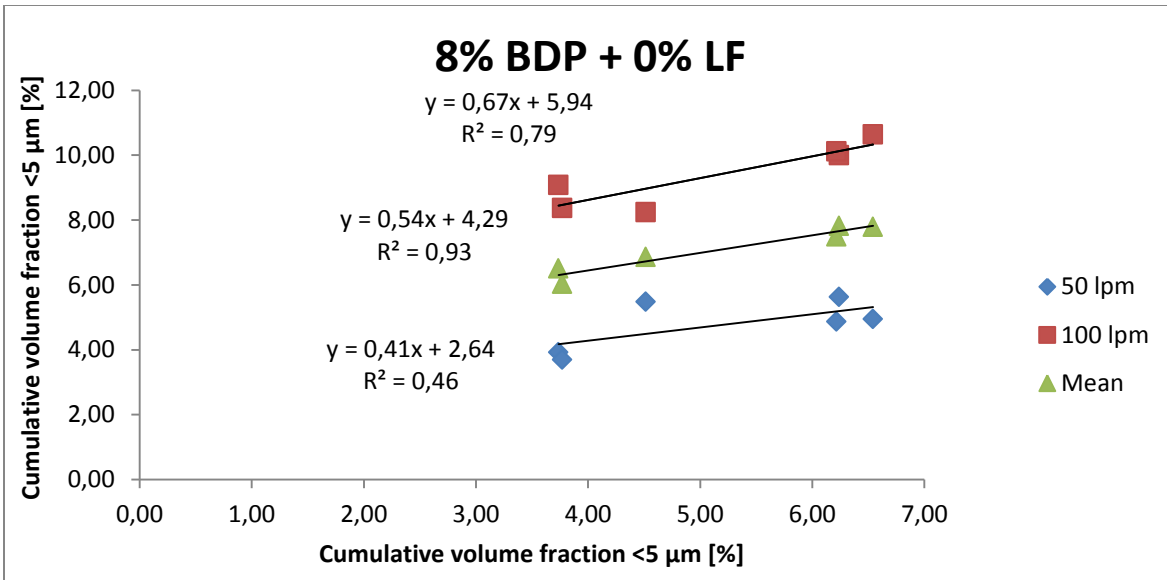


Figure E: Correlation between Sympatec Inhaler and NGI for coated formulation containing 8% BDP and 0% added LF.

### Standard formulations

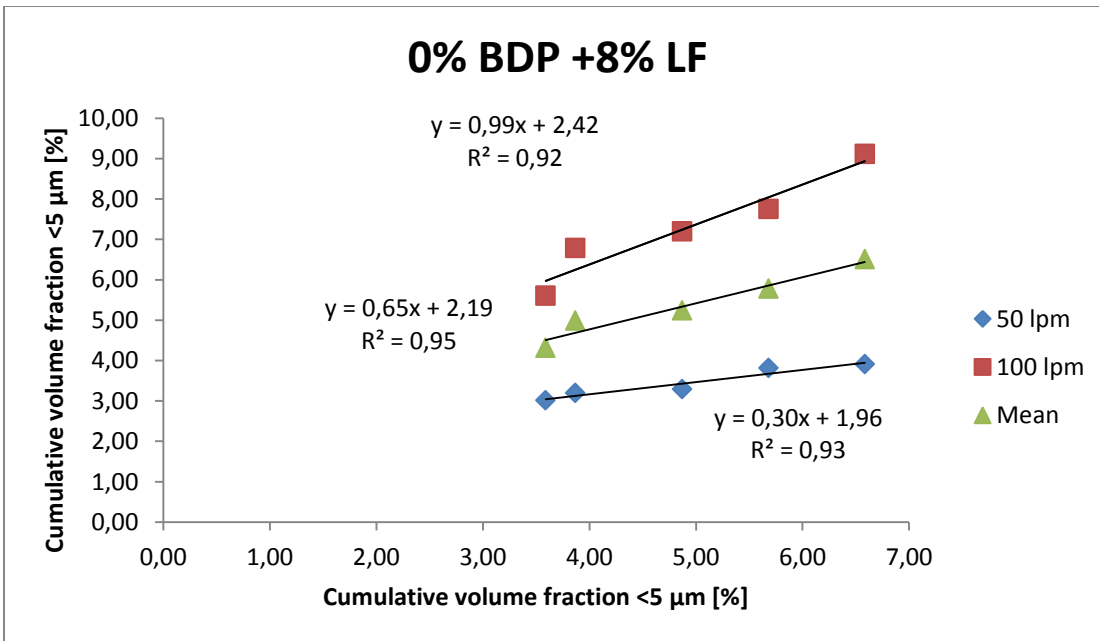


Figure F: Correlation between Sympatec Inhaler and NGI for standard formulation containing 0% BDP and 8% added LF.

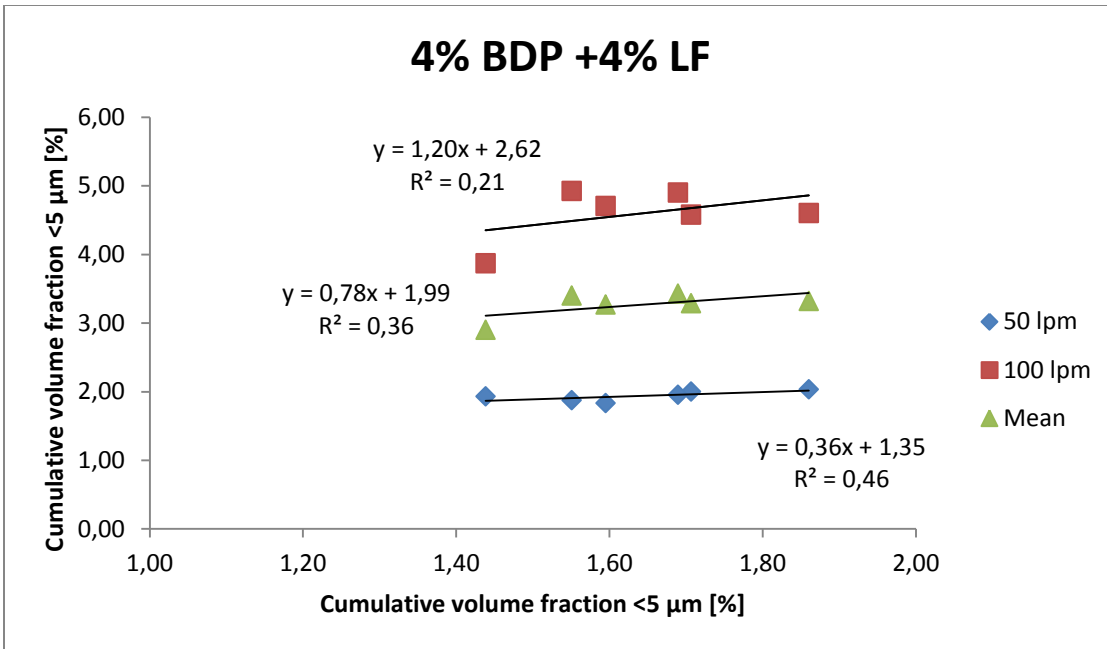


Figure G: Correlation between Sympatec Inhaler and NGI for standard formulation containing 4% BDP and 4% added LF.

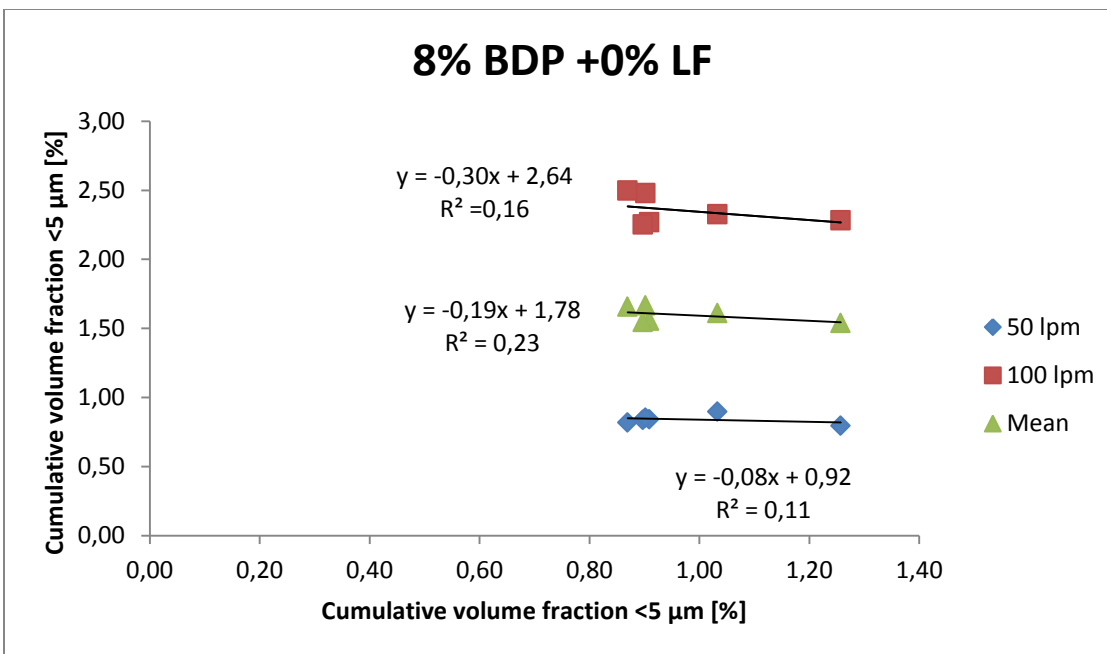


Figure H: Correlation between Sympatec Inhaler and NGI for standard formulation containing 8% BDP and 0% added LF.